EXTRACTION, CONCENTRATION, AND DETECTION OF FOODBORNE PATHOGENS USING GLYCAN-COATED MAGNETIC NANOPARTICLES AND A GOLD NANOPARTICLE COLORIMETRIC BIOSENSOR

By

Emma Faith Dester

A THESIS

Submitted to
Michigan State University
in partial fulfillment of the requirements
for the degree of

Biosystems Engineering – Master of Science

2022

ABSTRACT

EXTRACTION, CONCENTRATION, AND DETECTION OF FOODBORNE PATHOGENS USING GLYCAN-COATED MAGNETIC NANOPARTICLES AND A GOLD NANOPARTICLE COLORIMETRIC BIOSENSOR

By

Emma Faith Dester

In this work, a rapid method for foodborne pathogen extraction and concentration using magnetic nanoparticles (MNPs) was integrated with a gold nanoparticle (GNP) colorimetric DNA biosensor for fast and accessible detection of target bacteria. Experiments for both extraction and detection were conducted first using pure cultures without interfering food matrix components and followed by testing in food matrices commonly associated foodborne outbreaks. Magnetic concentration was tested with three bacterial species: *Listeria* spp., *Escherichia coli* O157, and *Staphylococcus aureus.* Then, a colorimetric GNP biosensor was developed and tested for *E. coli* O157.

Glycan-coated MNPs are ideal for foodborne pathogen concentration due to their low cost, simple storage conditions, and bacteria binding capabilities. Meanwhile, GNPs visibly change color upon aggregation, which allows for easy use in colorimetric biosensors without the need for expensive analytical equipment. Results from this study indicate concentration of bacteria to up to 60 times its initial concentration in buffer solution and 11 times in select food matrices. In addition, the colorimetric biosensor was capable of differentiating between target and non-target DNA from pure cultures at concentrations as low as 2.5 ng/µL. Finally, the integrated extraction and detection assay was capable of detecting *E. coli* O157 from contaminated flour. This assay shows immense promise for rapid foodborne pathogen detection, and evidence-based recommendations for continued optimization have also been identified.

ACKNOWLEDGEMENTS

This research was funded by the Michigan State University Targeted Support Grant for Technology Development (TSGTD) and supported by Dr. Evangelyn Alocilja's Nano-Biosensors Laboratory.

TABLE OF CONTENTS

LIST OF TABLES

LIST OF FIGURES

KEY TO ABBREVIATIONS

Units

ºC: degrees Celsius

µL: microliter

µM: micromolar

CFU/mL: colony forming units per milliliter

g: grams

hr: hour(s)

log CFU/mL: log base 10 of colony forming units per milliliter

mg: milligrams

min: minute(s)

mL: milliliter

mM: millimolar

pg: picogram

rpm: rotations per minute

s: second(s)

Chemical Abbreviations

$C_{12}H_{25}NaO_4S$: sodium dodecyl sulfate (SDS)

$C_6H_{12}O_6$: dextrin

COOH: carboxylic acid

Co: colbalt

Fe: iron

Fe_2O_3: iron oxide, maghemite

Fe_3O_4: iron oxide, magnetite

$HAuCl_4$: gold (III) chloride trihydrate

HCl: hydrochloric acid

$HS(CH_2)_{10}CO_2H$: 11-mercaptoundecanoic acid (MUDA)

Na_2CO_3: sodium carbonate

NaOH: sodium hydroxide

Ni: nickel

Ti: titanium

$Ti(OH)_4$: titanium hydroxide

$Zn(OH)_4$: zirconium hydroxide

Research-Related Acronyms

α: confidence level for statistics

C: control

CF: concentration factor

DNA: deoxyribonucleic acid

GNP: gold nanoparticle

MNP: magnetic nanoparticle

NT: non-target

OA: oxford agar

PBS: phosphate buffer solution

SPR: surface plasmon resonance

T: target

TEM: transmission electron microscopy

TSA: tryptic soy agar

TSB: tryptic soy broth

ZP: zeta potential

Literature Review and Background-Related Acronyms

BDC: buoyant-density centrifugation

CFC: continuous flow centrifugation

DFE: dielectrophoretic filtration efficiency

ELISA: enzyme-linked immunosorbent assay

IMS: immunomagnetic separation

LAMP: loop-mediated isothermal amplification

LFA: lateral flow assay

mPCR: multiplex polymerase chain reaction

NASBA: nucleic acid sequence-based amplification

NTA: non-target sample aggregation, referring to colorimetric GNP biosensor assays

PCR: polymerase chain reaction

qPCR: quantitative or real-time polymerase chain reaction

RCA: rolling circle amplification

RNA: ribonucleic acid

SDA: strand displacement amplification

SERS: surface-enhanced Raman spectroscopy

TA: target sample aggregation, referring to colorimetric GNP biosensor assays

Chapter 1: Introduction

1.1 Introduction

Globally, foodborne pathogens are responsible for approximately 600 million illnesses and 420,000 deaths each year, with the burden especially high for children under the age of five and low-income communities [1]. Within the United States, foodborne disease outbreaks also strain the healthcare system, leading to over 3,000 deaths and 128,000 hospitalizations annually [2]. *Listeria monocytogenes*, *Staphylococcus aureus*, and *Escherichia coli* are some of the many bacterial species implicated in foodborne illness [3]. Outbreaks can occur in a variety of food matrices, including fresh fruits, vegetables, meats, milk, and dairy products [3]. Fruits and vegetables are often especially dangerous, as they are commonly consumed fresh and therefore not cooked to sufficient temperatures for bacteria death [4]. Thus, timely detection of contaminated foods is essential to protect the health and safety of all consumers.

Many obstacles currently exist for rapid and accessible detection of foodborne pathogens. As traditional enumerative techniques require days of culture time for quantitative results, efforts have been made to develop rapid methods to more effectively protect consumers [5], [6]. Most commonly, polymerase chain reaction (PCR) techniques have been implemented to reduce detection time from days to hours [7]. However, PCR assays require advanced laboratory equipment, costly reagents, and trained personnel that increase detection cost and reduce accessibility [8]. In fact, the recent COVID-19 pandemic has drawn attention to the limited availability of PCR-equipped laboratory facilities in many low-income and middle- income countries [9], [10]. As foodborne illness is a global concern, it is of the utmost importance that low-cost, accessible, and rapid techniques are developed for foodborne pathogen detection. Several other rapid detection methods have been tested, including immunological assays and

many types of biosensors. However, they are sometimes still associated with high cost or equipment needs, and others can have low specificity or sensitivity when implemented in foods [6], [11], [12].

In addition to concerns related to accessible detection, pre-treatment of food samples to isolate and concentrate bacteria is often a significant challenge. It is typically necessary to increase the initial bacterial concentration in foods to allow for successful detection; furthermore, food components can often interfere with rapid detection techniques if not properly removed [13], [14]. Traditional pre-treatment methods utilizing incubation in selective media for isolation of target bacteria are effective but time-consuming [15]. Thus, physical, chemical, and biological processes have been tested and implemented as rapid methods for bacterial concentration directly from foods. Although some chemical and biological processes, such as immunomagnetic separation (IMS), are highly effective, they are also commonly associated with higher costs and specific storage conditions [16], [17]. Meanwhile, physical methods such as centrifugation and filtration often encounter issues with effective food matrix removal and selectivity [18], [19]. As a result, the search for a rapid and cost-effective assay for extraction, concentration, and detection of foodborne pathogens is still ongoing.

This research sought to address the limitations of current foodborne pathogen extraction and detection techniques through the design of a cost-effective and rapid assay with limited needs for laboratory equipment. To achieve this, glycan-coated magnetic nanoparticles were used for direct extraction and concentration of bacteria, and a colorimetric gold nanoparticle (GNP) biosensor was used for detection of target DNA. Figure 1.1 summarizes these steps in a graphical outline. The end goal of this research was to analyze the effectiveness of these two combined methodologies for detection of bacteria directly from contaminated food matrices.

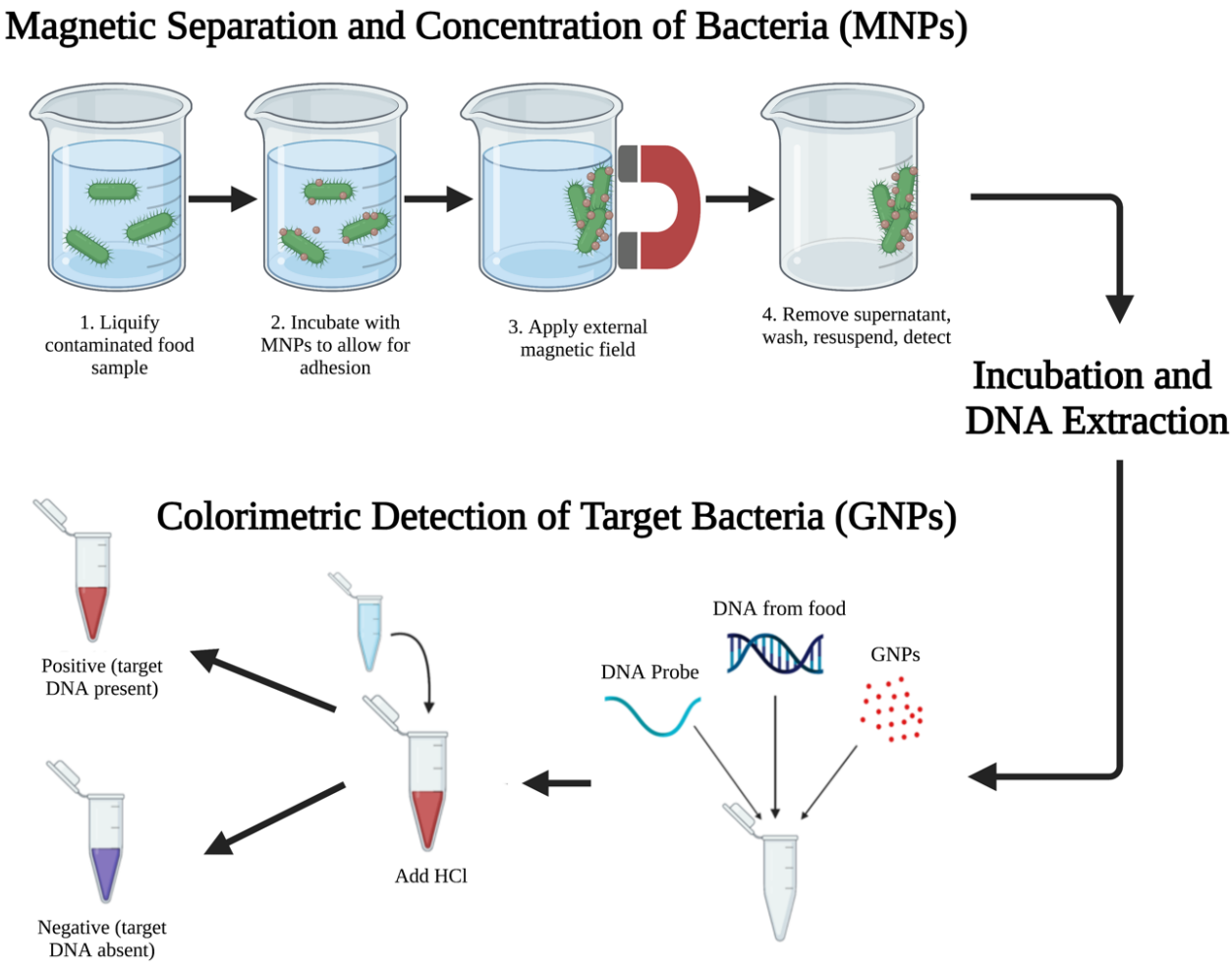

Figure 1.1 Graphical outline of thesis methods (created with Biorender).

1.2 Hypothesis and Aims

The overall hypothesis of this thesis is that methods using magnetic and gold nanoparticles can be implemented for rapid concentration and detection of bacteria directly from contaminated food matrices. This hypothesis was divided into two specific aims. The first aim was to determine the effectiveness of glycan-coated MNPs for capturing and concentrating (a) *Listeria* spp., (b) *S. aureus*, and (c) *E. coli* O157:H7 from various food matrices. The second aim concerned the development of a gold nanoparticle-based colorimetric biosensor for detecting *E. coli* O157:H7 DNA from food matrices. Each of these aims included several key objectives, outlined further in the following section.

1.3 Specific Objectives

A full summary of all objectives, aims, and methodologies is summarized in Table 1.1. The first aim, concentration of bacteria using glycan-coated MNPs, consisted of five specific objectives. The first was to visualize binding of MNPs to bacterial cells on a microscopic level in order to confirm successful adhesion and gain further insight into the adhesion mechanism. Both transmission electron microscopy (TEM) and confocal laser microscope imaging were used to capture images of bacterial samples previously extracted using MNPs. The second objective was to analyze the effect of pH on MNP bacterial capture in order to determine potential aspects of the glycan-bacteria adhesion mechanism and optimize cell capture. This was accomplished through several large-volume experiments in Phosphate-Buffered Saline solution (PBS) adjusted to various pH values. The third objective centered on comparing MNP concentration capabilities for different bacterial species and concentrations. To accomplish this, the three aforementioned bacterial species were extracted from PBS at 5 different inoculation concentrations; in addition, morphological bacterial cell characteristics were used to hypothesize differences in capture of various species. The fourth objective was to expand upon the hypothesized mechanism for MNP-bacteria adhesion using both experimental data and literature sources. Finally, the fifth objective was to examine the effect of various food matrices on MNP bacterial capture through direct extraction from contaminated and liquified food samples.

The second aim, development of a GNP colorimetric biosensor, consisted of three specific objectives. First, it was necessary to optimize the existing biosensor assay to have a quantitatively and qualitatively detectable color difference between target and non-target DNA samples. This was accomplished through design of a DNA probe specific to *E. coli* O157, followed by optimization of HCl volume and incubation time used in the procedure. Qualitative

results were observed visually, and quantitative results were analyzed using absorbance spectra collected from a NanoDrop One. The second objective was to analyze the sensitivity and specificity of the biosensor for each target pathogen. This was accomplished through statistical analysis of biosensor results using several non-target DNA samples at varying concentrations. The third and final objective concerned analysis of the sensitivity and specificity of the biosensor for DNA samples extracted from food. For this objective, bacterial samples concentrated from food matrices using MNPs were incubated in Tryptic Soy Broth (TSB) for 4 hr, followed by DNA extraction. Samples were then tested alongside target and non-target DNA from pure cultures to determine the biosensor's capability for detection of DNA from foods.

Table 1.1 Overview of aims, objectives, and approaches.

Aim 1: Determine the effectiveness of MNPs for capturing and concentrating *L. monocytogenes*, *S. aureus*, and *E. coli* O157:H7 from various food matrices.			
Objective	**Current technology**	**Approach**	**Sources**
Visualize binding of MNPs and bacteria on a microscopic level	MNP-bacteria binding has been visualized for these MNPs, but binding locations have not quantitatively analyzed.	Use TEM for confirmation of MNP binding, followed by confocal laser microscopy to quantify binding site locations.	[20], [21]
Analyze the effect of pH on MNP bacterial capture	Surface charge is known to play a role in glycan-protein interactions, but the known effect on bacterial capture is limited.	Conduct large-volume MNP capture experiments using in various pH buffer solutions and study whether there is a correlation between bacterial capture and charge difference.	[22], [23], [24], [25]
Analyze the effect of bacterial species and concentration on MNP bacterial capture	Studies with other glycan-coated MNPs have shown little effect of bacterial concentration on MNP capture, but studies have not been conducted with these MNPs and *S. aureus* capture from food has not been tested.	Conduct MNP extraction experiments in 100 mL PBS bags inoculated with varying bacterial concentrations. Test for correlation between concentrations, and compare results for different species.	[26], [27]
Confirm and elaborate upon hypothesized mechanism for MNP-bacteria adhesion	The theory of glycan-protein interactions is well-researched but rarely applied to optimizing applications of glycan-coated MNPs	Determine whether lab results confirm the applicability of literature sources on glycan-protein interactions and MNP interactions. Analyze how theories can be used for optimization.	[28], [29]
Examine the effect of various food matrices on MNP bacterial capture	Few glycan-coated MNP extractions have been conducted directly from food, and all use small sample volumes.	Directly extract bacteria from artificially inoculated food samples at liquified sample volumes of 100 mL.	[26], [30], [27]
Aim 2: Develop a gold nanoparticle-based colorimetric test for detecting *E. coli* O157:H7 DNA extracted from various food matrices.			
Objective	**Current technology**	**Approach**	**Sources**
Optimize test for quantitatively and qualitatively detectable color difference between target and non-target DNA samples.	GNP colorimetric biosensors have demonstrated potential for accessible and rapid detection. However, a biosensor with rapid GNP-probe functionalization has not been tested or optimized.	Utilize Nanodrop absorbance measurements and visual results to optimize assay for easy detection.	[31], [32]
Analyze sensitivity and specificity of optimized biosensor with pure DNA cultures.	Existing biosensors for rapid foodborne pathogen detection often sacrifice either sensitivity or accessibility, with sensitivity low in the most affordable options.	Statistically analyze key absorbance measurement differences between target and non-target samples at varying concentrations	[6], [12]
Analyze sensitivity and specificity of optimized biosensor with DNA cultures extracted from food samples.	Few GNP colorimetric biosensors have been tested directly for detection of DNA extracted from food, and 6+ hr of sample incubation is often required.	Extract DNA from magnetically extracted food samples after 4 hr of incubation and determine whether target DNA can still be visually identified.	[31], [32], [33]

Chapter 2: Literature Review

Sections 2.1, 2.3, and 2.4 of this chapter are adapted from the open access article "Current Methods for Extraction and Concentration of Foodborne Bacteria with Glycan-Coated Magnetic Nanoparticles: A Review," previously published in *Biosensors* [34].

2.1 Introduction

Traditional foodborne pathogen detection methods use several types of culture media to isolate and enumerate bacterial cells [5], [6]. Although sensitive and widely used, these preferred methods can be time-consuming and laborious, often requiring up to a week for conclusive results [5], [15]. In recent years, rapid detection methods have explored to reduce the time and labor necessary for foodborne pathogen detection. Nucleic acid-based analyses, for instance, can reduce detection time from days to hours with high sensitivity [35]. However, high equipment costs can limit their applicability in low-resource regions [36]. Immunological methods, such as lateral flow assays, have been shown to reduce costs but often sacrifice sensitivity [37]. Several types of biosensors have also demonstrated success in rapid foodborne detection, which convert biological, chemical, or biochemical elements into measurable signals [38].

Before detection, concentration and/or extraction of bacteria is often an important step. Conventional microbiological protocols typically accomplish this through overnight cultures, requiring 24-48 hr of incubation in selective media [15]. This pre-enrichment step is used to increase the target bacterial concentration, preceding further analysis and standard biochemical identification [6], [15]. As mentioned previously, however, this labor-intensive and time-consuming process is not conducive to rapid detection. Rapid detection methods such as biosensors and PCR often employ techniques such as centrifugation [39], [40], filtration [40],

dielectrophoresis [41], metal hydroxides [42], [43], and magnetic nanoparticles (MNPs) [26], [29], [44], [45] to concentrate and remove bacteria from foods without overnight culturing. These concentration methods can be broadly characterized as either physical or chemical/biological; however, some methods may incorporate characteristics of both categories [46]. Although these methods have been explored with varying degrees of success, complex food matrices often make rapid bacterial concentration more difficult. For instance, food macromolecules can block the interactions between target molecules and receptors in many biosensors, as well as interfering with PCR [13], [14].

Nanoparticles have attracted attention for both foodborne pathogen concentration and detection due to their unique properties, low cost, and functionalization capabilities [31], [47]–[49]. For instance, glycan-coated MNPs show promise as an affordable and rapid method for food pathogen concentration through carbohydrate-lectin interactions [26], [29]. Meanwhile, gold nanoparticles (GNPs) feature unique colorimetric properties that make them an optimal material for simple and cost-effective foodborne pathogen biosensors [31], [33]. This review seeks to summarize existing rapid methods for concentration and detection of bacteria from food matrices. Special attention is paid to the current state and future potential of glycan-coated MNPs for extraction and concentration of bacteria. In addition, a review of gold nanoparticle colorimetric biosensors is provided. Current limitations and knowledge gaps for these two nanoparticle-based assays are discussed in detail.

2.2 Current Food Extraction Methods: Physical

Physical methods for foodborne pathogen extraction typically use bacterial characteristics such as bacteria density, target bacteria size, and solution density to physically separate target

bacteria from the food matrix [46]. They are usually less selective than chemical or biological methods that utilize specific biological or chemical characteristics of the target cells [46]. The most commonly used methods, described in Table 2.1, include centrifugation and filtration.

Table 2.1 Overview of physical methods.

Method	Description	Advantages	Disadvantages	References
Centrifugation	Bacteria are concentrated by centrifugation and food solution can be removed. Pellet can be resuspended in a smaller solution volume.	Can concentrate from large sample volume, 5-30 min assay	Labor-intensive for effective food matrix removal, not selective for target pathogen, loss of bacteria adhered to food particles	[39], [50]–[55]
Filtration	Samples are passed through filters with various pore sizes, allowing bacteria to flow through while eliminating the larger food particles	1-10 min assay, remove inhibitors in food matrix	Filter clogging is common, non-target bacteria often concentrated	[40], [50], [56]–[58]

2.2.1 Centrifugation

Centrifugation is a common method for bacterial concentration in which the bacteria is pelletized and the supernatant is removed. Samples can be resuspended in a smaller solution volume, allowing for bacterial concentration. Centrifugation can typically take 1-30 min [52], [53], [55], although complex procedures may incorporate multiple centrifugation steps and washes that increase procedure duration [51]. Multiple centrifugation techniques have been developed to extract and concentrate bacteria from various food matrices, including continuous flow centrifugation (CFC) [52] and buoyant-density centrifugation (BDC) [51], [53].

Centrifugation has been tested for decades to extract and concentrate bacteria from food matrices [59]. However, recent developments have improved the efficiency of this method, as well as the purity of samples for further testing. For example, buoyant-density centrifugation methods have successfully eliminated PCR-inhibiting food substances, allowing for detection

without sample culturing after DNA extraction [53], [51]. In addition, continuous flow centrifugation has allowed for concentration of bacteria from higher sample volumes, leading to higher total bacterial capture [52], [54].

Despite these advancements, centrifugation of bacteria from foods still faces several challenges. Separation of food particles, although remediated through techniques such as BDC, requires multiple labor-intensive steps and still may not eliminate all food particles [51]. In addition, centrifugation does not allow for selective separation of a target pathogen. It will also concentrate non-target pathogens, including natural microflora [53]. A recent study of *Staphylococcus epidermis* in human milk samples also noted that cells could remain attached to fat during the centrifugation process and be lost [55]. Not only does this reduce capture efficiency, but there is also evidence this may lead to a DNA profile that is not representative of all bacterial cells in the food [55].

2.2.2 Filtration

Filtration is a physical method for bacterial extraction and concentration that relies on passing samples through filters with various pore sizes [58]. This method utilizes the size difference between bacterial cells and food particles to eliminate interfering components and quickly produce a purified sample. Filtration is often combined with centrifugation to increase bacterial capture efficiency. One study, for example, found that combining CFC with glass wool filtration significantly increased bacterial capture in ground beef samples [54]. With a pre-filtration step, recovery of *Escherichia coli* O157:H7, *Salmonella enterica*, and *Listeria monocytogenes* increased from 18, 27, and 32% to 48, 62, and 97%. Pre-filtration also eliminated the large amount of solid retentate aggregated in the collection bowl for unfiltered samples [54].

This method has several key advantages, including the rapid nature of the filtration process itself. Filtration can take as little as 1-10 min to effectively separate bacteria from a food matrix [50]. In addition, they advantageously remove inhibitors in the food matrix, reducing interference during subsequent pathogen detection. For example, using filter paper and a membrane filter, one author effectively performed PCR on food samples inoculated with pathogenic *E. coli* [40]. This method successfully detected 100% of beef, pork, and leafy vegetable samples with target bacteria concentrations of 2 log CFU/g [40].

Table 2.2 Recent advances in physical methods for foodborne pathogen extraction.

Method	**Sample size**	**Bacteria**	**Matrix**	**Capture**	**Source**
BDC	0.9 mL	*E. coli* O157:H7	Beef, minced beef	20-45%	[53]
BDC (multi-step)	220 mL	*S. enterica, E. coli, Yersinia enterocolitica, Campylobacter jejuni, Vibrio* spp., *Providencia alcalifaciens*, *Aeromonas hydrophila, B. cereus, S. aureus, Clostridium perfringens*	Beef, bovine liver, pork, chicken, processed cheese, scrambled egg, tofu, Chinese noodle, bread, jack horse mackerel, chort-neck clam, hamburger steak, whole milk	11% (2.0-23%)	[51]
CFC	250 mL (60 mL/min)	*E. coli* O157:H7, *Salmonella enterica*, *Listeria monocytogenes*	Ground beef, ground pork, ground turkey, spinach	47% (18-75%)	[54]
CFC and GW filtration	250 mL (60 mL/min)	*E. coli* O157:H7, *Salmonella enterica, Listeria monocytogenes*	Ground beef	69% (48-97%)	[54]
CFC	3.7 L (1 gal)	*Bacillus* spp., *Clostridium sporogenes*	Whole and skim milk	55-88%	[52]
Filtration (paper, membrane)	50 mL	Pathogenic *E. coli*	Beef, pork, leafy vegetables	N/A	[40]
Filtration (vacuum pump)	5, 15, 30 mL	*L. monocytogenes*	Dairy products, seafood, meat, vegetables	N/A	[18]

BDC: buoyant density centrifugation
CFC: continuous flow centrifugation

Although sometimes remediated by multi-step filtration methods, large food particles can often clog filters, limiting filtration effectiveness [56]. In addition, the success of this method

heavily depends on the matrix studied. One study used a vacuum pump filtration method for concentration and enumeration of low levels of *L. monocytogenes* from a variety of food matrices [18]. The experimenters noted important differences in the success of filtration on different food types. Although almost all seafood, vegetable, and meat products were successfully filtered, all samples containing dairy products were rejected due to either filtration problems or high levels of natural microflora [18]. Thus, both the food matrix components and non-target bacteria present in the food matrix may reduce filtration effectiveness.

2.3 Current Food Extraction Methods: Chemical and/or Biological

Chemical or biological methods for food extraction and concentration, sometimes referred to as adsorption methods, typically rely on a biosorbent matrix consisting of an affinity agent and a solid support [50]. Affinity agents such as carbohydrates, antibodies, and charged particles attach to bacterial cells through physicochemical interactions, including Van der Waal's forces, electrostatic interactions, and hydrogen bonding [46]. Solid supports are bound to the affinity agent and necessary for the extraction process. These components can best be illustrated through examples. In the case of immunomagnetic separation, for instance, the MNPs are the solid support. The affinity agent is the antibodies that coat the nanoparticles and selectively bind to target bacteria [16]. In other chemical methods, one element acts as both the solid support and the affinity agent, such as the electrode used in dielectrophoresis [50].

Chemical or biological methods for extracting and concentrating foodborne pathogens can be either nonspecific or highly specific to a target bacterial species. Immunomagnetic separation, as mentioned previously, adheres to bacterial cells through antibody-antigen interactions. These electrostatic interactions are highly specific to the bacteria with the target

antigens and do not bind to non-target species [17], [21]. Other methods utilize aspects of affinity that nonspecifically adhere to a variety of bacterial cells. For example, the presence of negatively charged elements in the bacterial cell membrane leads to the vast majority of bacterial species having a net negative charge at room temperature [60]. Thus, many extraction methods can use positively charged residues to nonspecifically adhere to bacterial cell membranes, such as some MNP-based techniques and dielectrophoresis [46]. Common chemical and biological methods are summarized in Table 2.3.

Table 2.3 Overview of chemical and biological methods.

Method	Description	Advantages	Disadvantages	References
Metal hydroxides	Immobilization of titanium or zirconium hydroxides to bacteria through chelation followed by centrifugation	Rapid, cost-effective, maintains cell viability	Centrifuge required, needs enrichment step, limited research in foods	[6], [42], [46], [61],
Dielectrophoresis	Nonuniform electric field used to manipulate bacterial cells	Rapid, option for selectivity, maintains cell viability	Remaining food particles in sample, potentially low capture rate in foods	[41], [46], [62]–[64]
Glycan-coated MNP separation	Glycans on MNPs electrostatically bind, extract, and concentrate bacteria	Rapid, cost-effective, option for selectivity	May bind to food particles, limited research in foods	[26], [46], [21], [20], [30], [65]
Immunomagnetic separation	MNPs coated with specific antibodies bind, extract, and concentrate target bacteria.	High specificity, rapid	Costly synthesis and storage, not standardized	[17], [44], [66]

2.3.1 Metal hydroxides

Metal hydroxides have shown promise as a potential nonspecific technique for isolating bacteria from food matrices. As first reported in 1976, the hydroxides titanium, $Ti(OH)_4$, and zirconium, $Zn(OH)_4$, can successfully immobilize to cells through a chelation process [61]. In this process, amino acids on the bacterial cell surface covalently bind with the metal hydroxide

hydroxyl groups, leading to effortless concentration of cells and removal of the sample matrix through a centrifugation process and subsequent supernatant removal [58].

In more recent years, metal hydroxides have been used for direct extraction and concentration of bacteria from food matrices. For instance, one author successfully used zirconium hydroxide and titanium hydroxide to extract *Salmonella enterica* serovar Enteritidis for PCR detection [42]. The researchers found metal hydroxide immobilization increased their DNA yield compared to centrifugation alone, with zirconium hydroxide having higher yields than titanium hydroxide. With a 4-hr enrichment period after extraction, metal hydroxide immobilization combined with nested PCR led to sensitivity as low as 1 CFU/mL [42]. Another study used zirconium hydroxide to extract *S. aureus*, *V. parahaemolyticus*, *E. coli*, and *E. faecalis* from pudding, coffee, and non-fat milk [43]. When combined with mass spectrometry for detection after a 5-8 hr enrichment period, this method successfully detected the foodborne pathogens. For detection of milk contaminated with *E. faecalis*, the detection limit was as low as 32 CFU/mL [43].

Metal hydroxide immobilization has proven to be a rapid and inexpensive method for nonspecific extraction of bacteria from food matrices that maintains cell viability [43], [61]. Unfortunately, there are only limited studies of its application in food matrices, and most studies still include 4-8 hr enrichment steps before detection. Centrifugation is also required, leading to additional equipment requirements [42], [43]. In addition, the nonspecific nature of the metal hydroxides may lead to concentration of food particles as well as the bacterial cells, which could potentially interfere with detection assays [58].

2.3.2 Dielectrophoresis

Dielectophoresis (DEP) is the electrokinetic motion of dielectrically polarized particles in a nonuniform electric field that acts as an electrostatic transport mechanism [62]–[64]. Since most biological cells behave as dielectrically opposed particles when exposed to this external electric field, DEP can be used to manipulate a wide variety of cells, including bacteria [67]. Both positive and negative DEP can be implemented for bacterial cell concentration applications [41], [67], [68]. This technique has been successful for removal and filtration of foodborne pathogens. For example, one study designed a DEP-based filtration system to remove *E. coli* O157:H7, *Listeria monocytogenes*, *Salmonella* Typhimurium, and *Staphylococcus aureus* from water samples [63]. The 5-hr process successfully removed 99.99% of the bacteria with a combination of DEP and mechanical filtration. Dielectrophoretic efficiency alone was found to be 85.71% [63].

DEP can be used in combination with several types of biosensors and biochips to enhance the detection of foodborne pathogens. For instance, DEP has been used to improve immunocapture and detection of *Salmonella* Typhimurium suspended in water using non-flow through biochips [67]. The introduction of DEP improved immunocapture efficiencies from 10.4% and 17.6% to 56.0% and 64.0% for 15 and 30 min of immunocapture, respectively [67]. DEP-treated foodborne bacteria have also been tested with other detection methods such as surface-enhanced Raman spectroscopy (SERS) [68], impedance-based biosensors [41], and microwire sensors [64], among any others. In addition, some combined DEP/biosensor technologies have been implemented to directly detect bacteria from food matrices. Notably, one author used an integrated microsystem device with positive DEP to detect *E. coli* O157 from raw

chicken samples [41]. Concentration and detection were effectively accomplished in only 6 min with a detection limit of 3.36 x 10^6 CFU/mL [41].

Dielectrophoresis has shown promise as a potential method for foodborne pathogen concentration. One key advantage is the rapid nature of these processes; many biosensors and other detection methods combined with DEP have been able to concentrate and detect target bacteria in under 30 min with minimal cell damage [41], [64], [67], [68]. It also has the potential for specificity, with some systems capable of separating viable and nonviable cells before detection, or even selectively concentrating certain target bacterial species [62]. However, the capture efficiency of DEP techniques can highly vary depending on device design [62]. Limited studies exist for capture directly from food matrices and capture efficiency is often not calculated, but the high detection limits in some research suggest a lower capture efficiency than experiments performed with pure cultures [41]. In addition, the remaining presence of food particles in the concentrated sample may negatively impact some biosensor-based detection methods [64].

2.3.3 Immunomagnetic Separation

Immunomagnetic separation (IMS) utilizes antibodies immobilized to MNPs to extract and concentrate target bacteria. The first step of IMS is to capture the bacteria, which is facilitated by the binding of a specific antibody to antigens on the target cell [16]. Several factors can influence the capture efficiency of IM particles, including particle composition/size, particle concentration, bacteria concentration, and amount of time IM particles are incubated with the target bacteria [13], [17], [66]. Immunomagnetic separation of target bacteria from food has been

employed with a variety of detection methods, including fluorescence methods [69], Surface Plasmon Resonance (SPR) [70], [71], and other biosensors [31], [45].

IMS has also been implemented in automated foodborne pathogen extraction systems. One study developed an automated IMS platform to extract and concentrate *E. coli* O157:H7 from contaminated milk [13]. The platform had a 20% capture efficiency and could concentrate target bacteria to 100 times its initial concentration with a total experimental time of 2 hr [13]. This automated system was also tested with an enzyme-based colorimetric assay for bacteria detection [72]. The combined extraction and detection assay was capable of detecting *E. coli* O157 in milk samples at concentrations as low as 3×10^2 CFU/mL [72].

One of the most notable advantages of IMS is its high selectivity; the use of antibodies allows for specific extraction of target bacteria and exclusion of natural microflora [44]. The method is also rapid in comparison to other techniques, with most sources successfully implementing the entire extraction procedure in under 2-3 hr. The separation process can also remove PCR inhibitors, reducing purification steps required before detection [14]. Finally, IMS allows for processing of large sample volumes. When the sample is resuspended in a low-volume solution, this can lead to significant concentration of the bacteria [13].

However, the presence of immunomagnetic beads in the concentrated sample introduces challenges for sample detection. For many common detection methods such as PCR, it is necessary to extract DNA from the concentrated sample. One paper tested the success of nine different DNA extraction kits on *B. anthracis* DNA extracted from apple juice, ham, whole milk, and bagged salad [14]. Only one of the 9 DNA extraction methods successfully detected *B. anthracis* using qPCR [14]. Immunomagnetic separation is also costly compared to conventional methods [16]. In addition to the cost of the experimental components themselves, antibody-MNP

complexes used in IMS are typically stored at 4 ºC until use [17], [66], [69]. This storage cost further increases the total cost of IMS and limits its potential use in low resource areas. Although this method could become more inexpensive through automation techniques currently being explored [13], the current cost does not permit its widespread implementation to detect foodborne pathogens.

Table 2.4 Recent advancements of chemical and biological methods for foodborne pathogen extraction.

Method	**Bacteria**	**Matrix**	**Capture**	**Source**
Zirconium titanium hydroxides	*S. enterica*	Pork sausage	N/A	[42]
Zirconium hydroxides	*S. aureus, V. parahaemolyticus, E. coli, E. faecalis*	Non-fat dry milk, pudding, coffee	99.97%*	[43]
Microsystem device with positive DEP	E. coli O157	Raw chicken	N/A	[41]
DEP with non-flow through biochips	*Salmonella* Typhimurium	Water	56-64%	[67]
Dielectrophoretic filtration	*E. coli* O157:H7, *L. monocytogenes*, *S.* Typhimurium, *S. aureus*	Water	85.71%**	[63]
Immunomagnetic Separation	*E. coli* O157:H7	Whole milk	20%	[13], [72]
Immunomagnetic Separation	*L. monocytogenes*	Soybean sprouts	1-10%	[73]
Immunomagnetic Separation	*E. coli* strains (STEC)	Unclarified apple juice	39-105%	[44]
Immunomagnetic Separation	*Salmonella* Typhimurium	Mixed vegetable salad, chicken, egg, minced pork meat	85-95%	[17]
Immunomagnetic Separation	*Salmonella* Typhimurium	Chicken, duck	88%*	[66]
*Data for pure bacterial cultures, no capture efficiency data available for food samples **Dielectrophoretic filtration efficiency (DFE)				

2.4 Glycan-Coated Magnetic Nanoparticles

2.4.1 Properties of Magnetic Nanoparticles

Nanoscale materials often exhibit physicochemical properties such as strength, magnetism, and chemical reactivity disparate from their macro scale properties [74]. MNPs in particular feature several properties that allow them to be used for countless applications in

health, science, and technological innovation [47]–[49], [75]. A variety of materials can be used to synthesize MNPs, including pure metals (Fe, Co, Ti, Ni), metal oxides, ferrites, and metal alloys. The most common MNP core materials are iron oxides, such as magnetite (Fe_3O_4) and maghemite (Fe_2O_3) [76], [77]. Several methods can be used to synthesize these nanoparticles, including coprecipitation, high-temperature thermal decomposition, hydrothermal processes, and microemulsion, among many others. Cardoso et al. [77] provides a comprehensive review of these synthesis methods and materials, as well as the many biomedical applications of MNPs.

As noted previously, MNPs have several advantageous and unique properties that contribute to their widespread applicability. One significant characteristic of MNPs is their superparamagnetic properties, meaning they have no net magnetization and do not aggregate without application of an external magnet [26]. This property typically emerges at a particle size of 10-20 nm, and MNPs of this size can rapidly disperse through liquid and also be manipulated by an external magnet [26], [78]. Thus, MNPs can be suspended in solutions for bacterial capture before separation from the supernatant using a magnet [22], [79]. They can also be utilized for efficient capture of other elements, including nucleic acids and proteins [80].

Another attractive MNP property is their high surface area to volume ratio. This trait leads to a potentially high capture efficiency for target cells due to the high adsorption capacity [74]. Typically, MNPs are also much smaller than bacterial cells. As a result, multiple particles can often attach to a single cell, potentially increasing the probability of bacterial capture. Multiple studies have demonstrated this behavior through microscopic imaging [20], [26]. TEM and confocal laser microscope images captured in the Nano-Biosensors Laboratory have also demonstrated this behavior (Figure 2.1).

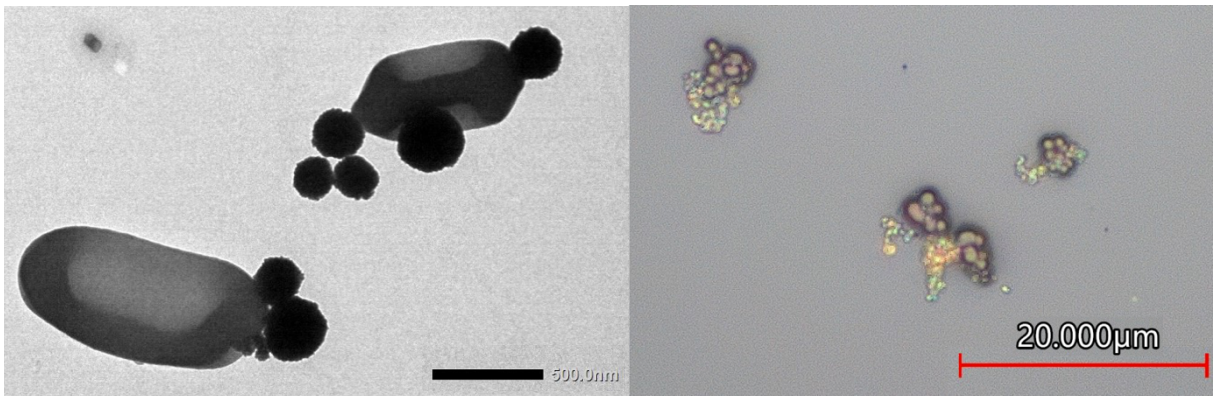

Figure 2.1 (A) TEM image of multiple MNPs bound to *Listeria* cells; (B) confocal laser microscope image of multiple MNPs bound to clusters of *S. aureus* cells.

2.4.2 Surface coating

A wide variety of materials can be used as MNP coatings for stabilization, modification, or introduction of active groups [16], [79]. In order coat the MNP surface, physical adsorption or covalent bonding is commonly used to produce a "core-shell" formation [81]. While the metallic core of MNPs determines the magnetic properties, surface coatings can be used to control MNP selectivity and other application-specific characteristics. Common MNP coatings include surfactant molecules, silica, and colloidal gold [81]. Glycans, or complex carbohydrates, are another common MNP coating. As reviewed by Fratila et al. [82], this coating can be achieved during MNP synthesis or as a post-synthetic functionalization step. During MNP synthesis, glycan coatings are accomplished through the presence of carbohydrates as the nanoparticles are synthesized, which allows for ligand adsorption onto the MNP surface. For post-synthetic methods, introduction of functionalized carbohydrates to the MNP surface is accomplished by ligand exchange, covalent linking, or non-covalent functionalization [82]. For applications involving bacterial capture, many glycans have been employed as MNP coatings, including mannose, galactose, fucose, and chitosan [20], [29], [83]. Further modification of the glycan-coated MNPs may include the addition of other materials, such as amino acids [27], [30].

Glycans play an essential role in many cellular mechanisms such as cell-cell interaction and bacterial infection [23]. These interactions often occur between surface proteins (e.g., lectins) and glycans [84], [21]. Uropathogenic *E. coli*, for instance, has FimH proteins localized to the tip of their pili that target the glycan mannose on urinary epithelial cells [85]. In addition to their role in bacterial infection, glycan interactions between neighboring cells play a role in the formation of bacterial biofilms [86]. Glycan-protein interactions are electrostatic and non-covalent, often consisting of van der Waals interactions and hydrogen bonds. The hydrogen bonds may specifically occur between hydroxyl and amino groups present on the carbohydrate and microbial protein surface [24], [25].

Due to their prevalence in natural biological processes, researchers have explored utilizing these protein-glycan interactions to extract and detect bacterial cells. Bacterial lectins typically have broad specificities for complex carbohydrates [25]. Therefore, glycan-coated MNPs can mimic the role of cell surface glycans and adhere to a proteins on various bacteria cells through non-covalent electrostatic interactions [22], [23]. After adhesion occurs, the superparamagnetic nature of MNPs allows for rapid extraction of the MNP-bacteria complexes with the application of an external magnetic field [29]. Extraction and concentration of bacteria using glycan-coated MNPs has been successfully employed for many applications. For instance, one author utilized chitosan-coated iron oxide nanoparticles to concentrate *Mycobacterium* tuberculosis from sputum [29]. The magnetically activated cell enrichment allowed for rapid detection of the bacteria with a colorimetric biosensing assay in only 20 min, with a total cost of only $0.50/test [29]. Glycan-coated MNPs have also been employed to capture bacteria such as *Helicobacter pylori* [83] and *Pseudomonas aeruginosa* [87], among many others.

Nonspecific capture of bacterial cells by glycan-coated MNPs may also be enhanced by the positively charged nature of some glycan coatings. Both Gram-positive and Gram-negative bacteria have a net negative charge under physiological conditions, primarily due to negative cell wall components such as teichoic acids and lipopolysaccharides [60], [88], [89]. As glycans must be in close proximity to bacterial lectins to achieve adhesion, generalized electrostatic attraction between these oppositely charged components may promote bacterial capture [28]. This generalized electrostatic attraction is often improved through the addition of amino acids to the MNP coating and is theorized to play a role in many glycan-coated MNP applications [27], [29], [30].

2.4.3 Glycan-Coated Magnetic Nanoparticles for Foodborne Pathogen Extraction

For MNP-based food pathogen extraction, most studies follow similar methodologies for bacterial extraction regardless of the surface coating [17], [26], [27], [70], [90]. This generalized method is demonstrated in Figure 2.2. First, MNPs are added to a liquified food sample contaminated with one or more bacterial species. Once MNPs have dispersed throughout the liquid, sample incubation allows MNPs to adhere to target cells. Incubation times often vary from as little as one minute to up to an hour, depending on the MNP surface coating and specific methodology. After incubation is complete, application of an external magnet concentrates the MNP-bacteria complexes. The supernatant is then removed and the remaining sample is re-suspended. Some procedures call for washing steps to remove remaining food matrix components, and many re-suspend the MNPs in a lower volume for bacterial concentration. Detection methods, including biosensors or PCR, can then be implemented [17], [27], [70], [90].

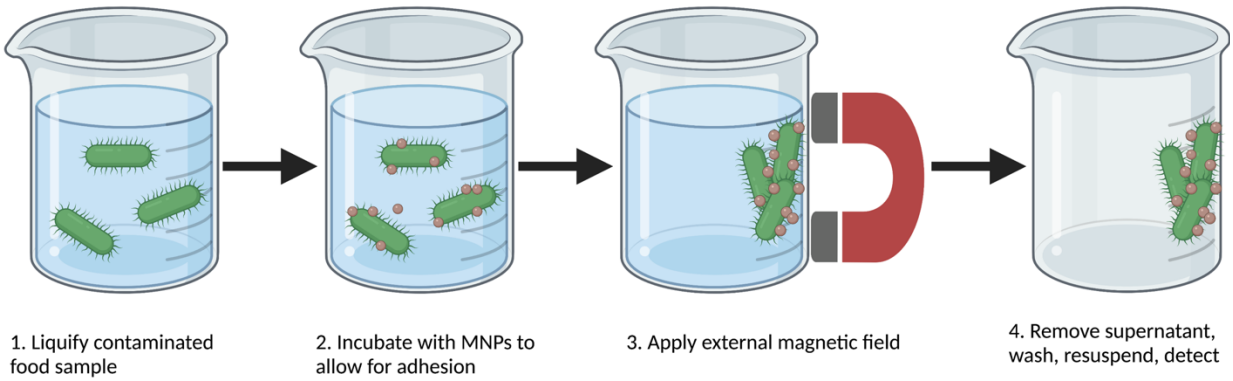

Figure 2.2 Overview of magnetic separation of bacteria from food samples (created with Biorender).

Multiple studies have successfully utilized glycan-coated MNPs for direct capture and concentration of bacteria from food matrices. One study utilizing two unspecified glycan coatings on MNPs successfully extracted *Salmonella* Enteritidis*, Escherichia coli* O157:H7*,* and *Bacillus cereus* from milk samples [26]. MNPs were added to 25 mL milk samples before inoculation with bacteria concentrations between 2.9 and 4.5 log CFU/mL. After 10 min of room-temperature incubation, the sample was mixed and magnetically separated. Supernatant removal was followed by resuspension in 1 mL of milk. The method was successful for all three bacterial species, with capture efficiencies ranging from 73-90% on a log scale. In addition, simultaneous capture of all three bacterial species was successful, with similar capture efficiencies [26]. Another author co-crystallized short chain glucans (SCGs) with dextran coated iron oxide nanoparticles for extraction of *E. coli* O157:H7 cells from liquified sausage [27]. The resulting glycan-MNPs were also functionalized with lysine, a positively charged amino acid, to ensure the MNPs had a positive surface charge. After 10 min of suspension in pure bacterial samples, the MNPs had successfully captured 90% of the bacteria cells. In sausage samples, extraction and concentration was combined with a colorimetric biosensor. The combined method had a limit of detection of 30.8 CFU/mL with 95% confidence [27].

While the aforementioned glycan coatings were used for nonspecific bacterial capture, specificity can also be achieved through the design of specific carbohydrate epitopes. For example, one study designed biotinylated oligosaccharides immobilized to streptavidin-coated magnetic beads to selectively capture *E. coli* strains containing the *pap* pilus genotype [65]. MNPs were incubated in PBS containing bacteria samples for 1 hr before magnetic separation. The glycan-coated MNPs were highly specific to the *pap*-containing uropathogenic (UPEC) strains when compared to three *E. coli* strains without the *pap* pilus genotype. A BacTiter-glo assay substrate was used to quantify capture efficiency, which was found to be 17-34% for the three target *E. coli* strains [65].

Although most glycan-coated MNP extraction methodologies follow the strategy outlined in Figure 2.2, other methods have also been explored. In one study, cysteine-glycan coated iron oxide MNPs were affixed to plastic strips and inserted into the liquid food sample, as opposed to being directly suspended in the solution [30]. The MNP-coated strips were suspended in the matrix for 10 min before use in a cyclic voltammetry detection method. This procedure was successfully performed with homogenized egg, vitamin D milk, and apple cider inoculated with *Salmonella* Enteritidis*, Escherichia coli* O157:H7*,* and *Listeria monocytogenes.* This combined extraction and detection method distinguished between target samples and negative controls with 95% confidence [30].

These carbohydrate functionalized MNPs have several key advantages over many other methods, particularly their low cost. For instance, one study noted that their glycan-coated MNP assay was 25% the cost of a comparable antibody-based assay [26]. Furthermore, glycan-coated MNPs do not require special storage conditions, further reducing overall expenses when compared to IMS [21]. One study, for example, observed the stability of iron oxide MNPs coated

in alginate or chitosan and suspended in buffer solutions [48]. After 6 months of storage at room temperature, the researchers found no evidence of flocculation or settling in the samples. These storage conditions further emphasize the low cost of this technique, as well as its accessibility in low-resource settings. Finally, glycan-coated MNP assays typically have shorter incubation times with target bacteria than IMS, with many methods only requiring 5-10 min [26], [20]. Thus, the economical and efficient nature of glycan-coated MNPs for foodborne pathogen extraction are key advantages. Applications of glycan-coated MNPs for extraction and concentration of foodborne pathogens are summarized in Table 2.5.

Table 2.5 Glycan-coated MNPs for extraction and concentration of foodborne pathogens.

Coating	**Bacteria**	**Matrix**	**Capture**	**Detection Method**	**Source**
Glycan (not specified), cysteine-glycan	*S.* Enteritidis, *E. coli* O157:H7, *B. cereus*	Milk (vitamin D, reduced fat, fat-free)	73-90%*	N/A	[26]
Cysteine-glycan	S. Enteritidis, *E. coli O157:H7, L. monocytogenes*	homogenized egg, vitamin D milk, apple cider	N/A	Cyclic voltammetry	[30]
Lysine-SCGs	*E. coli* O157:H7	Sausage	>90%**	Colorimetric biosensor	[27]
Biotinylated oligosaccharides	*E. coli* (UPEC)	PBS	17-34%	N/A	[65]
Mannose Galactose	*E. coli* strains (3)	PBS	10-65% 15-75%	BacTiter-glo assay	[20]

SCG: Short chain glucan
*log basis
** Data for pure bacterial cultures, no capture efficiency data available for food samples

Despite its low cost and experimental duration, the nature of glycan-coated MNPs may lead to complications in complex food matrices. Due to their similar chemistries, glycans can also electrostatically bind to carbohydrate elements of the food matrix [30]. This may result in issues with subsequent pathogen detection, depending on the method employed. In addition, most glycan coatings tested in foods are non-specific [26], [30], [27], which could potentially

cause complications in matrices with high levels of natural microflora. However, the current primary drawback to glycan-coated MNP separation from food is the limited research. Although extraction of foodborne pathogens from pure cultures is described in some studies [20], [65], aforementioned papers by Matta & Alocilja [26] and You et al. [27] were the only research found describing direct bacterial extraction from food using glycan-coated MNPs.

2.5 Current Food Pathogen Detection Methods

2.5.1 Immunological Assays

Immunological assays for detection of foodborne pathogens rely on antibody-antigen interactions, in which a selected antibody will bind to a specific antigen present on the target cells [6]. These methods can use both monoclonal and polyclonal antibodies, with monoclonal antibodies allowing for increased sensitivity and specificity as they are composed of a single antibody [91]. One of the most common immunological methods for this application is the enzyme-linked immunosorbent assay (ELISA), which utilizes an antibody attached to a solid matrix that will bind to the target antigen if present in an enriched culture [92]. Then, an enzyme substrate is used to visualize the presence of bound targets [93]. ELISA has been used for detection of bacteria extracted from foods on many occasions, with one study successfully detecting *Salmonella enterica* from a variety of food matrices with 100% sensitivity and 81% specificity [11]. Although more rapid than traditional culture methods, the assay did include a 48 hr culture of contaminated samples before detection. This need for cultural enrichment due to low sensitivity is common among ELISA techniques in food pathogen detection [92].

Lateral flow assays (LFAs) offer a more cost-effective alternative to ELISA. These assays are on simple test strips composed of several overlapping membranes, with successful

capture of the target antigen typically indicated by the presence of a colored line on the strip [37]. These assays can be useful tools for on-site and rapid testing. For example, one report detailed the design and implementation of a handheld multiplexed LFA that successfully detected *E. coli* O157 and *Salmonella* Typhimurium directly from liquified lettuce at concentrations of approximately 10^4 CFU/g [94]. This high limit of detection hinders its use for sensitive detection of pathogens in foods; however, a 6 hr incubation could reduce detection limits to as low as 1 CFU/g. With the LFA itself capable of producing results in only 22 min, sensitive and accurate detection could be accomplished within a single work day [94].

Immunological assays show promise as a rapid method for food pathogen detection. However, ELISA techniques typically require specialized personnel and equipment, reducing its accessibility [6]. Although lateral flow assays are far more accessible and cost-effective, they often have a potential for false positives due to non-specific binding and typically can only be used for qualitative detection [37], [95]. Yet advancements in immunological assays are continuing to address these concerns. For instance, one study incorporated SERS with an LFA, leading to a detection limit as low as 75 CFU/mL for *L. monocytogenes* and *Salmonella* Typhimurium [96]. With further work, these immunological techniques may eventually balance low cost and accessibility with high sensitivity and rapid results.

2.5.2 Nucleic Acid-Based Methods

Nucleic acid-based methods for foodborne pathogen detection target DNA or RNA sequences specific to the pathogen of interest [7]. Most common among the nucleic acid-based methods is polymerase chain reaction (PCR). In this method, a target DNA sequence is amplified in a three-step process utilizing single strand DNA primers that anneal to DNA after denaturing

of target DNA at a high temperature [91]. After amplification, results are visualized on electrophoresis gel using stains such as ethidium bromide or SYBR Green [6], [93]. Advancements in PCR have led to more rapid and robust variations of this technique as well. Multiplex PCR (mPCR), for instance, allows for simultaneous detection of multiple targets by using multiple sets of primers [95]. Quantitative or real-time PCR (qPCR), offers the advantage of simultaneous detection and quantification of PCR products through the use of fluorescent molecules [93], [97]. Thus, results can be analyzed more quickly, and electrophoresis gel is not required.

These PCR techniques have been widely applied for rapid food pathogen detection. In one paper, the authors utilized real-time PCR to detect 12 different foodborne pathogens, including *E. coli* O157:H7, *S. enterica*, and *S. aureus* [97]. For detection from artificially inoculated minced meat samples, the matrix was homogenized with PBS before direct DNA extraction of 1 mL of the homogenate. The researchers were able to detect bacterial concentrations in the food samples as low as 10^3-10^4 CFU/g with only a 1 hr detection assay duration [97]. PCR methods are also often integrated with other techniques to increase sensitivity. For instance, one study combined magnetic separation, mPCR, and capillary electrophoresis for detection of *Staphylococcus aureus*, *Escherichia coli* O157.H7, *Salmonella* Typhimurium, and *Listeria monocytogenes* directly from artificially contaminated food matrices [98]. With a total detection assay time of 2.5 hr, this method had a limit of detection as low as 10^1 CFU/mL from contaminated samples of milk, pears, chicken sausage, and biscuit.

In recent years, other nucleic acid detection methods have also been developed that do not require thermal cycling conditions. Loop-mediated isothermal amplification (LAMP), for instance, can result in 10^6-10^9 copies of target DNA in under an hour [99]. This PCR alternative

is low-cost and easy to operate; in addition, it maintains the high sensitivity and specificity typical of nucleic acid-based methods [6], [100]. Other isothermal nucleic acid amplification options include nucleic acid sequence-based amplification (NASBA), rolling circle amplification (RCA), and strand displacement amplification (SDA) [91]. These options could potentially increase the accessibility of nucleic acid-based foodborne pathogen detection methods.

Nucleic acid methods offer key advantages for foodborne pathogen detection, including high specificity and sensitivity with a short assay time. In addition, techniques such as mPCR allow for detection of multiple pathogens simultaneously, increasing their real-world applicability. However, nucleic acid methods also typically require trained personnel and costly equipment [8]. Although the cost and equipment requirements of many PCR techniques are resolved by isothermal methods such as LAMP, these methods offer their own difficulties and limitations, such as complex primer design [6]. In addition, food matrix components can often interfere with PCR, leading to added pre-processing steps or higher limits of detection [95], [98].

2.5.3 Biosensing Techniques

Biosensors are analytical devices that utilize biological or biochemical reactions to detect target analytes and convert the results into measurable signals [38], [101]. Biosensors can be classified by several different methods, including their data output system, target analyte, or label dependence [91], [102]. For the purposes of this brief overview, biosensors classified as optical and electrochemical based on their overall mechanism with be discussed. However, a variety of other biosensing techniques have been used to detect foodborne pathogens, including cyclic voltammetry [30], fluorescence methods [20], and quantum dot biosensors [101], as well as

colorimetric gold nanoparticle biosensors [31], which will be discussed separately in the following section.

One of the most common types of biosensors for foodborne pathogen is optical biosensors, with commercialized systems also available [103]. These biosensors are highly sensitive and label-free, but they are often associated with a high cost [6]. Surface Plasmon Resonance (SPR) is one type of optical biosensor which uses refractive index measurements to measure the binding of an analyte to its ligand in real time [104]. These biosensors often rely on antibody-antigen interactions for target detection, similar to immunological assays [105]. For instance, one study reported the use of an SPR biosensor for detection of *E. coli* and *Salmonella* spp. from cucumber and hamburger samples in under 80 min [106]. The system was incredibly sensitive to *E. coli*, with a limit of detection as low as 17 CFU/mL for *E. coli* in hamburger. However, detection limits for *Salmonella* were above 10^3 CFU/mL [106].

Electrochemical biosensors are another detection option for foodborne pathogen detection. In these biosensors, the bio-recognition element is fixed to an electrode which detects the recognition of the target analyte and converts this into an electrical signal [12]. These biosensors are typically categorized by the produced electrical signal, with some classifications including impedimetric, potentiometric, electrochemiluminescent, and conductometric methods [38]. One author successfully designed an impedimetric biosensor for detection of *S.* Typhimurium using screen-printed electrodes (SPE) [107]. With an assay time of only 30 min, the label-free biosensor was capable of detecting the target bacteria at concentrations as low as 10^1 CFU/mL and was highly specific to *S.* Typhimurium [107].

Although a wide variety of biosensors are currently under development, they often share some advantages for foodborne pathogen detection. As shown in the studies discussed,

biosensors are incredibly rapid and often highly sensitive to their target pathogen. In addition, biosensors typically do not require highly trained personnel, unlike conventional nucleic acid-based methods [95]. These key characteristics enhance the applicability of biosensors for use in low-resources areas or for on-site detection. However, sensitivity to low levels of microorganisms is still a challenge for many electrochemical biosensors [12]. Meanwhile, optical biosensors have higher sensitivity but also higher costs, reducing their accessibility [6].

2.6 Gold Nanoparticle Biosensors

2.6.1 Synthesis and Properties of Gold Nanoparticles

GNPs feature many properties typical of nanomaterials, such as a high surface area to volume ratio, that improves their performance in analyte capture and sensing applications [108]. In addition, GNPs are chemically stable and easily modified with biomolecules for biosensor applications [109], [108]. These nanoparticles also have relatively simple preparation methods, with the most common synthesis routes being the Turkevich-Frens and Brust-Schiffrin methods [110]. The Turkevich-Frens method utilizes sodium citrate to produce spherical GNPs in a single-phase metal salt redox reaction [111], [112]. Meanwhile, the Brust-Schiffrin method is a two-phase reduction reaction utilizing a thiolate for stabilization [110], [113]. Seeding/growth assays have also gained popularity in recent years due to their simplicity and versatility [111]. A comprehensive review of current GNP synthesis methods is detailed by Zhao et al. [110].

In addition to the aforementioned advantages of GNPs, they also feature unique optical properties. Colloidal GNP solutions have free electrons whose coherent oscillation produces a strong SPR band [111]. This SPR band is strongly distance-dependent, meaning aggregation of the nanoparticles will lead to a visible color change [109]. Small and dispersed gold

nanoparticles will appear red in color, with a peak absorbance around 520 nm, while aggregated particles will absorb higher wavelengths, leading to a visible color change to blue or purple [114]. As a result of these properties, GNPs have been utilized in a variety of biosensing techniques, including fluorescence sensing [109], SERS [108], electrochemical biosensing [115], and colorimetric detection [32].

2.6.2 Gold Nanoparticles for Colorimetric DNA Detection

Colorimetric GNP biosensors can be implemented to detect a wide variety of targets, including DNA, proteins, antigens, and other small molecules [109], [111], [116]. Most methods rely on introduction of a ligand to the GNP surface that will bind to the target; however, some methods do exist that rely on the intrinsic interactions between the GNP surface and the molecule of interest [111], [117]. Regardless of the functionalization, colorimetric GNP biosensors rely on the previously described optical properties of GNPs, in which an increase in particle size or aggregation leads to a visible color change [114]. Detection of DNA using GNPs conjugated with oligonucleotide probes was first explored in 1996, when researchers attached DNA oligonucleotides capped with thiol groups to the surface of GNPs [118]. This thiol-gold chemistry is still the most common method for functionalization of GNPs with DNA probes [109], [119]. The oligonucleotide probe is specific to the target genome and will therefore adhere to the target DNA when subjected to denaturation temperatures, followed by hybridization temperatures [33].

As mentioned previously, GNP colorimetric biosensors are dependent upon the aggregation of GNPs leading to a visible color change of the solution. However, methods utilizing DNA probes typically follow two separate overarching methodologies: assays with

target sample aggregation (TA), and assays leading to aggregation of non-target samples (NTA). NTA biosensors typically use one probe sequence attached to GNPs that will bind to target DNA [119]. Nanoparticle aggregation and the resulting color change is achieved through the addition of salt after DNA hybridization has occurred. GNP-probe complexes attached to target DNA are protected and remain red in color, while samples with no or non-target DNA will aggregate and turn purple or blue [31], [32].

TA biosensors can proceed through multiple approaches. The first involves a crosslinking assay, which uses two probes attached to GNPs that will form a polymeric network with target DNA [119]. The formation of this polymeric network will lead to GNP aggregation and a color change; thus, target samples will turn blue while non-target samples remain red. For other TA methods, GNPs are typically not functionalized with the DNA probe before addition of a DNA sample [33]. As a result, target DNA will hybridize to the probe upon heating, leaving the GNPs exposed. However, samples without target DNA will not hybridize to the probe, and the unhybridized probe will adsorb to the GNP surface [33], [120]. Therefore, GNPs in the target samples are left unprotected and will aggregate upon the addition of a salt, while non-target samples are protected and remain red in color. This typical mechanism of non-functionalization TA methods is compared to NTA methods in Figure 2.3.

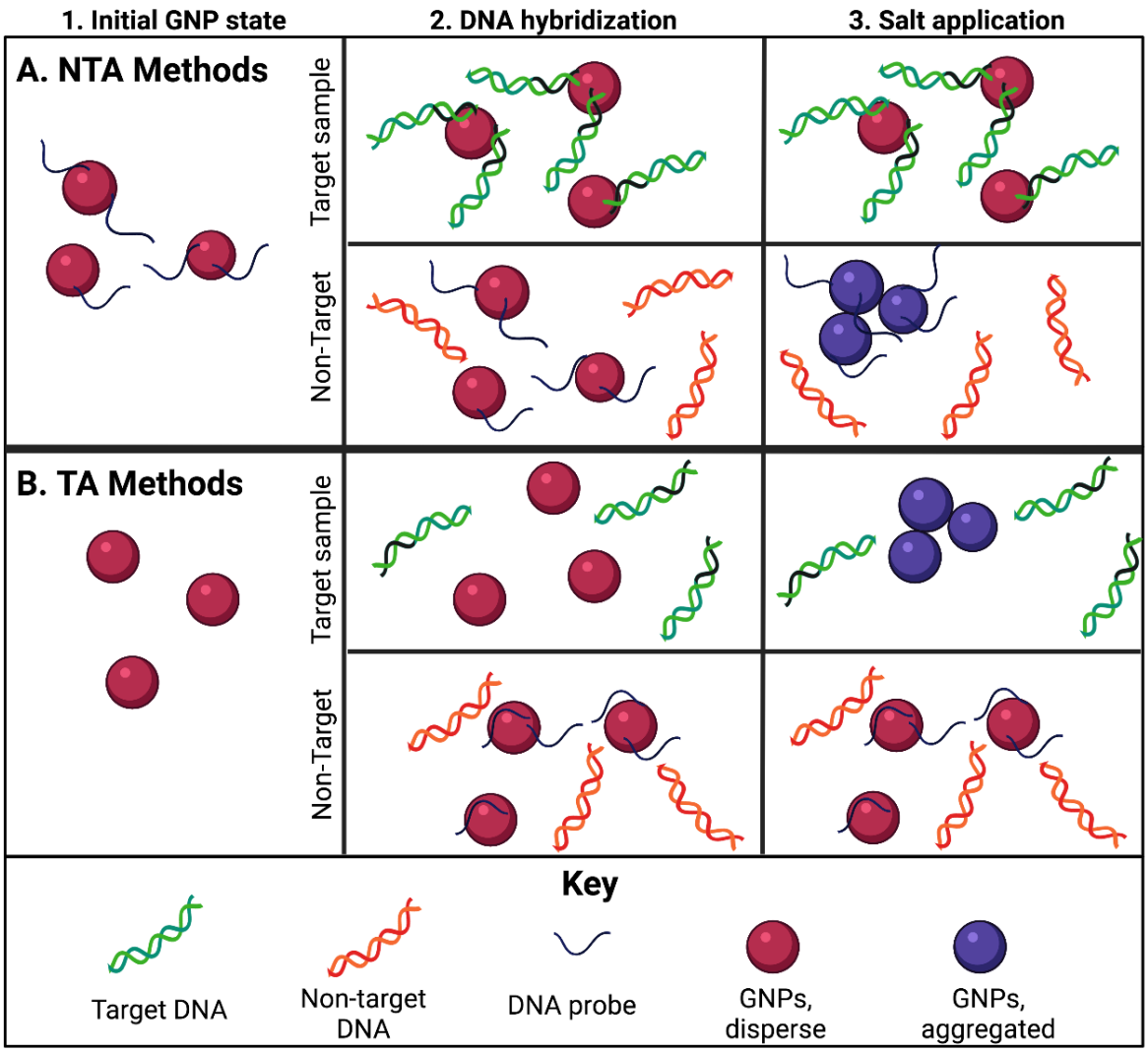

Figure 2.3 Comparison of NTA colorimetric GNP biosensors to non-functionalized TA biosensors (created with Biorender).

2.6.3 Food Applications of Gold Nanoparticle Colorimetric Biosensors

Colorimetric GNP biosensors have been utilized for detecting a variety of targets, including illicit drugs [121], protein biomarkers for cancer [114], and viral DNA [119]. However, this brief overview will specifically focus on DNA detection of foodborne pathogens or other components within food matrices. Both TA and NTA assays have been successfully developed for foodborne pathogen detection. For instance, one TA biosensor was capable of detecting concentrations of *Klebsiella* Pneumoniae as low as 9 pg/µL in under an hour [33].

Similarly, one NTA method detected uropathogenic *E. coli* strains in pure culture with a limit of detection of 9.4 ng/μL, with a total detection assay time of only 30 min [32]. NTA assays have also been conducted in food matrices, with one author detecting 10 CFU/g of *Salmonella* spp. in inoculated blueberry and chicken samples through pre-treatment with IMS and 6 hr of sample incubation [31].

These biosensors have also been implemented for direct detection of food matrix components. In one study, DNA was extracted from 100 mg of meatballs composed of various meat products, and the DNA was used in a TA assay. The oligonucleotide used in this study was for pork DNA, and it was capable of detecting the presence of pork in the meatballs when 20% or more of the total meatball weight was from pork [120]. This report demonstrates another application of GNP biosensors for rapid detection of adulterated food products. Similar GNP-based biosensors with added electrochemical components have been capable of higher sensitivities, detecting pork concentrations of 10% by weight [122].

Colorimetric GNP biosensors still face some challenges as a foodborne pathogen detection mechanism. For instance, applications in food matrices may require additional pre-treatment steps and culturing for bacteria to reach detectable levels [31]. In addition, for NTA assays, GNP functionalization with the oligonucleotide probe can take several days, increasing the required labor for this assay [31], [32]. DNA extraction can also potentially increase experimental cost due to the need for extraction kits; however, a simple boiling method for DNA extraction can eliminate this need and has been proven viable for use in a DNA biosensor [33]. Despite these challenges, GNP colorimetric DNA biosensors demonstrate several key advantages. In particular, the cost-effectiveness and small size of these biosensors increases their accessibility [114], [119]. The colorimetric nature of the biosensor itself is also noteworthy; as

results are visually detectable, the presence of a pathogen can potentially be determined without costly analytical equipment. Unlike other GNP-based biosensors (impedimetric assays, SPR, and SERS), analytical tools such as spectropolarimeters and spectrometers can be eliminated from the biosensing system [106], [123]–[125]. Another advantage of these biosensors is their rapidity, with DNA-based detection typically accomplished in under one hour [32], [114]. Thus, the rapid and cost-effective nature of this technique indicates its future potential as a foodborne pathogen biosensing method.

Table 2.6 Gold nanoparticle biosensors for detection of foodborne pathogens or food components.

Method	**Target DNA**	**Matrix**	**LOD**	**Reference**
NTA	*Salmonella* spp. strains (19)	Inoculated chicken and blueberry samples	<10 CFU/g	[31]
NTA	Uropathogenic *E. coli* (UPEC)	Pure culture, spiked urine	54 ng	[32]
TA	*Klebsiella* Pneumoniae	Pure culture	9 pg/µL, or 15 x 10^5 CFU/mL	[33]
TA	Pork	Meatballs	20% pork samples	[120]

2.7 Conclusions and Knowledge Gaps

Current methods for bacterial capture and concentration from foodborne pathogens have demonstrated significant advantages over the traditional culture method. Many of the techniques discussed in this review, including dielectrophoresis, centrifugation, filtration, and MNP-based methods have successfully concentrated bacteria from foods to detectable levels without the need for cultural enrichment. Further, the short assay times and cost-effectiveness of these methods enhance their applicability. However, the physical methods discussed still face challenges with rapid removal of the food matrix and lack the potential for targeting specific bacterial species. Similarly, many chemical methods have their own challenges. For instance, studies using dielectrophoresis typically have high limits of detection in their subsequent biosensing assay.

Meanwhile, metal hydroxides lack specificity and require a cultural enrichment step before detection. Although IMS has been widely successful, the lack of standardization and high experimental cost are limiting factors.

Glycan-coated MNPs offer a cost-effective alternative to antibody-based magnetic separation. Their low-cost and room-temperature storage conditions, along with the potential for specificity, demonstrate their potential for rapid and cost-effective foodborne pathogen extraction. However, there are still few published works on extraction of bacteria directly from food matrices using glycan-coated MNPs. In addition, the variability of glycan coatings and experimental methods in these studies increases the difficulty of fully analyzing their potential. Due to this lack of standardization between studies and the limited research available, few sources fully hypothesize the mechanism of bacterial adhesion. Although literature sources in this review describe many elements of the mechanism, some details of the process are still unclear. Further research must be conducted to both confirm existing elements of this theory and discover new potential factors. A deeper understanding of this mechanism, as well as the factors that can improve adhesion, could improve optimization and standardization of glycan-coated MNP separation.

Many rapid methods have been explored to replace traditional foodborne pathogen detection assays. The most widely used PCR assays, however, often require costly equipment and skilled technicians for successful detection. Although some immunological assays can significantly lower costs, they often have higher limits of detection. Meanwhile, several types of biosensors have been shown to achieve specificity and sensitivity, although cost and sample preparation requirements widely vary. In particular, GNP colorimetric biosensors have shown immense promise as a rapid detection technique that can eliminate the need for high-cost

equipment. These biosensors have been successfully implemented for a wide variety of applications, from illicit drug detection to cancer screening. However, there are limited studies performed with DNA extracted directly from food, and short culture times are still necessary. In addition, NTA assays typically require overnight processes to achieve GNP functionalization with a DNA probe. Thus, further research must be conducted into reducing the duration of preparatory steps, as well as determining its effectiveness in detection of bacteria extracted from food. With these advancements, GNP colorimetric biosensors can become an accessible and rapid detection method for foodborne pathogens.

Chapter 3: Glycan-Coated Magnetic Nanoparticles for Foodborne Pathogen Extraction

3.1 Introduction

Foodborne illnesses can be caused by a variety of pathogens with a multitude of infectious consequences, ranging from mild illness to hospitalization and death. For instance, although primarily associated with nosocomial infections [126], *S. aureus* is also a cause of toxin-related food poisoning [127]. Foods can be contaminated through interaction with animals or farm workers, as well as human handling of foods during preparation [128], [129]. Consumption of contaminated foods can lead to gastroenteritis, vomiting, diarrhea, and other severe symptoms [127]. Meanwhile, Shiga-toxin producing *E. coli* (STEC), often *E. coli* O157, is a common foodborne pathogen that is increasing in prevalence, with over 3,000 recorded U.S. cases in 2019 [130]. Although serious symptoms are rare, it can cause hemolytic uremic syndrome which can lead to acute renal failure, particularly in children [131]. *Listeria* spp., specifically *L. monocytogenes*, is another dangerous foodborne bacteria species. Although less common than STEC, illness often has fatal results in high risk groups such as the elderly, immunocompromised, children, and pregnant women [132]. For instance, of the 134 U.S. *Listeria* cases reported in 2019, 98% of these individuals were hospitalized, and 21 cases ended in death [130]. Listeriosis is a global problem as well, with one 2017-2018 outbreak in South Africa leading to 1060 laboratory-confirmed cases and 216 deaths [133].

These pathogens are commonly implicated in ready-to-eat foods or fresh fruits and vegetables, meaning they are not typically cooked by consumers to sufficient temperatures for bacteria death to occur [4], [129], [132]. As a result, it is essential that these pathogenic bacteria species are detected before reaching the consumer to prevent infection, illness, and death. Traditional concentration methods relying on bacterial culture often require 24-48 hr of

incubation in selective media [15]. Thus, rapid extraction methods have been explored to enhance detection, including centrifugation [39], [40], filtration [40], dielectrophoresis [41], and magnetic nanoparticles (MNPs) [26], [29], [44], [45]. However, as discussed previously, many of these methods have challenges with specificity, cost, and efficiency when implemented in food matrices (Table 2.1 & 2.3).

Glycan-coated MNP extraction offers a potential alternative to many current methods. Although similar in mechanism to IMS, glycan-coated MNP extraction relies on glycan-protein interactions for bacterial capture instead of antibody-antigen interactions. As a result, this method has a reduced cost and simplified storage conditions when compared to IMS [16], [17], [48], [66], [69]. However, limited research has been conducted with glycan-coated MNPs for foodborne pathogen extraction, and aspects of the bacterial adhesion mechanism have not been fully confirmed (Section 2.4). Thus, additional research must be conducted to determine its applicability and efficiency for bacterial concentration directly from food matrices.

MNPs coated with the glycan chitosan were used in this study to extract foodborne bacteria species from 100 mL liquid samples. Results were quantified using colony counts of plated samples, through which the MNP-treated bacterial concentration was compared to a control. Factors affecting bacterial capture, such as bacterial species, initial bacterial capture, and solution pH were analyzed through pure culture studies, and microscopic imaging was used to visualize MNP-bacteria adhesion. Several potential factors for optimization were identified, including solution pH and MNP net charge. This analysis also provided further evidence of successful glycan-protein binding. Finally, extraction experiments directly from four food matrices were completed for each bacterial species, with foods selected based on foodborne outbreak data. Results indicate viable capture of target cells from all matrices studied, with

successful concentration of target bacteria from several foods. As an initial design, this foodborne extraction assay is a cost-effective and rapid bacterial concentration method that can be applied directly to food matrices with a large sample volume.

3.2 Materials and Methods

3.2.1 Materials

Bacterial strains of *E. coli* O157:H7, *S. aureus* (ATCC 12600), and *Listeria* spp. (strain J1-101) were obtained from frozen cultures in Dr. Evangelyn Alocilja's Nano-Biosensors Laboratory of Michigan State University (MSU). Chitosan-functionalized magnetic nanoparticles (100-200 nm in diameter) were used as prepared. Hydrochloric acid (ACS reagent, 37%), Tryptic Soy Agar (TSA), Tryptic Soy Broth (TSB), Oxford Agar (OA), and Oxford Listeria Supplement were purchased from Sigma Aldrich (St. Louis, MO). Phosphate Buffer Solution (PBS), pH 7.4, was also purchased from Sigma Aldrich and prepared as directed. CHROMagar for *E. coli* O157 and *S. aureus* were purchased from DRG International (Springfield, NJ). Sodium Hydroxide (NaOH) pellets were purchased from VWR International (Radnor, PA) and prepared as directed.

Gram staining material (Gram Iodine, Gram's Safranin Solution, ethanol, and Crystal Violet) was purchased from VWR International (Radnor, PA). Glutaraldehyde, cacodylate buffer, and uranyl acetate stain used for TEM were provided by the MSU Center for Advanced Microscopy (CAM). TEM grids (formvar/carbon 200 mesh copper) were purchased from Electron Microscopy Systems (Hatfield, PA).

Whirl-Pak bags (92 oz. and 18 oz.) were purchased from VWR International. Magnetic racks, SpheroTech Fleximag Separators, were purchased from Spherotech Inc (Lake Forest, IL).

Spinach, romaine lettuce, milk, flour, precooked sausage, deli ham, and chicken salad were purchased from a local seller. All food materials were stored at 4 ºC before use, excluding flour which was stored at room temperature.

3.2.2 Microscopic Imaging

Microscopy was used to examine individual interactions between magnetic nanoparticles and bacterial cells. Both Transmission Electron Microscopy (TEM) and a confocal laser microscope were used to visualize these interactions. Confocal laser microscopy was performed in the Nano-Biosensors Laboratory using a Keyence VK-X1000 3D Scanning Confocal Microscope. TEM was achieved at MSU CAM using the JEM-1400Flash, with an LaBC6 crystal electron source operated at 100 KV.

For TEM imaging, 2-3 colonies grown on an overnight TSA culture plate were suspended in 0.9 mL PBS. Then, 100 µL of MNPs were added to the sample, mixed, and incubated at room temperature for 5 min to allow for binding. Next, the samples were subjected to magnetic separation for 1 min. After supernatant removal, the sample was resuspended in 100 µL of 2.5% glutaraldehyde in 0.1 M cacodylate buffer. Then, 5 µL of the MNP-bacteria solution was dropped onto the black side of a grid for 20-30 s before washing with 5 µL distilled water. After being dried with filter paper, 5 µL of 0.1% uranyl acetate stain was added. Excess stain was removed after 5-10 s and allowed to air dry before being loaded into the TEM specimen holder. Images were taken in the range of 5000-25000 x magnification.

For confocal laser microscope imaging, 1 mL overnight cultures of each target pathogen were centrifuged at 8000 rpm for 5 min and resuspended in sterile water. Then, 100 µL of MNPs were added to the sample, mixed, and allowed to incubate for 5 min. Tubes were then

magnetically separated with a magnetic rack for 1 min before supernatant removal and re-suspension in 1 mL sterile water. Next, 10 µL of each sample was placed on a glass slide and allowed to dry before heat treatment. Samples were then Gram-stained using Crystal violet, iodine, 90% ethanol solution, and safranin before use in the microscope. Images were taken at 1000 x magnification.

3.2.3 Bacterial Culture

Frozen stock cultures of each bacterial species were stored at -80 ºC. Master plates were created using a 10 µL loopful of stock culture streaked on TSA and incubated at 37 ºC for 24-48 hr. The master plates were stored at 4 ºC for a maximum of six weeks before replacement. Fresh bacterial cultures were created for each experiment by transferring a single colony from the master plate into 9 mL TSB. After overnight incubation at 37 ºC, 1 mL of the bacterial culture was transferred to 9 mL of new TSB. This "spiked" sample was incubated at 37 ºC for an additional 4 hr to achieve logarithmic growth.

3.2.4 MNP Bacterial Capture in PBS

For bacterial inoculation, 4 hr spiked bacterial cultures were serially diluted to a concentration of approximately 10^5 CFU/mL, unless otherwise specified. The serial dilution was continued to a 10^{-6} dilution, and 10^{-5} and 10^{-6} dilutions were plated to confirm the initial concentration. One milliliter of the diluted sample was then added directly to a Whirl-Pak bag containing 101 mL of PBS and mixed. Before magnetic extraction, 1 mL of the sample was removed and plated to serve as the control. Next, 1 mL of MNPs were added to the Whirl-Pak bag, mixed by hand, and allowed to incubate at room temperature for 5 min. The Whirl-Pak bag

was then attached to a magnetic rack. After 5 more min, a pipet was used to remove the supernatant, and the remaining sample was re-suspended in 1 mL PBS. The final sample was serially diluted and plated on selective media to determine the final bacterial concentration. All plates were incubated at 37 ºC for 24 hr before analysis.

Concentration of bacteria by MNPs was accomplished through colony counting of plates with 20-300 individual colony forming units (CFUs). Concentration factor was used to quantify the concentration, using the following formula:

$$Concentration\ Factor = \frac{CFUs\ in\ treated\ sample}{CFUs\ in\ control}$$

In order to analyze MNP capture at varying pH values, the PBS pH was adjusted before inoculation using HCl or NaOH. Bags were adjusted to pH levels of 5, 6, 7, 8, 9, and 10, and the final pH was confirmed using pH test strips. After pH adjustment, the aforementioned procedure was conducted in triplicate at each pH. The relationship between concentration factor and solution pH was analyzed using the correlation coefficient r. The significance of the relationship was determined using a two-tailed t-test at the 95% significance level.

For analysis of MNP capture at varying bacterial concentrations, serial dilutions were used to create 1 mL bacterial cultures at the original, 10^{-1}, 10^{-2}, 10^{-3}, and 10^{-4} concentrations. Bags of PBS were inoculated and treated as described previously, with experiments conducted in triplicate at each inoculation concentration. Results for each bacterial species were analyzed separately. For these calculations, results were linearized by taking the logarithm (base 10) of bacterial concentration. Correlation between concentration factor and the initial sample concentration was examined using the correlation coefficient r. The significance of the relationship was determined using a two-tailed t-test at the 95% significance level.

3.2.5 Effect of pH on Surface Charge

For each bacterial species, three overnight cultures were centrifuged at 8000 rpm for 5 min. After supernatant removal, 1 mL of each culture was re-suspended in sterile water with an adjusted pH, with a total of three samples at each pH level for each bacterial species. Water was adjusted to pH levels of 4, 5, 6, 7, 8, or 9, which was confirmed using pH test strips. Ten to thirty min after re-suspension, samples were analyzed using a ZetaSizer (Malvern Nano-ZS) to detect their net zeta potential (surface charge). Net charge measurements were collected in triplicate for each sample, leading to a total of 9 measurements at each pH for a tested bacterial species. Measurements were then analyzed to calculate mean zeta potential at different pH values. This procedure was also conducted with the MNPs from the Nano-Biosensors lab. Net charge difference between the collected data and known MNP charges at each pH were then calculated.

3.2.6 MNP Bacterial Capture from Food Matrices

For foodborne pathogen extraction, the procedure was adapted to follow Bacteriological Analytical Manual (BAM) protocols, beginning with artificial contamination. The overall method is detailed in Figure 3.1. First, 25 g of the food matrix was weighed in a Whirl-Pak bag. For bacterial inoculation, 1 mL of a 4 bacterial culture was serially diluted to approximately 10^5 CFU/mL and added to the Whirl-Pak bag. The serial dilution was then continued to a 10^{-6} dilution, and 10^{-5} and 10^{-6} dilutions were plated to confirm the initial concentration. Following artificial contamination of food samples, the bacteria were allowed to acclimate for 1 hr at room temperature. Then, 225 mL of PBS was added to each sample in sterile Whirl-Pak bags before being placed in a stomacher for 2 min. The liquified food matrix was then removed from the initial bag and separated into two Whirl-Pak bags with 100 mL of liquified food each. One bag

was designated as the control and plated to determine the initial bacterial concentration. The other bag was designated as the treatment bag and subjected to magnetic extraction.

As with PBS experiments, 1 mL of MNPs were then added to the Whirl-Pak bag, mixed, and allowed to incubate at room temperature for 5 min. The Whirl-Pak bag was then attached to a magnetic rack. After 5 min more, a pipet was used to remove the supernatant, and the remaining sample was re-suspended in 1 mL PBS. The final sample was serially diluted and plated on selective media to determine the final bacterial concentration. All plates were incubated at 37 ºC for 24 hr before analysis, and experiments were conducted in triplicate for each food matrix. Manufacturer instructions for selective media were used to distinguish between target bacterial colonies and natural microflora, if present.

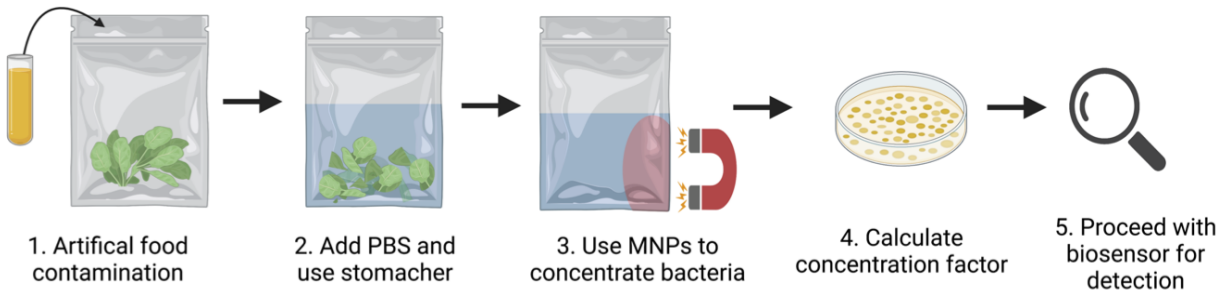

Figure 3.1 MNP-based food extraction procedure (created with Biorender).

3.3 Results and Discussion

3.3.1 Microscopic Imaging and Analysis

In order to confirm MNP-bacteria adhesion and visualize the interaction, TEM images were collected for all three bacterial species (Figure 3.2, A.1). These images confirmed bacteria-MNP adhesion, with MNPs typically clustered around the bacterial cell walls. For *Listeria* spp. and *E. coli* O157:H7, images identified MNPs bound to both clusters of bacteria and isolated bacterial cells. However, all *S. aureus* images displayed clusters of cells surrounded by MNPs.

This clustering behavior may be partially responsible for the increased MNP capture of *S. aureus* when compared to other bacterial species, which will be discussed in future sections.

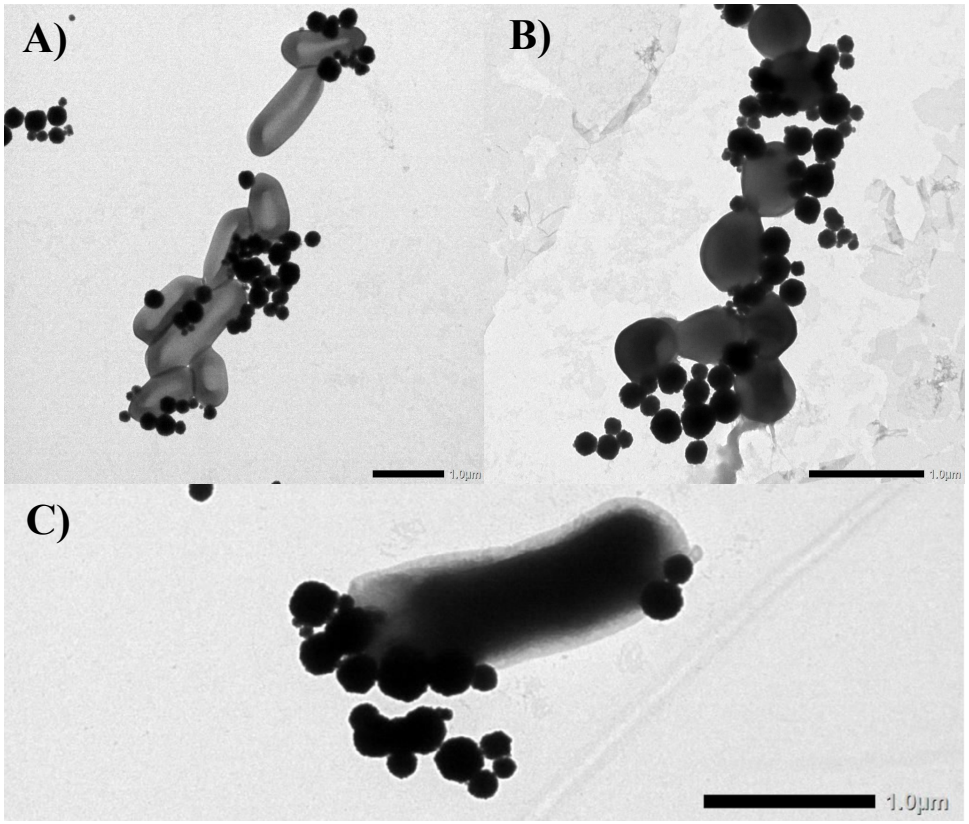

Figure 3.2 TEM image of (A) *Listeria*-MNP interaction, (B) *S. aureus*-MNP interaction, and (C) *E. coli* O157-MNP interaction.

This microscopic analysis also confirms that initial MNP adhesion does not lead to lysis of the target cells. Chitosan, the glycan coating of these MNPs, is known to be an antimicrobial agent with cell lysis properties [134]. However, literature suggests that the rapid nature of magnetic separation eliminates any negative effects on the target bacteria [22]. This microscopic analysis confirms that claim for the nanoparticles used in these trials, as little to no cell lysis was noted in the TEM images.

Although TEM images offer high-definition visualization of MNP-bacteria adhesion, the time-consuming nature of this microscopy technique resulted in a small sample set of images. To

further understand and quantify MNP-bacterial adhesion, extensive confocal laser microscopy analysis was conducted (Figures A.2, A.3, & A.4). In addition to further visualizing MNP-bacteria adhesion, it was possible to categorize the binding into two separate locations for the rod-shaped bacterial species (*E. coli* O157 and *Listeria* spp.). All MNP-bacteria interactions were categorized as occurring on the curved end of the rods or on the flat sides. Examples of these two categories are demonstrated in Figure 3.3.

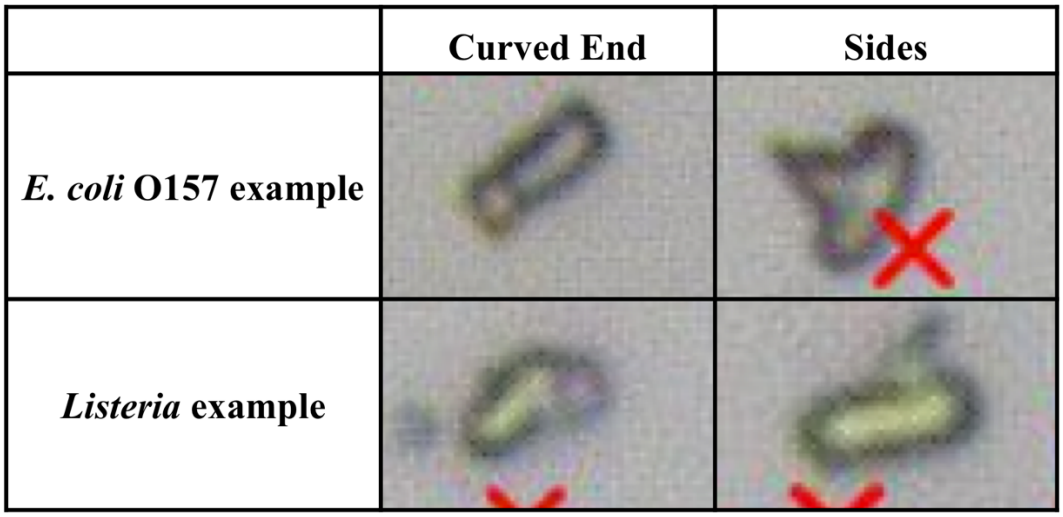

Figure 3.3 Example categorization of MNP-bacteria binding sites.

Over 100 bacterial cells were categorized for each species, including cells with MNP binding occurring in multiple sites. Results are summarized in Table 3.1. Sample size indicates the total number of bacterial cells analyzed for each bacterial species.

Table 3.1 Summary of binding site analysis, *E. coli* O157 and *Listeria* spp.

	***E. coli* O157**	***Listeria***
Sample size	101	113
Binding on curved end present	90.1%	88.5%
Binding on sides present	25.7%	23.0%

As shown in the table, 90.1% and 88.5% of bacterial cells bound to MNPs (*E. coli* O157 and *Listeria* spp., respectively) demonstrated binding on the curved end of the rod-shaped bacteria. Meanwhile, only 23-26% of the cells had binding on the sides of the bacterium. Thus, MNPs primarily bind to curved ends of these two rod-shaped bacterial species. Many, but not all, cells with binding on sides of bacterium were surrounded by large clusters of MNPs also attached to curved ends. These results suggest that MNPs may preferentially adhere to certain locations on the bacterial cell membrane. This could be explained by the presence of specific glycan-binding sites on bacteria. Glycans on host cells are often targeted by bacteria surface proteins to initiate infection, and these proteins are sometimes localized to specific locations on the cell membrane [28]. In addition, chitosan-coated nanoparticles have been shown to adhere to membrane proteins of *E. coli* and *S. aureus* cells [134]. *E. coli* cells in particular are known to have many glycan-protein interactions as part of their infection mechanism [135].

However, this data collected does not conclusively indicate adhesion is due to glycan-protein interactions. For instance, chitosan can non-covalently bind to teichoic acids on the surface of Gram-positive bacteria, and similar electrostatic interactions may take place with lipopolysaccharides in Gram-negative bacterial cell walls [136]. Regardless, the targeted locations of the MNP binding sites shown in microscopic analysis suggest these specific glycan-protein interactions may play a role. For instance, the external wall teichoic acids in *L. monocytogenes* are extremely prevalent and there is no indication they would be isolated to specific regions of the cell membrane [137], [138]; thus, it is unlikely that the interactions with MNPs shown through microscopic analysis are solely due to these interactions. As many glycan-protein interactions are still undiscovered, this may be the cause of the specific binding sites seen in this analysis.

3.3.2 Effect of pH on Surface Charge and Concentration Factor

In order to determine the effect of pH on concentration factor, 100 mL bags of PBS were modified to pH values of 5, 6, 7, 8, 9, and 10. The experiment was completed in triplicate at each pH for PBS contaminated with *Listeria* spp., *S. aureus,* and *E. coli* O157. Results are represented graphically in Figure 3.4, with *E. coli* O157 shown separately for scale. The graph results indicate a negative correlation between concentration factor and sample pH for all bacterial species.

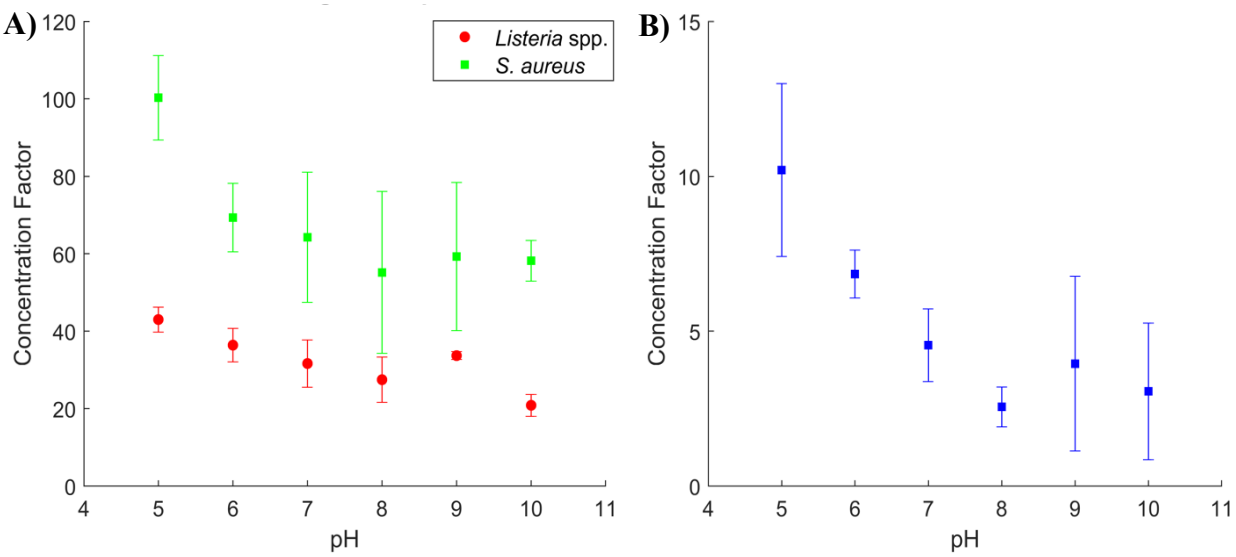

Figure 3.4 Average CF versus pH for (A) Gram-positive bacteria (*Listeria* spp. and *S. aureus*) and (B) *E. coli* O157, with error bars indicating standard deviation.

Statistical testing was used to evaluate this perceived correlation. The correlation coefficient and significance testing values are summarized in Table 3.2 at the 95% confidence level. These results were calculated using the raw data set with 3 measurements at each pH value for every bacterial species. At 95% confidence, these results indicate a significant negative correlation between pH and concentration factor for *E. coli* O157 and *Listeria* spp. This is demonstrated by p-values lower than the alpha of 0.05 for 95% significance and high r-values. The only experiment without significant results at this level is *S. aureus,* most likely due to the

high variability between replicates in this data set. However, results still indicate a significant negative correlation at 90% confidence, and the r-value of -0.458 indicates a medium-strength correlation. Thus, the majority of pH experiments support the hypothesis that the MNP-based extraction method produces higher concentration factors at a lower sample pH. The lowest pH tested, 5, produced the highest concentration factors.

Table 3.2 Statistical correlation results from pH experiments.

Name	**r**	**Tcalc**	**Tcrit**	**Pcalc**	**α**
S. aureus	-0.458	-1.857	2.160	0.0861	0.05
***E. coli* O157**	-0.737	-4.357	2.120	0.0005	0.05
***Listeria* spp.**	-0.785	-5.066	2.120	0.0001	0.05

The observed relationship between pH and capture efficiency may result from the electrostatic MNP interactions with bacterial cell walls. As pH decreases, for instance, the amino groups on chitosan will become protonated, leading to a net positively charged MNP surface [49], [139]. Bacteria, meanwhile, have a net negatively charged cell membrane under physiological conditions, although this can vary with pH [88]. Thus, there will often be an electrostatic attraction between positively charged glycan coatings and negatively charged bacterial cell membranes that enhances cell capture. As a result, using pH to maximize the surface charge difference between the bacterial cell wall and MNP surface could in turn optimize bacterial capture.

To further elucidate the relationship between pH, surface charge, and concentration factor, a Zetasizer was used to measure the zeta potential (surface charge) of bacterial species at suspended in water of varying pH. As predicted by literature, all bacteria had a net negative charge in pH 7 water. *E. coli* O157 was the least negatively charged, at -4.0 mV in pH 7 PBS. *S.*

aureus and *Listeria* spp. were notably more negatively charged, with zeta potentials of -35.0 and -42.8 at pH 7, respectively. However, net surface charge for all three bacteria also varied with solution pH. Zeta potential at all pH values are summarized in Figure 3.5.

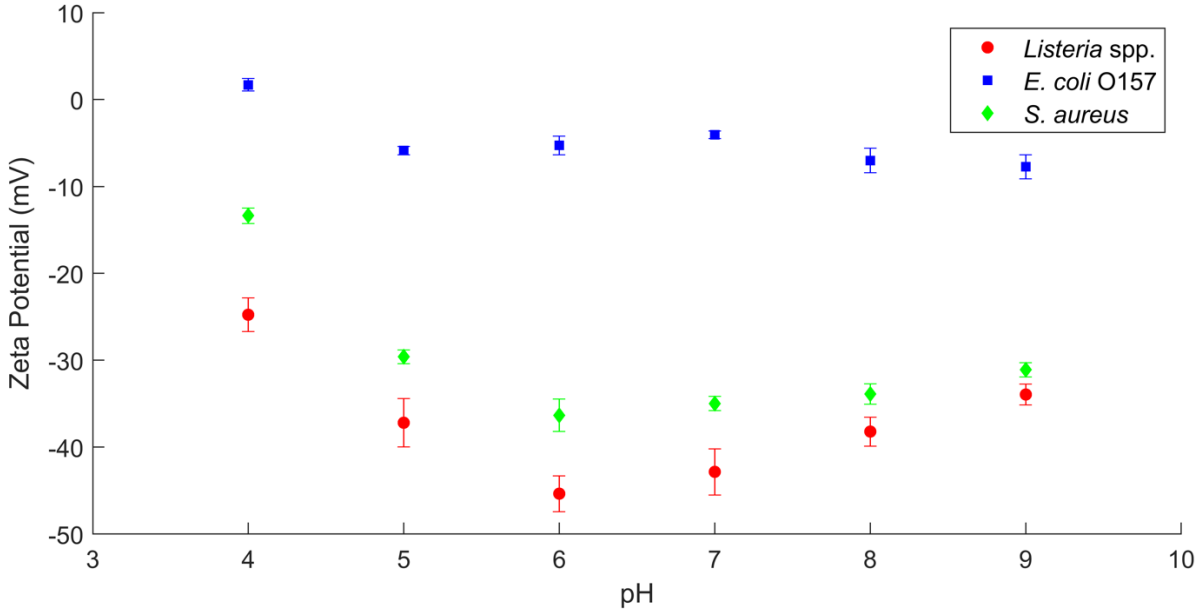

Figure 3.5 Zeta potential versus water pH for *Listeria* spp., *E. coli* O157, and *S. aureus*.

For *Listeria* spp. and *S. aureus,* zeta potential became increasingly negative from pH 4 to 6. From pH 7 to 9, the zeta potential became less negative, although the bacteria retained a net negative surface charge at all pH values tested. *E. coli* O157 did not demonstrate the same trend as the other bacteria and appeared to have increasingly negative surface charges with increasing pH, aside from a slight increase between pH 5 and 7. The similar trend seen in the Gram-positive species may be due to specific acid resistance mechanisms. Although both *E. coli* and *L. monocytogenes* use the glutamate decarboxylation system, other systems implemented by both *L. monocytogenes* and *S. aureus* are unique [140]. For instance, acid resistance mechanisms of both species appear to include F_1F_0 ATPase [140], [141]. By actively exporting protons to maintain the proton-motive force, it can increase intracellular alkalinity. Similarly, *L. monocytogenes* and

S. aureus also utilize the arginine deiminase pathway [142], [143]. It possible that these acid resistance mechanisms in particular are responsible for the relationship between surface charge and pH specifically for *S. aureus* and *L. monocytogenes.*

After analysis of bacterial zeta potential was complete, measurements of each bacteria were subtracted from the MNP zeta potential at each pH tested. These numerical differences are represented in Table 3.3.

Table 3.3 Average zeta potential difference between bacteria and MNPs at pH 4-9 (mean ± standard deviation).

	Average Zeta potential difference from MNPs (mV)		
pH	***Listeria***	***S. aureus***	***E. coli* O157**
4	61.2 ±2.3	49.8 ± 1.5	34.8 ± 1.4
5	44.4 ±3.3	36.8 ± 1.9	13.0 ± 1.8
6	31.4 ±3.1	22.4 ± 2.9	-8.7 ± 2.5
7	15.2 ±2.8	7.3 ± 2.8	-23.6 ± 0.9
8	6.5 ± 1.8	2.2 ± 1.8	-24.7 ± 1.6
9	-18.8 ± 6.95	-21.6 ± 7.0	-45.0 ± 7.0

As shown in the table, the net charge difference, not only charges of MNPs and bacteria individually, varied with solution pH. The charge difference for *Listeria* and *S. aureus* was positive when suspended in water with pH 4-8, indicating the MNPs were more positively (or less negatively) charged than the bacteria. However, at a pH of 9, the MNPs were more negatively charged than the bacteria. For *E. coli* O157, this reversal occurred earlier at pH 6. This is most likely due to the less negative surface charge of *E. coli* O157 compared to the other bacterial species. Since any net charge difference should indicate oppositely charged residues on the bacteria and MNP that enhance binding, the absolute value of this net charge difference at each pH was plotted in Figure 3.6.

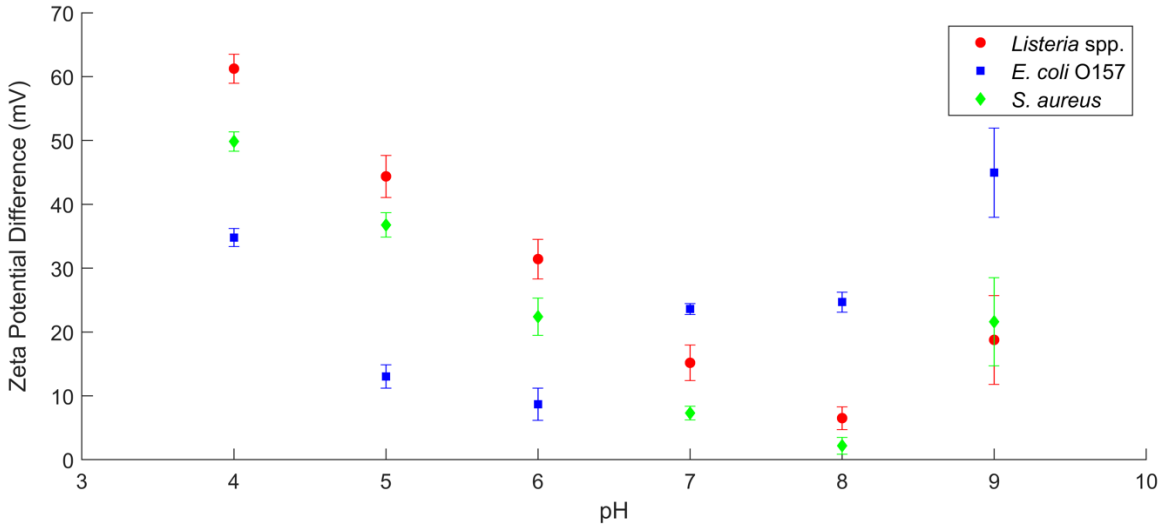

Figure 3.6 Absolute zeta potential (ZP) difference between MNPs and bacteria in water, pH 4-9.

Once again, *Listeria* and *S. aureus* showed the most consistent trends, with the net surface charge difference decreasing from pH 4-8 and increasing at pH 9. For *E. coli*, the zeta potential difference generally decreased from pH 4-6 and increased from pH 7-9. These trends were analogous to the results for concentration factor versus solution pH, particularly for *Listeria* spp. and *S. aureus* (Figure 3.4). For these two species, both concentration factor and net surface charge decreased until pH 8 before slightly increasing at pH 9. These similar trends suggest that a higher surface charge difference between MNPs and bacteria is correlated with a higher concentration factor, emphasizing the importance of electrostatic forces in the adhesion mechanism.

However, the results do suggest that binding is not completely due to electrostatic attraction between net oppositely charged MNPs and bacteria. Above pH 5, both MNPs and bacteria had a net negative charge, yet concentration of the bacteria still occurred. In fact, the concentration factor increased for *Listeria* spp. and *S. aureus* at pH 9 compared to pH 8. Thus, it is hypothesized that binding occurs through the electrostatic attraction of oppositely charged residues on the MNP and bacteria, instead of the total surface charge. This hypothesis aligns with

existing literature on bacterial cell membranes that describe the presence of both negative and positive cell wall components [60].

Despite the success of pH reduction in PBS experiments for increasing CF, some negative effects of a low pH solution were also observed. Despite the higher concentration factor, lower bacterial concentrations were noted in the control plates for the pH 5 experiments for *S. aureus* and *E. coli* O157, as well as the MNP-treated plates for *S. aureus*. Bacterial concentrations for control and treated plates at a pH 5 and pH 7 are compared in Table 3.4. Although the reduction was slight, particularly in the treated plates, this suggests the low pH may lead to inhibition of colony formation or even the death of some bacterial cells. This may be a concern in future work; however, using stationary phase cells instead of log phase cells could reduce this impact. Additionally, stationary cells are more representative of bacteria on food surfaces and commonly used in foodborne pathogen studies [144], [145].

Table 3.4 Bacterial concentrations from pH experiments, pH 5 and 7 (mean ± standard deviation).

	S. aureus	***E. coli* O157**	***Listeria* spp.**
pH 7 concentration, control plates (log CFU/mL)	4.67 ± 0.06	5.38 ± 0.13	5.02 ± 0.08
pH 5 concentration, control plates (log CFU/mL)	4.25 ± 0.02	5.04 ± 0.14	5.02 ± 0.02
Reduction, control plates (log CFU/mL)	0.42 ± 0.06	0.35 ± 0.19	0.00 ± 0.08
pH 7 concentration, treated plates (log CFU/mL)	6.47 ± 0.09	6.03 ± 0.10	6.51 ± 0.03
pH 5 concentration, treated plates (log CFU/mL)	6.25 ± 0.03	6.03 ± 0.03	6.65 ± 0.01
Reduction, treated plates (log CFU/mL)	0.22 ± 0.09	0.00 ± 0.10	-0.14 ± 0.04

3.3.3 Effect of Bacterial Species on Concentration Factor

Concentration factor experiments in PBS were substantially different for the three bacterial species at a neutral pH, as shown in the pH experiments (Section 3.3.2). Numerical results at a neutral pH are shown in Table 3.4. *S. aureus* had the highest CF, followed by *Listeria*

spp., and *E. coli* O157 had the smallest CF. Several potential causes of these differences have been identified. For instance, the morphological characteristics of the bacteria may play a role. As shown through TEM imaging, *S. aureus* is spherical and typically exists in grape-like clusters [126]. The other bacteria are rod-shaped and, although they do exhibit some cell clustering under microscopic analysis, it appears to be to a lesser extent. This clustering behavior could increase the efficiency of MNP cell capture as more cells could potentially be magnetically separated by the same concentration of MNPs.

Table 3.5 Concentration factors in neutral pH PBS.

Bacteria	***S. aureus***	***Listeria* spp.**	***E. coli* O157**
CF in PBS pH 7 (mean ± SD)	64.27 ± 16.78	31.68 ± 6.10	4.55 ± 1.17

In addition, *E. coli* O157 is Gram-negative, while *Listeria* and *S. aureus* are Gram-positive. The different cell membrane components found in Gram-positive species, such as teichoic acid, may potentially improve MNP adhesion [60], [136]. Finally, the *E. coli* cell surface charge was found to be significantly less negative than *Listeria* spp. or *S. aureus* (Figure 3.6). As these MNP-bacteria interactions are electrostatic in nature, this may lead to reduced adhesion strength. For instance, for pH values of 4 and 5 at which MNPs were positively charged, the Zeta potential difference between MNPs and *E. coli* cells was relatively low (Table 3.3).

3.3.4 Effect of Bacterial Concentration on Concentration Factor

With artificial inoculation, all experiments conducted in PBS (Section 3.3.2) and food matrices (Section 3.3.6) had a final concentration of approximately 10^3-10^5 CFU/mL in the 100 mL bag, with variability due to bacterial growth. As bacterial concentrations widely vary in

naturally contaminated foods, it is important determine the applicability of this assay for various bacterial concentrations. Thus, additional trials were conducted to determine the effect of initial bacterial concentration on CF. Final bacterial concentrations in the PBS samples ranged from 2 x 10^2 CFU/mL to 4 x 10^6 CFU/mL. Lower concentrations could not be tested due to the lack of countable colonies on agar plates. Resulting concentration factors at each bacterial concentration are summarized in Figure 3.7. As visually evident from the figures, no overall correlation between initial bacterial concentration and CF was present.

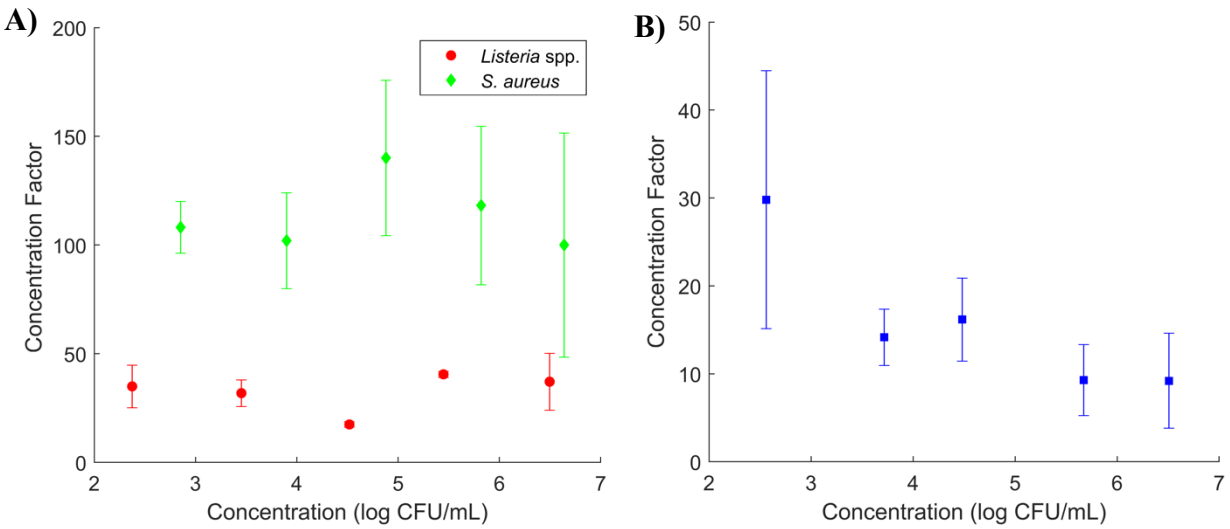

Figure 3.7 Average CF versus concentration for (A) Gram-positive bacteria (*Listeria* spp. and *S. aureus*) and (B) *E. coli* O157, with error bars indicating standard deviation.

Upon analysis of each bacterial species individually, the Gram-positive *Listeria* spp. and *S. aureus* showed little to no correlation between initial bacteria concentration and final CF. This was demonstrated by correlation coefficients close to zero and P-values greater than 0.05 for significance testing (Table 3.6). However, *E. coli* O157 had a significant negative correlation (r of -0.683), with the highest concentration factors at the lowest bacterial concentrations.

Table 3.6 Statistical correlation results from bacterial concentration experiments.

Name	r	Tcalc	Tcrit	Pcalc	α
S. aureus	0.014	0.049	2.160	0.962	0.05
***E. coli* O157**	-0.683	-3.375	2.160	0.005	0.05
L. monocytogenes	0.161	0.587	2.160	0.567	0.05

These results indicate that calculated concentration factors are not correlated with sample bacteria concentration for *S. aureus* and *L. monocytogenes*. Thus, it is reasonable to assume concentration factors in the tested food matrices will not significantly vary with different bacterial concentrations within the range tested. However, the relationship seen in the *E. coli* O157 experiments is of particular interest. The correlation coefficient indicates a relatively strong relationship, and the p-value also demonstrates significance with 95% confidence. It is possible that this negative correlation can be explained by the limited number of MNPs added to the solution; at high bacterial concentrations, there may not be enough MNPs to capture all bacterial cells. Therefore, a smaller proportion of the sample bacterial population is captured, resulting in the lower concentration factors seen at higher bacterial concentrations.

Why this relationship is only present for *E. coli* O157 and not the other bacterial species cannot be fully explained, but it may be related to the lower affinity MNPs have for this species compared to the others studied. Based on these results, it can currently be concluded that the concentration factors of *E. coli* O157 may vary depending on initial bacterial concentration. However, as these experiments were conducted only in PBS, it is unclear whether this correlation would maintain its significance in food matrices.

3.3.5 Hypothesized MNP-bacteria adhesion mechanism

Although literature sources fully outlining glycan-coated MNP interactions with bacteria are limited, a general hypothesis can be formulated through an accumulation of source material. Through literature analysis, this mechanism is hypothesized to be facilitated by a combination of forces within a fluid matrix, as summarized in Figure 3.8. As mentioned previously, glycans must be in close proximity to their target proteins for successful adhesion [28]. This proximity can be achieved in multiple ways. One potential mechanism is Brownian motion, the uncontrolled and random movement of particles in a fluid [29], [146]. Through this movement, bacterial cells can randomly become close enough to glycan-coated MNPs for adhesion to occur. This close proximity can also be achieved in a less random manner through generalized electrostatic interactions. MNPs with a positively charged surface coating should be electrostatically attracted to negatively charged cell membranes, drawing the particles towards the cells [27], [29], [30], [89]. Once the bacterium and glycan coating are in close proximity, adhesion can occur through non-covalent carbohydrate-protein binding, including van der Waals forces and hydrogen bonds [24], [25]. Adhesion can be improved through the use of a positively charged glycan coating that reduces electrostatic repulsion [29].

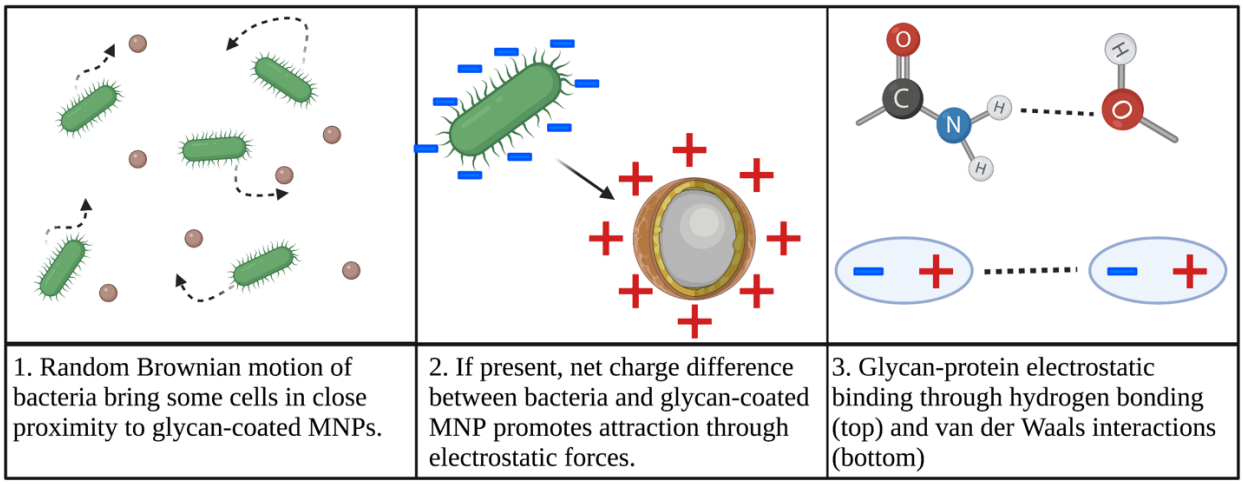

1. Random Brownian motion of bacteria bring some cells in close proximity to glycan-coated MNPs.	2. If present, net charge difference between bacteria and glycan-coated MNP promotes attraction through electrostatic forces.	3. Glycan-protein electrostatic binding through hydrogen bonding (top) and van der Waals interactions (bottom)

Figure 3.8 Overview of hypothesized mechanism of glycan coated MNP bacterial adhesion (created with Biorender).

For this work, the glycan chitosan was used to coat the MNPs and adhere to bacterial cells. Chitosan is a cationic polysaccharide derived from chitin that is often used for glycan-coated MNPs due to its biodegradability and biocompatibility [48], [147]. The polysaccharide has both hydroxyl (-OH) and amino ($-NH_2$) groups. At a low pH, the amino groups will be protonated, leading to a positively charged glycan coating [49], [139]. When suspended in solution, this positively charged MNP will be electrostatically attracted to negatively charged bacterial cells, bringing them in close proximity. Then, non-covalent interactions between chitosan on the MNPs and proteins on the bacterial surface can occur. At a higher pH, chitosan will be negatively charged and therefore should not have generalized electrostatic interactions with the bacteria. However, binding should still occur. MNP-bacteria adhesion can be accomplished at a high pH through hydrogen bonding interactions between negatively charged hydroxyl groups of chitosan and positively charged pockets on the cell membrane [26].

This binding theory is supported not only by literature, but by experimental data collected in this thesis. The pH experiments (Section 3.3.2), for instance, indicate that the highest concentration factors occur at low pH values when the MNPs are positively charged. This aligns

with the hypothesis that generalized electrostatic interactions can improve initiation of MNP-bacteria adhesion. Further, binding still occurred when both MNPs and bacteria had a net negative charge, evidenced by concentration factors above 1 at all pH values tested. This indicates that other factors, potentially glycan-protein interactions, must play a role. Finally, quantitative microscopic analysis (Section 3.3.1) also indicated the preferential selection of specific bacterial regions for binding. This further indicates the presence of glycan-protein interactions, which often occur at specific regions of the bacterial cell [28].

This theory offers opportunities for further optimization of this bacterial concentration assay. Due to the effect of generalized electrostatic interactions, this technique may be more effective at capturing bacterial species with more negatively charged cell membranes. A correlation between cell surface charge and bacterial capture was noted in this research as well, with *E. coli* having both the least negative cell surface charge and the lowest concentration factor at a neutral pH (Section 3.3.2). Similarly, modifying MNPs to have a net positively charged surface through addition of amino acids or other components may improve generalized bacterial capture. Finally, the nature of glycan-protein interactions also allows for possible design of species specific glycans for targeted bacterial concentration. This has already been accomplished in pure culture studies by some researchers [65].

Although this hypothesized mechanism focuses primarily on glycan-protein interactions, other factors may also play a role in this particular MNP-bacterial adhesion process. As mentioned previously, generalized electrostatic attraction can improve MNP capture. In addition, chitosan is known to interact with non-protein cell wall components, such as teichoic acids, through non-covalent interactions [136]. Fully elucidating the mechanism of action between these chitosan-coated MNPs and select bacterial species is beyond the scope of this work, but

both literature and experimental sources indicate both glycan-protein interactions and other electrostatic interactions play a role. This hypothesis can be expanded upon in future work and used as a framework for further experimental optimization.

3.3.6 Foodborne Pathogen Extraction

Four food matrices were selected for each bacterial species based on recent multistate outbreak data and other literature sources [148]–[150]. In addition, 2-4 of the matrices for each species were re-tested while suspended in PBS adjusted to a pH of 6 to determine the effect of pH reduction on CF in food. The PBS was not reduced to a pH below 6 as lower colony counts in initial trials indicated bacterial death was occurring (Table 3.4). Successful concentration of bacteria was defined as experiments with an average CF greater than 1, and numerical CF results can be found in Figure B.1.

S. aureus was successfully extracted from milk, sausage, deli ham, and romaine, as evidenced by the growth of viable colonies in selective agar plates. Despite the successful capture, concentration only occurred in trials with milk (pH 6), deli ham (pH 7), and romaine lettuce (pH 6 and 7). Reducing the PBS pH was unsuccessful at increasing CF for deli ham and only mildly successful in sausage and romaine. However, for milk samples, pH reduction led to a CF increase from 0.85 ± 0.15 to 11.62 ± 5.64 (mean ± standard deviation). This may be because milk typically has a higher pH than other tested matrices, such as romaine and spinach [151]. Therefore, the reduction in PBS pH may have had a greater effect on the total pH of the milk sample, leading to a more dramatic impact on CF. Experimental results for food trials with *S. aureus* are summarized in Figure 3.9.

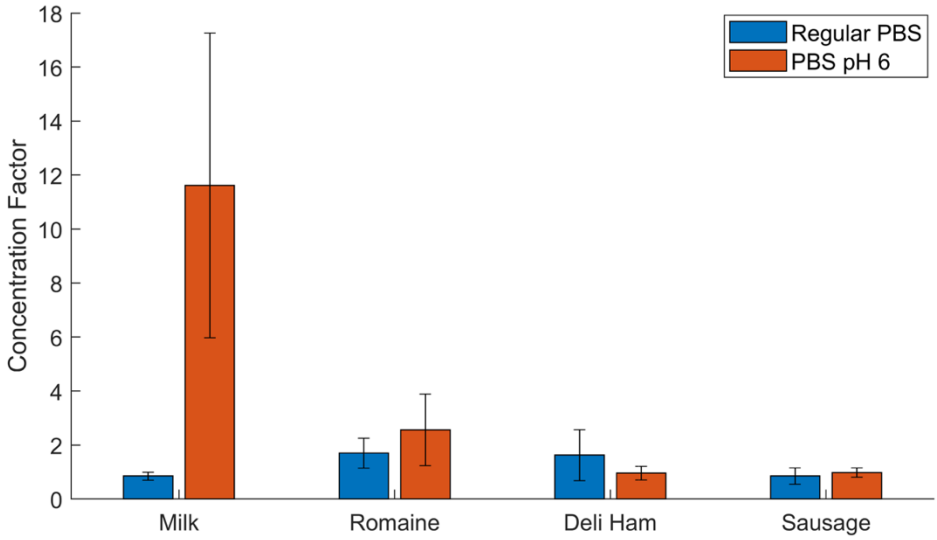

Figure 3.9 Concentration factor results for *S. aureus* from food matrices. Error bars represent standard deviation.

For *Listeria* spp. and *E. coli* O157, successful target bacterial capture from all tested matrices was similarly shown through the growth of viable cells in the treated sample plates. Successful concentration of bacteria occurred in some food matrices, specifically sausage (pH 7) for *Listeria* spp., and spinach (pH 6 and 7) and flour (pH 7) for *E. coli* O157 (Figure 3.10). Notably, pH reduction for *Listeria* spp. extraction from milk did not dramatically increase bacterial capture as it had for *S. aureus*. As the food matrix was identical, these vastly different results are hypothesized to be due to characteristics of the bacteria-MNP interactions. In PBS studies, the average CF for *S. aureus* is twice that of *Listeria* spp. If this is due to a naturally lower affinity of MNPs to *Listeria,* it is possible that within a food matrix the MNPs may preferentially bind to carbohydrates or other bacteria in the food matrix instead of the target bacterial cells. In addition, the MNP-*Listeria* affinity may not be strong enough to effectively capture *Listeria* cells already attached to food particles. Thus, pH modification may not sufficiently enhance the MNP-bacteria attraction to produce higher concentration factors for *Listeria* spp. in milk.

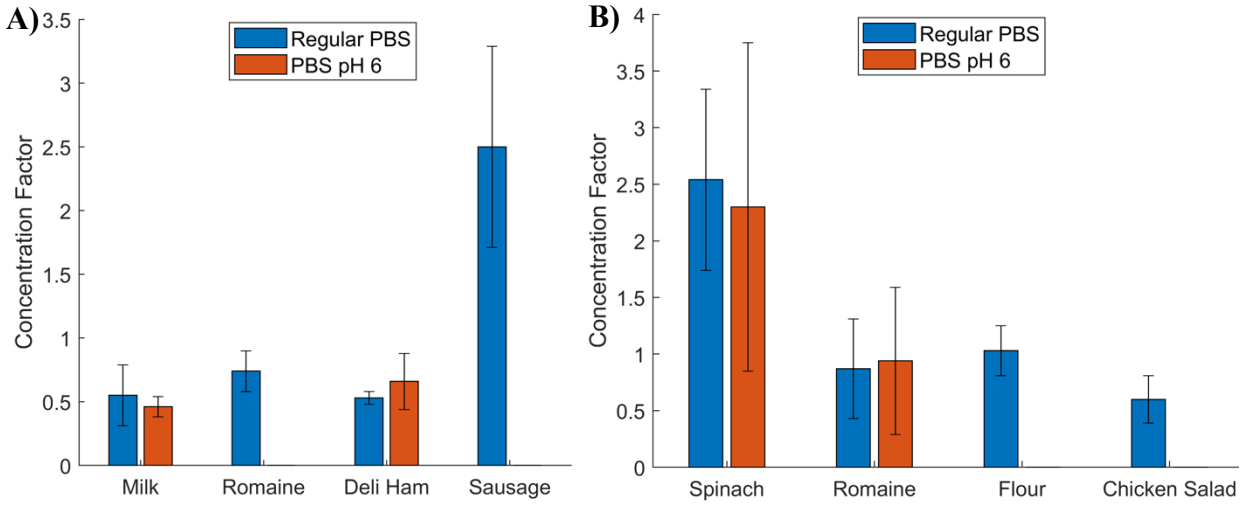

Figure 3.10 Concentration factor results for (A) *Listeria* spp. and (B) *E. coli* O157 extracted from food matrices. Error bars represent standard deviation.

As a whole, trials conducted in food matrices produced significantly lower concentration factors than those conducted in pure PBS. For instance, at a neutral pH, *Listeria* spp. CF decreased from 31.68 ± 6.10 in PBS to 0.53-2.50 in foods. The presence of natural microflora may be partially responsible for this reduced concentration factor. Several food matrices, including romaine lettuce, spinach, and chicken salad clearly had other bacterial species present in the sample. This was evidenced by the growth of colonies in control samples plated on non-selective media that had not been artificially inoculated. In addition, these inoculation-free plates often showed higher colony growth on MNP-treated plates than untreated plates, indicating concentration of natural microflora by MNPs. Resulting CFs calculated from countable control plates in various food matrices are shown in Table 3.7. As the glycan coating used in this assay, chitosan, binds to many bacterial species with varying affinities, it is possible that natural microflora may out-compete the target bacteria for MNP adhesion, reducing the target bacteria CF. This could be resolved in future research through the design of a species-specific glycan or implementation of this assay exclusively in foods without natural microflora.

Table 3.7 Concentration factors for natural microflora from various food matrices.

Food Matrix	**Chicken salad**	**Romaine**	**Spinach**
Concentration Factor*	3.96 ± 2.57	5.21 ± 2.10	3.57 ± 1.73

*Mean ± standard deviation, 3 trials for each matrix

However, other factors aside from the presence of natural microflora must also play a role in the reduced CFs seen in foods. Non-selective plating of control samples indicated low levels of native microbes in food matrices such as milk and deli ham, yet CFs for target bacteria were still significantly lower than CFs calculated in pure PBS trials. Thus, components of the food matrix itself may also alter MNP-binding affinity. For instance, carbohydrates in the food matrix may electrostatically bind to glycan-coated MNPs [30]. Therefore, carbohydrate-containing foods may interfere with MNP bacterial capture. In future work, MNP-bacterial attraction could be improved by using a positively charged coating, and food particles could be more effectively removed by implementing washing steps after magnetic separation and before re-suspension of the final sample.

Reduction of PBS pH in food sample trials did not successfully increase CF in all food matrices tested, unlike experiments conducted in pure PBS. This diminished effect may once again be due to food matrix effects such as the presence of natural microflora and carbohydrates that compete for MNP adhesion. In addition, the bacteria may be adhering to the surface of the food particles themselves. Even with a reduced pH, the MNP-bacteria attraction may not be sufficient to remove bacterial cells from the food. However, pH reduction was successful in increasing CF for select trials, such as those with *S. aureus* and milk. Regardless, the limited effect of pH modification on CF indicates that further elements of this assay must be improved to effectively concentrate bacteria from a wider array of food matrices.

3.4 Conclusions

As mentioned previously, existing work for foodborne pathogen applications of glycan-coated MNP extraction is limited. For instance, most glycan-coated MNP extraction studies utilize small sample volumes of 100 µL - 1 mL, not suitable for significant bacterial concentration directly from food matrices [27], [47], [65]. In fact, the highest sample volume found in existing research for foodborne applications in particular was 25 mL [26], [30]. In this work, higher initial sample volumes of 100 mL were used in all extraction experiments to gather new information about the large-scale implementation of this assay. Thus, the glycan-coated MNP extraction procedure could be easily integrated into existing BAM protocols for initial steps towards foodborne pathogen detection [15].

This work also took several key steps towards optimizing bacterial capture, primarily through the analysis of variables such as pH, bacterial species, and bacterial concentration. These analyses helped develop a deeper understanding of the glycan-coated MNP bacterial adhesion mechanism that can enhance future optimization studies. For instance, the clear correlation between pH and CF, as well as the similar trend shown between surface charge and pH, emphasizes the importance of electrostatic interactions for MNP-bacteria adhesion. Optimization of this electrostatic interaction through positively charged MNPs or low pH solutions may prove effective in improving CF. In addition, microscopic analysis provided a strong indication that glycan-protein interactions were occurring due to the location-specific adhesion of MNPs to bacteria (Table 3.1). This suggests the potential success of species-specific glycans for capturing only the target bacterial cells.

In comparison to existing extraction and concentration methods, glycan-coated MNPs offer key advantages of simple storage conditions and low cost. IMS, for example, is a similar

technique to the assay outlined in this study, except it utilizes antibody-coated MNPs. Although highly successful, IMS is costly compared to conventional methods [16]. They also require 4 ºC storage conditions before use, reducing their accessibility [17], [66], [69]. Meanwhile, the low-cost glycan-coated MNPs used in this study were stored for up to a year in powder form at room temperature and easily suspended in water for experimental use, with no need for refrigeration. These characteristics increase the accessibility of glycan-coated MNPs for application in regions with limited resources. Finally, this assay rivals IMS in terms of speed. IMS is already a rapid method, with successful implementation of the entire procedure typically requiring less than 2-3 hr [13], [17], [73], [152]. For IMS, the incubation time in which MNPs are exposed to the sample before magnetic separation, typically varies from 10-45 min [16], [44], [66], [73], [152]. The glycan-coated MNP assay used in this work had an even shorter experimental duration due to the use of a rapid 5-min incubation period.

However, current results for bacterial capture from food matrices indicate obstacles for widespread implementation of this assay. Although the MNPs did capture target bacteria, concentration factors directly from foods were low compared to current methods using IMS [13], [66], [72]. While this glycan-coated MNP extraction method is advantageous in terms of cost, storage, and speed, it is currently lacking the efficiency within food matrices necessary to dramatically improve the sensitivity of subsequent detection methods. Further optimization is required to specifically apply this magnetic separation technique to complex food matrices. In particular, the glycan coating itself can be modified for further improvement. Addition of amino acids, for example, could assist in creating a positively charged MNP without the need for pH reduction. As shown in this work through solution pH modification, enhancement of the

generalized electrostatic attraction between MNPs and bacterial cells can vastly improve non-specific bacterial capture.

Current findings indicate the simple and cost-effective nature of this extraction technique, as well as its potential for nonspecific concentration of foodborne pathogens. This procedure was incredibly effective at separating and concentrating some bacteria to over 60 times its initial concentration in PBS, and early trials indicate successful MNP-bacteria adhesion even within complex food matrices. Further, this technique also has the potential for automation, using techniques similar to those explored for IMS [13]. Although challenges still exist for direct food pathogen extraction, these results indicate the potential for further assay optimization that will enhance its applicability.

Chapter 4: Gold Nanoparticle Biosensor for Detection of Foodborne Pathogens

Parts of this chapter have previously been published in the open access article "Detection of Unamplified *E. coli* O157 DNA Extracted from Large Food Samples using a Gold Nanoparticle Colorimetric Biosensor" in the *Biosensors* journal and are reprinted here alongside new unpublished results [153].

4.1 Introduction

Gold nanoparticles have wide applications in diagnostics and biomolecule detection due to their unique colorimetric properties. As a result, they have been utilized in a variety of biosensors for foodborne pathogens, including fluorescent probes [154], SPR [155], and lateral flow assays [156], [157]. However, these biosensing options are often limited in terms of accessibility or sensitivity. For instance, one lateral flow biosensor had a sensitivity of 0.1 pg/µL of *Phytophthora infestans* DNA, but it also required an asymmetric PCR assay before implementation [157]. Meanwhile, a more accessible LFA utilizing antibodies had a much higher limit of detection of 10^3-10^4 CFU/mL [155]. Although promising, Surface-Plasmon Resonance techniques often utilize antibodies and detection equipment that increase assay cost [6], [158], [159].

Directly utilizing GNPs for visual colorimetric detection may increase accessibility through a simplified assay and reduced equipment needs. Colorimetric DNA biosensors have been previously used for detection of foodborne pathogens, with sensitivity as low as 9 pg/µL of DNA in some research [33]. However, only one study could be found that tested detection of pathogens extracted from foods [31]. Although a high sensitivity of <10 CFU/mL was achieved, a 6 hr incubation for sample enrichment was required. In addition, the thiol-gold chemistry

commonly implemented to functionalize thiolated DNA probes to GNPs requires 1-2 days of preparation [31], [32]. Thus, further work is required to develop an accessible and rapid colorimetric GNP biosensor for direct food pathogen detection.

In this work, a colorimetric GNP biosensor for *E. coli* O157 DNA was designed for detection of bacteria extracted from food matrices. Unlike existing assays, the biosensor utilizes non-covalent interactions for GNP-probe functionalization. GNPs were coated in 11-mercaptoundecanoic acid (MUDA) using thiol-gold chemistry, and aminated DNA probes non-covalently bound to -COOH groups on the coating. Thus, probe functionalization was achieved almost instantaneously. This biosensor was successfully optimized for specificity against non-target DNA and high sensitivity with DNA extracted from pure cultures. Although a short sample incubation period could not be eliminated, results in MNP-extracted bacteria from flour indicate successful detection of *E. coli* O157:H7 after 4 hr of incubation, with specificity against food samples with non-target bacteria achieved. This biosensor shows promise as a more rapid alternative to current GNP colorimetric biosensors, with successful implementation even in complex food matrices.

4.2 Materials and Methods

4.2.1 Materials

Bacterial strains of *E. coli* O157:H7, *Salmonella enterica* serovar Enteritidis, *B. cereus,* and *Listeria* spp. (strain J1-101) were obtained from Dr. Alocilja's Nano-Biosensors Lab at MSU. *Listeria monocytogenes* EGD-e*,* used in food studies, was obtained from Dr. Bergholz's Lab at MSU. *E. coli* C-3000 (15597) was obtained from the American Type Culture Collection (ATCC). DNA extraction materials, the Powerlyzer Microbial Kit and AE buffer solution, were

purchased from Qiagen (Germantown, MD). DNA concentrations and absorbance spectra data were collected using a NanoDrop One purchased from ThermoFisher Scientific (Waltham, Massachusetts).

Hydrochloric acid (ACS reagent, 37%), 11-mercaptoundecanoic acid (MUDA, $HS(CH_2)_{10}CO_2H$), sodium dodecyl sulfate (SDS, $C_{12}H_{25}NaO_4S$), gold (III) chloride trihydrate ($HAuCl_4$), sodium carbonate (Na_2CO_3), and dextrin from potato starch ($C_6H_{12}O_6$) were purchased from Sigma Aldrich (St. Louis, MO).

4.2.2 Probe Design and PCR confirmation

The oligonucleotide probe was designed to specifically target *E. coli* O157, with a genome size of approximately 5.5 Mb [160]. The probe specifically targeted the Shiga toxin Stx1 subunit A (StxA1) gene with the following sequence: TC TGC CGG ACA CAT AGA AGG AAA CTC ATC A. The probe was designed using NCBI BLAST (National Center for Biotechnology Information Basic Location Alignment Search Tool) and purchased with 5' amination and a poly-A tail from Integrated DNA Technologies (Coralville, Iowa).

Targeting the same gene, *E. coli* O157 primers (Stx1F934 and Stx1R1042) recommended by the Bacteriological Analytical Manual (BAM) [161] were also purchased from Integrated DNA Technologies. For confirmation of biosensor results, PCR was conducted on pure *E. coli* O157 DNA samples and samples extracted from flour using the Qiagen Powerlyzer kit. The PCR protocol and gel electrophoresis was adapted from existing protocols amplifying Stx genes [162].

4.2.3 GNP Synthesis and Surface Coating

Dextrin-coated gold nanoparticles were synthesized using the procedure developed by Yrad et al. [163]. First, 5 mL of 2 mM gold (III) chloride trihydrate ($HAuCl_4$) was swirled into 24.5 mL sterile type 1 water within an Erlenmeyer flask. Then, 0.5 mL of 10% sodium carbonate (Na_2CO_3) solution was added in a dropwise manner to the flask with continuous swirling. Swirling was continued for 3 min after dropwise addition of sodium carbonate was complete. Then, 20 mL of dextrin was added with swirling, and mixing was continued until the mixture turned pale yellow. The flask was covered in foil and a stir bar was added before being placed on a hot plate pre-heated to 150 ºC. Then, the solution was heated with stirring at 350 rpm for 40-50 min until the solution turned wine red. After the color change occurred, the sample was slowly cooled with mixing for an additional 3 min.

After GNP synthesis, 400 µL of 0.025 M SDS was added to 9.20 mL GNPs and incubated at room temperature with shaking for 30 min. Then, 400 µL of 25 µM MUDA was added to the mixture and samples were incubated with shaking for an additional 30 min. Then, the GNPs were centrifuged at 10,000 rcf and 15ºC for 15 min. After supernatant removal, the GNP pellet was re-suspended in 500 µL borate buffer.

4.2.4 Biosensor Design and Optimization

First, 5 µL DNA probe, 10 µL sample DNA, and 5 µL GNPs were combined in a single tube. As the MUDA-coated GNPs have carboxylic acid (-COOH) groups, they form non-covalent interactions with the amine groups on the probes, leading to almost instantaneous GNP-probe functionalization. Samples were then heated in the thermocycler to allow for hybridization

of the probe to target DNA. The tubes were subjected to 5 min at 95 ºC (for denaturing) and 10 min at 55 ºC (for annealing) before being cooled down to room temperature.

Upon heating in the thermocycler, target DNA (if present) would hybridize to the GNP-probe. In samples without target DNA, the DNA would not hybridize. Then, HCl is added to the sample. Electrostatic repulsion from the dextrin coating on the GNPs typically prevents particle aggregation, with introduction of HCl disrupting these forces and inducing particle aggregation [111], [120], [164]. However, the presence of target DNA bound to the GNP-probe protects GNPs from aggregation. Thus, samples with target DNA remained redder in color while non-target samples turned purple or blue. This led to a quantifiable shift in peak wavelength on absorbance spectra. Non-target samples aggregated quickly to a purple/blue shade, with a shift to higher peak wavelengths farther from 520 nm. Target samples remained redder in color and retained a peak wavelength closer to 520 nm. The basic experimental procedure is outlined in Figure 4.1.

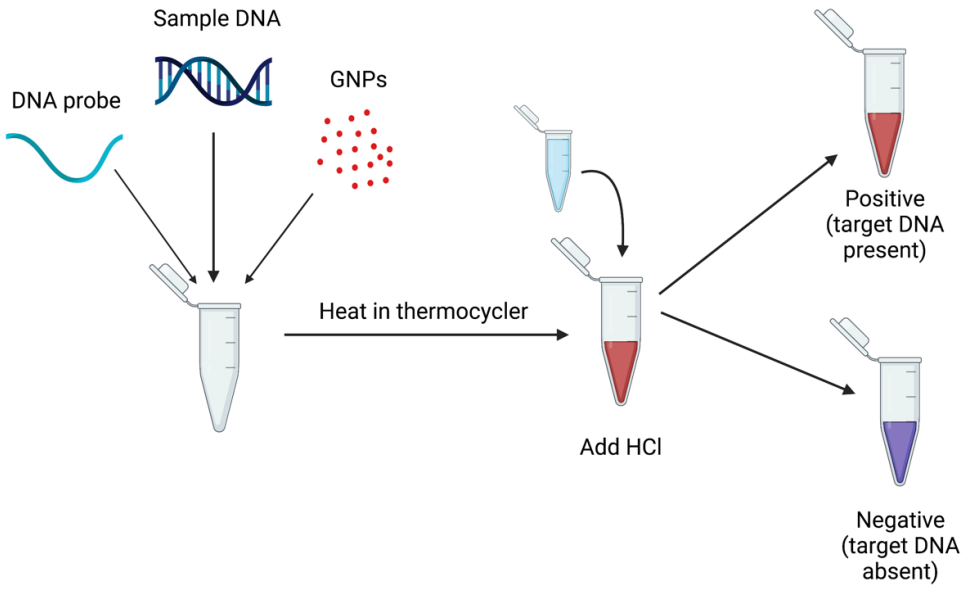

Figure 4.1 Basic procedure for GNP biosensor (created with Biorender).

Optimization variables included the amount of HCl added and the time between HCl addition and reading colorimetric results (5 - 15 min). The optimal HCl amount and aggregation time were determined through quantitative and qualitative analysis. First, HCl volume was optimized by adding 5 µL 0.1 M HCl at a time to negative control (water) and target (10 ng/µL *E. coli* O157 DNA) tubes at 1-min intervals until aggregation of the control without aggregation of the target tube was visually observable. The lowest HCl volume with visible control tube aggregation was then used to compare target samples to multiple non-targets, all at 10 ng/µL. Absorbance spectra readings were taken at 5-min intervals after HCl application until visible aggregation of the target samples occurred. Thus, the optimized procedure had the greatest and most consistent peak shift difference between target and non-target samples, along with a visibly red target sample when compared to the non-target and control.

4.2.5 Sensitivity and Specificity Testing

A series of 9 trials was conducted with the biosensor to determine its specificity. A DNA concentration of 10 ng/µL was used for all samples, with four non-target bacterial species represented. These non-targets were DNA from other foodborne pathogens, specifically *E. coli* C-3000, *S.* Enteritidis*, L. monocytogenes,* and *B. cereus.* A negative control with water and no DNA was also included for each trial.

For genomic DNA extraction, all samples were collected using the Qiagen Powerlyzer DNA extraction kit. Colonies were transferred into 9 mL of broth and incubated overnight, with 1.8 mL of the resulting transfer used for each DNA collection tube. Extracted DNA was measured and diluted to 10 ng/µL using Nanodrop dsDNA measurements for use in specificity testing. During specificity testing, absorbance measurements and images were collected after

HCl application at the previously optimized time. Results were analyzed through the generation and inspection of absorbance spectra. In particular, the wavelength corresponding to peak absorbance, referred to as "peak wavelength," was compared for target and non-target samples. Statistical analysis utilized 95% confidence intervals of peak wavelength for each sample to compare target and non-target results. In addition, comparison of multiple groups was accomplished through the Kruskal-Wallis test and the non-parametric Student-Neumann Keuls test.

A separate series of trials were conducted to determine biosensor sensitivity. Nine replicates were tested for each DNA concentration. DNA was collected and quantified as previously described before being serially diluted to lower concentrations. For each replicate, a target DNA sample was compared to a non-target of the same concentration. Peak wavelength measurements were used to determine whether there was a difference in GNP aggregation and peak shift between the two samples. The detection limit was defined as the lowest concentration with a significant difference (95% confidence) between the target and non-target absorbance values.

4.2.6 Biosensing of Food Samples

Bacteria extracted from food using the MNP-based extraction procedure (Chapter 3) was also tested in the biosensors. First, 500 µL of the concentrated bacteria was transferred to 4.5 mL of Tryptic Soy Broth and incubated for 4 hr. DNA extraction was then performed using the Qiagen Powerlyzer kit. The resulting DNA was quantified using the NanoDrop, and samples with a yield > 10 ng/µL were selected for testing with the biosensor and pooled with other replicates from the same food matrix and with the same artificial inoculation.

For each food matrix, DNA extracted from target-inoculated samples was compared to two nontarget-inoculated DNA samples from the same food, as well as one sample from the food that was not inoculated. As with the target sample, DNA was extracted from a 4 hr spiked sample of the food matrix previously concentrated with MNPs without artificial inoculation. All DNA samples extracted from food were compared at their initial extraction concentrations. If initial concentrations between target and non-target samples differed by > 5 ng/µL, samples were tested again after dilution to the lowest concentration in the sample set for standardization.

4.3 Results and Discussion

4.3.1 Optimization and Specificity Testing of Pure *E. coli* O157 Cultures

Initial optimization of the *E. coli* O157 biosensor resulted in the application of 10 µL 0.1 M HCl for all further analysis (Figure C.1). The procedure was optimized for measurement 10 min after HCl application (Table C.1). Specificity trials were conducted with one water control, one target sample, and four non-target species and strains: *E. coli* C-3000 (NT1), *S.* Enteritidis (NT2), *L. monocytogenes* (NT3), and *B. cereus* (NT4). All DNA samples were diluted to 10 ng/µL using Nanodrop dsDNA measurements. Visual results are displayed in Figure 4.2.

Control (water)	**T (*E. coli* O157)**	**NT1 (*E. coli* C3000)**	**NT2 (*S. enteritidis*)**	**NT3 (*L. monocytogenes*)**	**NT4 (*B. cereus*)**

Figure 4.2 Visual results for one specificity trial using specific *E. coli* O157 biosensor.

As shown in Figure 4.3(A), absorbance spectra indicate a peak shift for the control and non-target species when compared to the target sample. Measurements of peak wavelength shift

for all nine replicates were used to establish 95% confidence intervals for each sample type, graphically represented in Figure 4.3(B). The target sample demonstrated substantially smaller peak wavelength shifts than the non-target and control samples. For instance, the mean wavelength shift was 64 nm for target samples and ranged from average shifts of 101-142 nm for non-target species. To determine the significance of this relationship, Kruskal-Wallis and non-parametric Student-Neumann Keuls tests were implemented (Table C.2, C.3 & C.4). The tests indicated at 95% confidence that there were significant differences between the wavelength shift of the target samples compared to all non-targets, as well as the control.

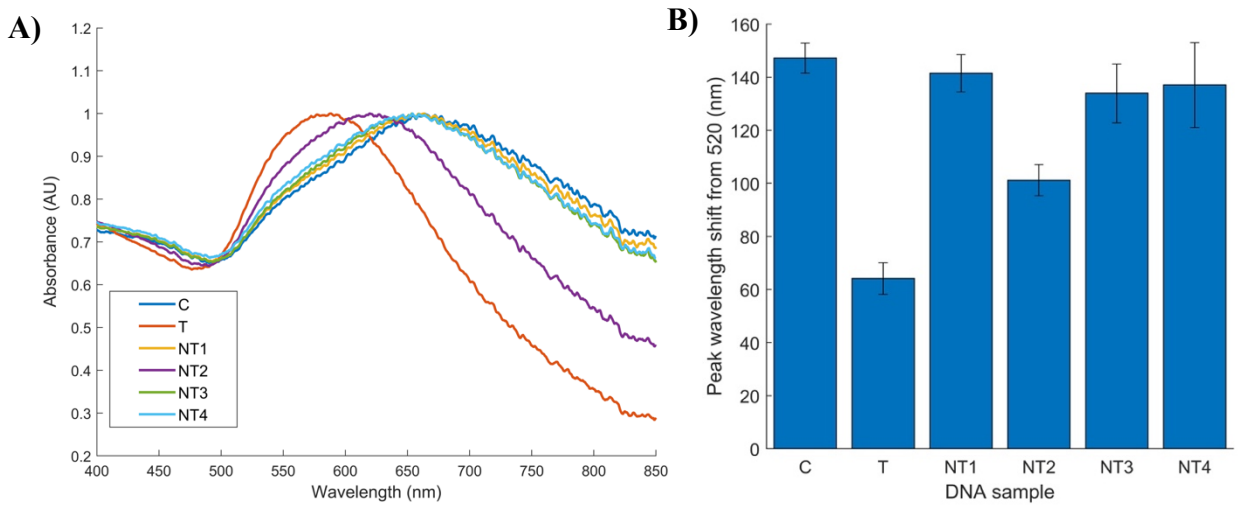

Figure 4.3 *E. coli* O157 biosensor specificity testing results with 10 ng/µL DNA for (A) absorbance spectra and (B) peak wavelength shift from 520 nm, with error bars representing 95% confidence intervals (C: water, NT1: *E. coli* C-3000, NT2: *S.* Enteritidis, NT3: *Listeria* spp., NT4: *B. cereus*).

Importantly, the results for *E. coli* C-3000 also indicated specificity of this biosensor for target strains within the *E. coli* species. As *E. coli* C-3000 does not contain the target gene (Stx1) or complementary sequence to the probe, the samples with this DNA display GNP aggregation consistent with a negative result. Thus, the biosensor can specifically detect Shiga-toxin producing *E. coli* strains, which contain the Stx1 virulence gene [131]. This specificity is

essential as non-STEC *E. coli* strains that do not cause disease are often found in natural microflora [165].

It should also be noted that there was a smaller peak wavelength shift for *S.* Enteritidis compared to other non-target DNA species. While peak wavelength shift ranged from 130-140 nm for other non-targets, the mean peak wavelength shift for *S.* Enteritidis was 101 nm (Figure 5(a)). The exact cause of this is unknown; due to the high specificity of the oligonucleotide probe for STEC, annealing to *S.* Enteritidis DNA is highly unlikely. Thus, factors unrelated to probe specificity are most likely contributing to these results. As wavelength shift is dependent upon GNP aggregation, it is possible that lower quality DNA could have interfered with the aggregation process. A260/A230 and A260/A280 ratios were within appropriate ranges, but compromised DNA quality is still possible. Despite the reduced wavelength shift, there was still a significant difference between this non-target and the target DNA with 95% confidence, indicating specificity.

4.3.2 Sensitivity Testing of Pure *E. coli* O157 Cultures

A sensitivity analysis was performed to determine the detection limit of this biosensor for *E. coli* O157. *Listeria* spp. DNA was used as the non-target species. *Listeria monocytogenes* is another dangerous foodborne pathogen, with a 98% hospitalization rate and 16% mortality rate in the United States in 2019 [130]. Thus, differentiating between these species in foodborne pathogen detection mechanisms is of the utmost importance. First, target and non-target DNA was diluted by a factor of two between concentrations of 20 and 1.25 ng/µL. Then, each trial compared the target and non-target peak wavelength shift for samples of the same concentration.

The mean difference between target and non-target peak wavelength values at each DNA concentration are graphically represented in Figure 4.4 with 95% confidence intervals.

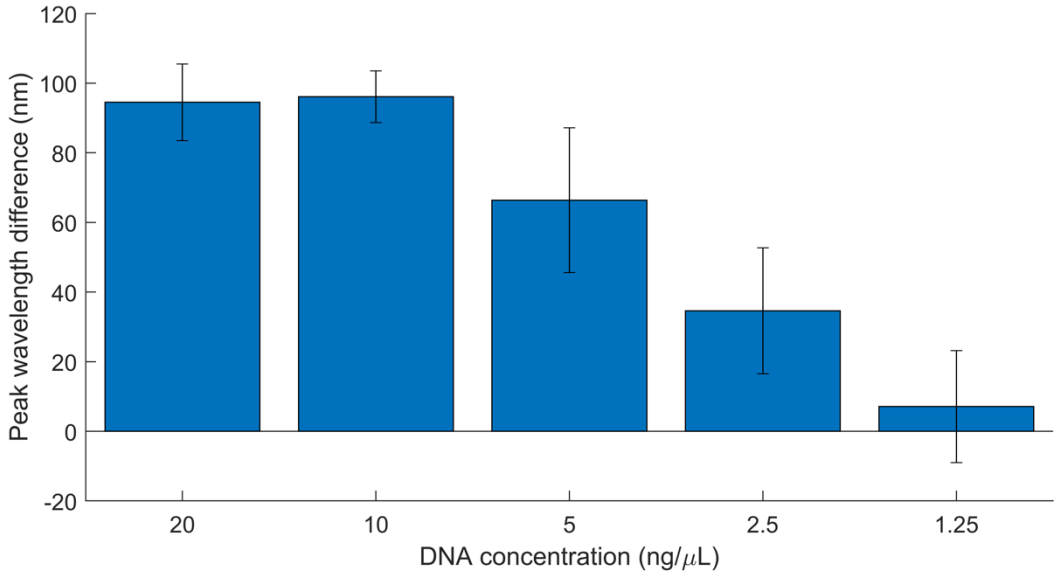

Figure 4.4 Paired mean difference between target (*E. coli* O157) and non-target (*Listeria* spp.) peak wavelength, 20-1.25 ng/µL. Error bars represent 95% confidence intervals.

Concentrations as low as 2.5 ng/µL showed a mean positive difference between the target and non-target peak wavelengths, with confidence intervals not overlapping zero. The lowest concentration of 1.25 ng/µL has a positive mean difference, but the confidence interval includes zero. Thus, reliable detection at this concentration cannot be established. This indicates the biosensor is reliably sensitive to a minimum of 2.5 ng/µL target DNA when compared to a non-target sample of the same concentration. Because lower concentrations do not produce consistent results, the lowest detection limit of the biosensor is 2.5 ng/µL when a target sample was compared to a non-target sample.

Sensitivity results also indicate that, while the biosensor can detect as high as 20 ng/µL (the highest concentration tested), the linear range of detection is between 2.5 and 10 ng/µL.

Above 10 ng/µL, data appears to be showing a hook effect, in which a high concentration of a biosensor's target ligand compared to the capturing molecule leads to decreased or no detection [166], [167]. In this case, the DNA concentration (target ligand) most likely oversaturates the probe concentration (capturing molecule), leading to the stagnation of peak wavelength difference shown at 20 ng/µL. If higher concentrations were tested, it is predicted that peak wavelength difference may begin to significantly decrease. Notably, the highest non-target DNA concentration tested (20 ng/µL) did have a reduced mean peak shift compared to lower non-target concentrations, although significance of this decrease at the 95% confidence level cannot be established (Figure 4.5). This trend may be explained by the high concentration of DNA strands in the sample interfering with tube aggregation. Thus, this may also contribute to the linear sensitivity trend disappearing at concentrations above 10 ng/µL.

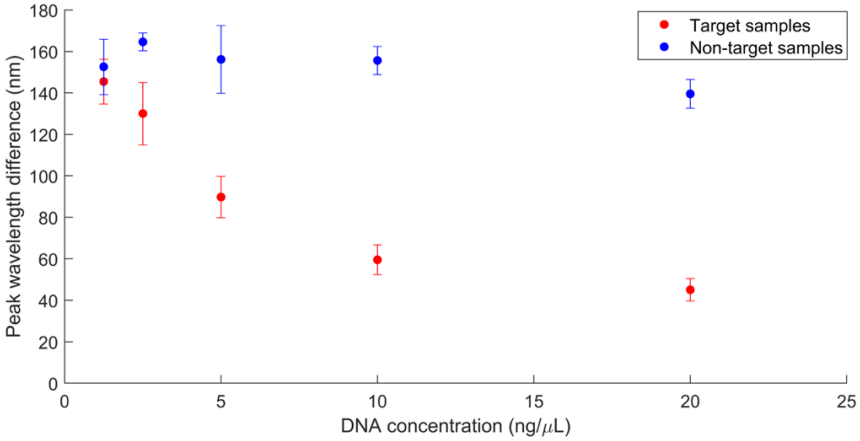

Figure 4.5 Target (*E. coli* O157) and non-target (*Listeria* spp.) peak wavelength shift from 520 nm at varying concentrations, 20-1.25 ng/µL. Error bars represent 95% confidence intervals of nine replicates.

4.3.3 Detection of DNA from food with *E. coli* O157 Biosensor

The *E. coli* O157 biosensor was first tested with DNA samples extracted from 4 hr spikes of bacteria previously concentrated from flour using MNPs. Based on plating of the concentrated sample before 4 hr incubation, the initial collected target bacteria concentration was

approximately 10^3 CFU/mL. This target sample from *E. coli* O157-inoculated flour was compared to a water control, two samples extracted from flour inoculated with other foodborne pathogens (*E. coli* C-3000, NT1, and *L. monocytogenes*, NT2), and one DNA sample extracted from magnetically separated flour that had not been artificially contaminated (NT3).

DNA extractions from flour not inoculated produced a DNA concentration of 55.6 ng/µL, while the *E. coli* O157-contaminated flour sample produced a concentration of 83.4 ng/µL. Thus, it may be assumed that this difference (approximately 28 ng/µL) is equivalent to the *E. coli* O157 DNA concentration in the target sample. Although variability in DNA yields must be acknowledged, this offers an estimate of the true target DNA concentration. To confirm that positive results for the target sample were not due to the higher DNA concentration, the biosensor was tested using all initial concentrations as well as a sample of the *E. coli* O157 DNA diluted to 60 ng/µL (T60). Results for six replicates are shown in Figure 4.6, with error bars representing 95% confidence intervals.

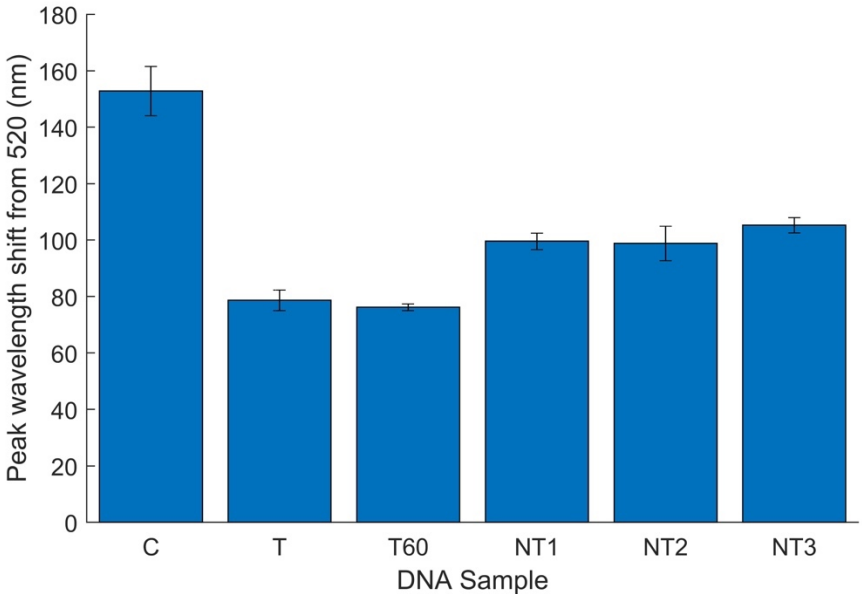

Figure 4.6 *E. coli* O157 specificity results in flour, analyzed by peak wavelength shift from 520 nm. 6 replicates total with DNA concentrations of 60 ± 4 ng/µL unless otherwise noted. Error bars represent 95% confidence intervals. (NC: water, T: *E. coli* O157 at 83.4 ng/µL, T60: *E. coli* O157 at 60 ng/µL, NT1: *E. coli* C-3000, NT2: *L. monocytogenes*, NT3: flour without artificial inoculation).

Both target samples (T and T60) showed significantly smaller peak shifts than all non-targets, indicating the success of this biosensor for direct detection of *E. coli* O157 from flour. Kruskal-Wallis and non-parametric Student-Neumann Keuls tests indicated significant differences between the wavelength shift of both target samples and all non-target samples with 95% confidence (Table 4.1, C.5, C.6, & C.7). The possible effect of DNA concentration on successful detection was also eliminated as the T60 sample and all non-targets had similar concentrations.

Table 4.1 Select results from non-parametric Student-Neumann Keuls testing for group comparisons, with a difference greater than the critical difference indicating significance. 6 replicates. (C: water, T: *E. coli* O157, NT1: *E. coli* C-3000, NT2: *Listeria monocytogenes*, NT3: flour without artificial inoculation).

	Difference	**Range**	**Critical Difference**
T60 vs C	176	6	104.00
T vs C	148	5	83.19
T60 vs NT3	130	5	83.19
T vs NT3	102	4	62.93
T60 vs NT1	93.5	4	62.93
T vs NT1	65.5	3	43.34
T60 vs NT2	88.5	3	43.34
T vs NT2	60.5	2	24.48

PCR amplification confirmed the presence of the target Stx1 gene in both pure cultures and DNA samples extracted from flour inoculated with *E. coli* O157 (Figure 4.7). Thus, the biosensor results aligned with PCR analysis.

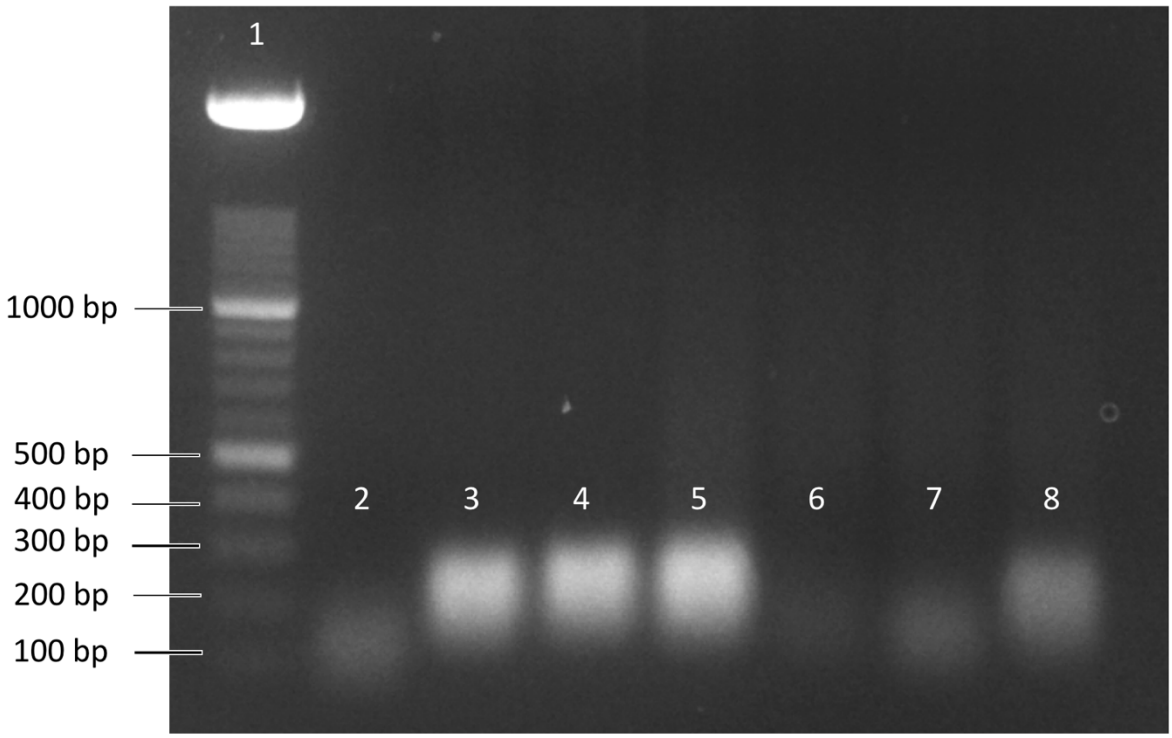

Figure 4.7 Gel electrophoresis results for PCR-amplified *E. coli* O157 DNA from flour.

Furthermore, as the T60 sample and all non-targets were of similar concentration, the effect of DNA concentration on successful detection was ruled out. The samples were then diluted to half their concentration (30 ng/µL total), at which the estimated target DNA concentration was approximately 10 ng/µL. At this concentration, the biosensor was not successful in detecting the target sample (Table 4.2). This lower sensitivity than pure DNA testing is most likely due to a "dilution effect," in which the presence of non-target DNA in a sample reduces the likelihood of successful detection [31], [168].

Table 4.2 *E. coli* O157 specificity results in flour samples diluted to 30 ng/µL, analyzed by peak wavelength shift from 520 nm. 6 replicates. (NC: water, T: *E. coli* O157, NT1: *E. coli* C-3000, NT2: *L. monocytogenes*, NT3: flour without artificial inoculation).

	NC	T	NT1	NT2	NT3
Average	659.75	610.17	610.25	614.08	649.67
Standard Deviation	14.35	7.78	8.29	8.78	34.98
95% Confidence Interval	14.34	7.77	8.28	8.77	34.95

As flour did not have a high concentration of natural microflora, with only a few colonies noted in MNP concentration experiments, it is likely that the other DNA present is from food matrix components that adhered to the MNPs during extraction. This is further evidenced by the extraction of 55.6 ng/µL of DNA from samples not artificially inoculated (NT3). This dilution effect may have had an even stronger impact on biosensor testing in spinach and romaine, both of which were shown to have significant natural microflora populations in initial MNP extraction tests. During biosensor testing, DNA samples extracted from *E. coli* O157-inoculated food were not statistically different than non-target food samples (Table 4.3).

Table 4.3 *E. coli* O157 specificity results in spinach and romaine samples at 25 and 12 ng/µL, respectively, analyzed by peak wavelength shift from 520 nm. 6 replicates. (NC: water, T: *E. coli* O157, NT1: *E. coli* C-3000, NT2: *L. monocytogenes*).

Sample	NC	T	NT1	NT2	NT3
Average (spinach)	655.42	653.75	648.75	650.83	689.75
Standard deviation (spinach)	11.87	8.99	10.38	9.49	6.85
Average (romaine)	645.08	629.25	621.92	608.5	647.00
Standard deviation (romaine)	0.20	8.70	7.15	4.67	2.92

Initial DNA concentrations were lower for spinach and romaine than they had been for flour, with yields of 24-27 ng/µL and 12-18 ng/µL, respectively. In fact, the difference between DNA yields for target-inoculated food and inoculation-free food was 0 ng/µL for spinach and 6 ng/µL for romaine. Thus, it is possible that little to no target DNA was present in these food

samples. Interference of food matrix components themselves may also play a role. For instance, humic acids are common in food and environmental samples and known to interfere with DNA-based detection assays if not properly removed [169]. In future work, DNA extraction kits specifically designed for bacterial extraction from these types of matrices, such as the Qiagen Powerlyzer PowerSoil kit, could improve results [170]. As a result of DNA extraction difficulties, as well as the high concentration of natural microflora, biosensor testing was unsuccessful at detecting target samples when compared to non-targets.

4.4 Conclusions

Experimental results indicate this colorimetric biosensor can successfully visually differentiate between target and non-target DNA at concentrations as low as 2.5 ng/µL. Unlike some colorimetric GNP biosensors [32], this procedure does not require a prolonged functionalization step for the GNP-probes before hybridization in a thermocycler. Due to the SDS-MUDA surface coating on the GNPs, aminated probes can quickly non-covalently bind to the GNP surface. As a result of this rapid non-covalent binding, the entire detection assay after genomic DNA extraction takes as little as 30 min. Due to the limited time and analytical equipment required, this biosensor can potentially increase the accessibility and affordability of rapid biosensors for *E. coli* O157.

Although the lowest detection limit of 2.5 ng/µL was achieved in pure cultures, the biosensor had a higher limit estimated to be above 8 ng/µL when detecting bacteria extracted from flour. There are multiple potential causes for this reduced sensitivity. For one, it is probable that DNA from the food matrix itself is extracted alongside bacterial DNA. Food particles were clearly visible in most concentrated samples, and the high concentration of DNA from pure flour

samples despite the lack of natural microflora on TSA plates indicates that food DNA was most likely extracted. In addition to the aforementioned dilution effect caused by the presence of food DNA, food particulates such as carbohydrates and fats are known to interfere with DNA-based detection assays [95], [98]. This presence of food particles could be potentially addressed through upstream process modifications; for instance, washing the concentrated sample in PBS and repeating magnetic extraction could reduce the food particles present in the sample selected for DNA extraction.

In addition, the failure of the biosensor to detect *E. coli* O157 from spinach and romaine may also be due to the high presence of natural microflora in the sample. In future studies, introducing a selective step before the biosensing itself may allow for more accurate detection from foods. One option could be the use of selective glycan coatings for specific concentration of target cells. Similarly, this colorimetric biosensor could be tested after sample treatment with the more thoroughly studied method of IMS, which would not only increase extraction specificity but also potentially lead to higher concentration factors [17]. Although IMS does not achieve the level of accessibility desired in this work, successful biosensor detection using this pre-treatment method could be used to establish a proof-of-concept for reliable foodborne pathogen detection while a species-specific glycan was designed. Finally, a selective broth, as opposed to Tryptic Soy Broth, could be implemented to reduce the growth of non-target pathogens during the 4 hr incubation period before DNA extraction. Many types of broth have been designed to selectively enhance the growth of *E. coli* O157 and other dangerous foodborne pathogens; however, the selectivity is typically analyzed only after 12-24 hr of incubation [171], [172]. Thus, the success of this technique on samples incubated for only 4 hr is currently unknown.

Despite the continued work required for reliable detection of pathogens directly from foods, initial results are promising. The biosensor has been shown to be highly specific and sensitive, with results in under 30 min after DNA extraction. The improved assay for probe functionalization also significantly reduced preparation time required before biosensor implementation [31]. Finally, successful food detection from flour was achieved after only 4 hr of incubation, rivaling existing work that required 6 hr of growth before DNA detection. With future improvements, this biosensor can be an accessible and rapid detection method for foodborne pathogens.

Chapter 5: Conclusions

The information collected throughout this thesis indicates the potential of a combined magnetic and gold nanoparticle technique for rapid and cost-effective foodborne pathogen detection. MNPs successfully captured target bacteria from all food matrices tested, and the GNP biosensor for *E. coli* O157 was sensitive to concentrations of DNA from pure cultures as low as 2.5 ng/μL. However, further optimization is required to prepare this technology for real-world applicability. For instance, although MNP concentration of bacteria was achieved to over 60 times its initial concentration from PBS samples, concentration factors in food ranged from 0.46 to 11.62. Similarly, the biosensor encountered issues with detecting *E. coli* O157 from some artificially inoculated food matrices, with detection achieved for flour but not for the leafy greens (romaine and spinach) tested. Thus, although proof-of-concept has been achieved, further work is required for this technology to compete with existing rapid detection methods directly from foods.

Several key steps were taken towards elucidating the mechanism of this assay, allowing for further optimization. For instance, there is no evidence in literature that glycan-coated magnetic separation has been conducted on sample volumes as large as 100 mL. Thus, data collected in this thesis is more directly applicable and comparable to existing BAM methods. In addition, the further studies into factors affecting the success of both magnetic extraction and biosensor detection allow for future improvements. Finally, this work successfully integrated an extraction and detection method for *E. coli* O157 from foods based on low-cost nanoparticle assays. Although results were mixed, the reliable detection of *E. coli* O157 from flour with this integrated procedure proves the capabilities of this combined assay for accessible and affordable foodborne pathogen detection within a single work day.

While low-cost materials and simple procedures are already used in this assay, accessibility can be further increased through future improvements. For instance, although colorimetric biosensor results were confirmed in this work through absorbance measurements on a NanoDrop, results could also be quantified without the need for spectrophotometry. Smart phone imaging has been shown to be capable of differentiating between aggregated and non-aggregated GNPs by identifying the color change [173], and a phone application could easily be designed for application with this biosensor. At its current state, the other significant equipment need in this assay is the thermocycler for DNA/probe hybridization. Due to the simple and static temperature conditions (95 ºC for 5 min and 55 ºC for 10 min), the need for a thermocycler could potentially be eliminated through the use of a hot water bath. Similar water bath usage has been suggested for isothermal nucleic acid based detection mechanisms [6], [100].

Optimization of this biosensing technique for detection of bacteria from foods would most thoroughly be improved through modifications to the upstream extraction and concentration process using MNPs. As noted previously, although successful MNP capture of target bacteria was achieved from all food matrices, the continued presence of food particles and natural microflora, as well as the limited concentration of target bacteria, may be responsible for the unsuccessful biosensor results with some food samples. Thus, three suggestions are proposed for future improvements. First, contamination with food particles should be reduced by implementing washing steps after initial magnetic separation. Second, generalized bacterial capture may be improved by functionalizing MNPs with amino acids to increase their positive charge. Third, in matrices with high levels of natural microflora, a species-specific glycan should be designed to selectively capture the bacterial species for which the food sample is being tested.

Foodborne illness is still responsible for hundreds of thousands of deaths in the world each year, and detection of contaminated foods before they reach the consumer is an essential step to reducing this statistic. However, current assays do not yet fulfill the need for affordable, accessible, and rapid detection. In this work, a novel technique using gold and magnetic nanoparticles was designed and tested to directly address these needs. Current results indicate that this integrated extraction and detection method can successfully detect bacteria directly from food matrices in approximately 6 hr. In addition, as specificity is based solely on the probe sequence, this assay can be easily modified to target a wide variety of foodborne pathogens. With further optimization and improvements in accessibility, this assay could be implemented in a wide variety of food matrices to prevent deaths and illnesses on a global scale.

APPENDICES

Appendix A. Additional Microscopic Imaging of MNP-Bacteria Interactions

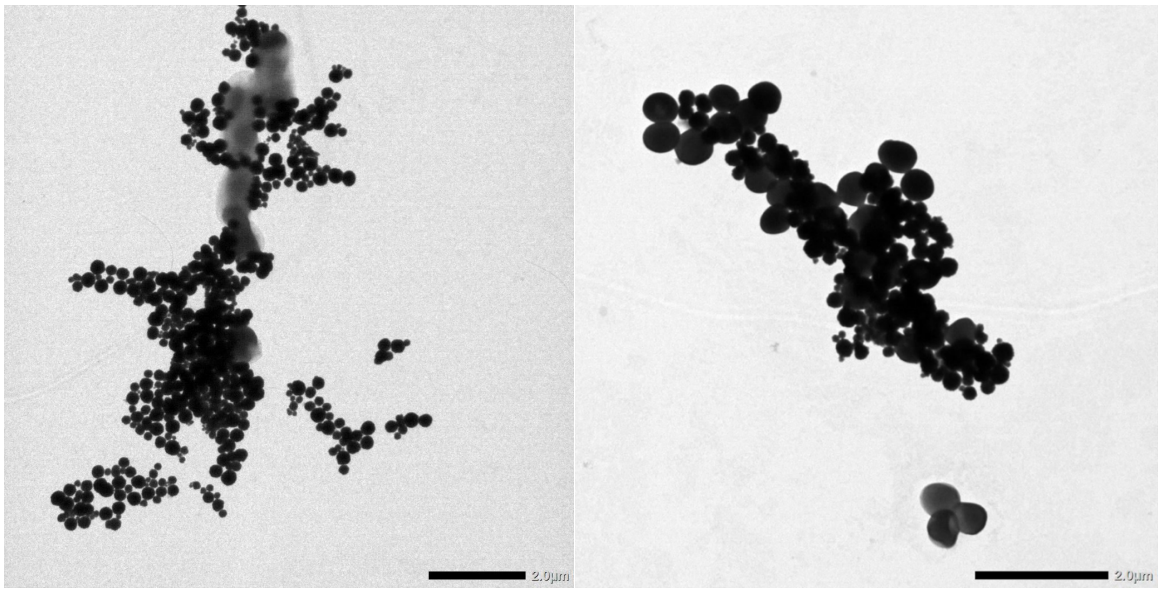

Figure A.1 TEM image of A) *E. coli* O157-MNP interactions and B) *S. aureus*-MNP interactions.

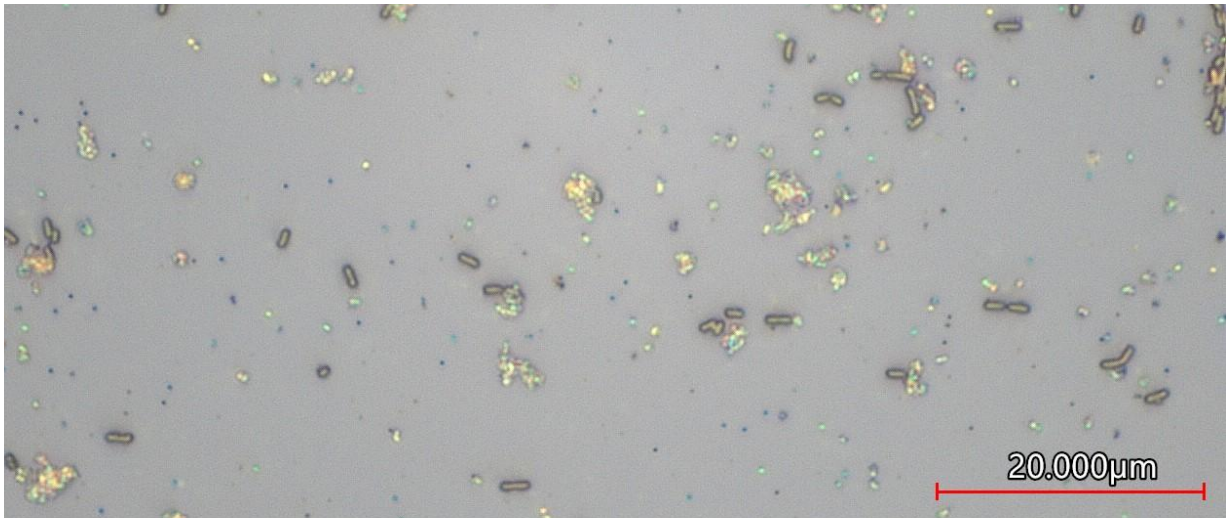

Figure A.2 Microscopic image of *Listeria*-MNP interactions with confocal laser microscopy.

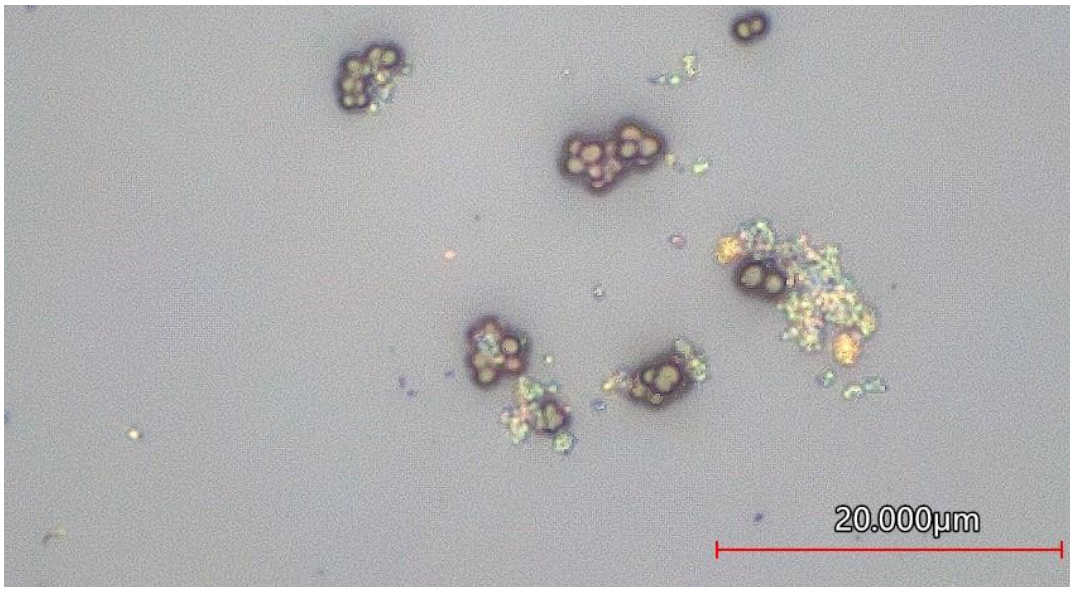

Figure A.3 Confocal laser microscope image of *S. aureus*-MNP interaction.

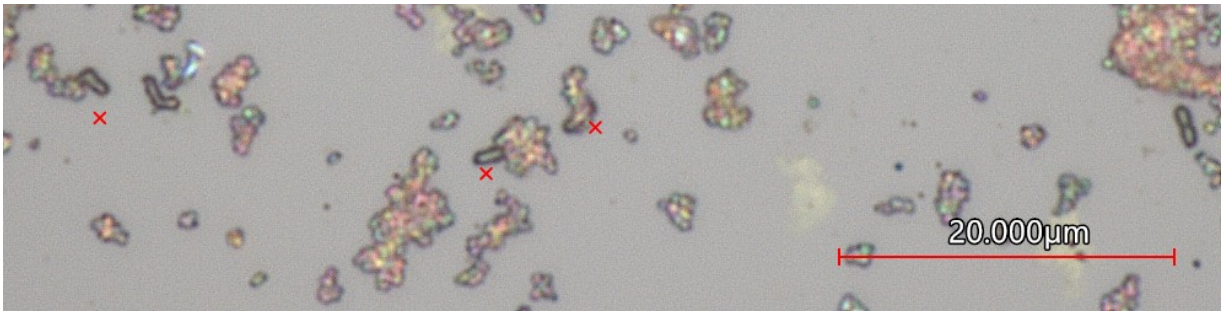

Figure A.4 Confocal laser microscope image of *E. coli* O157-MNP interaction.

Appendix B. Supplementary Data for Magnetic Nanoparticle Extraction

Table B.1 Food matrix extraction results.

Bacteria	**pH**	**Matrix**	**CF**	**Standard Deviation**
S. aureus	6	Milk	11.62	5.64
S. aureus	7	Milk	0.85	0.15
S. aureus	6	Sausage	0.98	0.17
S. aureus	7	Sausage	0.85	0.30
S. aureus	6	Deli Ham	0.96	0.25
S. aureus	7	Deli Ham	1.63	0.94
S. aureus	6	Romaine Lettuce	2.56	1.33
S. aureus	7	Romaine Lettuce	1.70	0.56
L. monocytogenes	6	Deli Ham	0.66	0.22
L. monocytogenes	7	Deli Ham	0.53	0.25
L. monocytogenes	6	Milk	0.46	0.08
L. monocytogenes	7	Milk	0.55	0.24
L. monocytogenes	7	Romaine Lettuce	0.74	0.16
L. monocytogenes	7	Sausage	2.50	0.79
E. coli O157	6	Romaine Lettuce	0.94	0.65
E. coli O157	7	Romaine Lettuce	0.87	0.44
E. coli O157	6	Spinach	2.30	1.45
E. coli O157	7	Spinach	2.54	0.80
E. coli O157	7	Flour	1.03	0.22
E. coli O157	7	Chicken Salad	0.60	0.21

Appendix C. Supplementary Data for *E. coli* O157 Colorimetric Biosensor

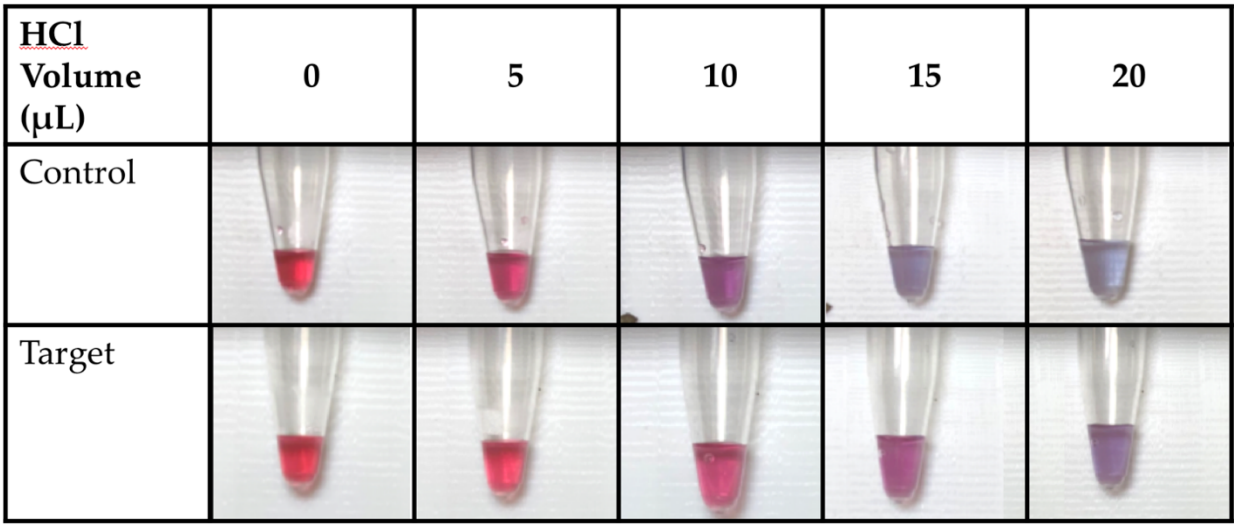

Figure C.1 Visual results for one optimization trial using specific *E. coli* O157 biosensor.

Table C.1 Statistical analysis of biosensor results after 5 and 10 min (9 replicates per sample). Readings were stopped after 10 min due to lack of visual differentiation between target and non-target tubes at 15 min.

	C	T	NT1	NT2	NT3	NT4
	Results after 5 min					
Average	118.1	54.2	106.8	83.1	103.1	106.9
SE	3.73	2.11	4.79	2.39	2.84	5.34
tcrit	2.26	2.26	2.26	2.26	2.26	2.26
95% CI	109.7 - 126.5	49.4 - 59.0	96.0 - 117.7	77.6 - 88.5	96.6 - 109.5	94.8 - 119.0
	Results after 10 min					
Average	147.2	64.2	141.5	101.2	133.9	137.1
SE	2.52	2.62	3.11	2.57	4.90	7.08
tcrit	2.26	2.26	2.26	2.26	2.26	2.26
95% CI	141.5 - 152.9	58.2 - 70.1	134.5 - 148.5	95.4 - 107.0	122.9 - 145.1	121.0 - 153.1

Table C.2 Peak wavelength shift data for 9 replicates in *E. coli* O157 GNP biosensor specificity testing and 95% confidence interval testing (C: water, NT1: *E. coli* C-3000, NT2: *S.* Enteritidis, NT3: *Listeria* spp., NT4: *B. cereus*, n: number of trials).

	Peak wavelength shift from 520 nm (nm)					
	C	**T**	**NT1**	**NT2**	**NT3**	**NT4**
Trial 1	143	52.5	133.5	107.5	133.5	133.5
Trial 2	157.5	67.5	141	91.5	113	133.5
Trial 3	134.5	75	134.5	99.5	134.5	169
Trial 4	153.5	68	153	91	139	142
Trial 5	157.5	68	157	111.5	157	145.5
Trial 6	144	58.5	133	112	145.5	88
Trial 7	144.5	56.5	145.5	99.5	145.5	144.5
Trial 8	144.5	58.5	145	99	119	138.5
Trial 9	146	73	131	99	118.5	139
Average	147.22	64.17	141.50	101.17	133.94	137.06
St. dev.	7.56	7.87	9.33	7.71	14.69	21.24
n	9	9	9	9	9	9
SE	2.52	2.62	3.11	2.57	4.90	7.08
tcrit	2.26	2.26	2.26	2.26	2.26	2.26
tcrit*SE	5.70	5.93	7.04	5.82	11.07	16.02
UL95%	152.92	70.10	148.54	106.98	145.02	153.07
LL95%	141.52	58.24	134.46	95.35	122.87	121.04

Table C.3 Statistical analysis of *E. coli* O157 GNP biosensor specificity using Kruskal-Wallis (C: water, NT1: *E. coli* C-3000, NT2: *S.* Enteritidis, NT3: *Listeria* spp., NT4: *B. cereus*, n: number of trials).

	Ranked data - Kruskal-Wallis					
	C	**T**	**NT1**	**NT2**	**NT3**	**NT4**
Trial 1	18	54	28.5	38	28.5	28.5
Trial 2	2.5	50	20	43	35	28.5
Trial 3	25	46	25	39.5	25	1
Trial 4	6	48.5	7	44	21.5	19
Trial 5	2.5	48.5	4.5	37	4.5	10.5
Trial 6	17	51.5	31	36	10.5	45
Trial 7	15	53	10.5	39.5	10.5	15
Trial 8	15	51.5	13	41.5	33	23
Trial 9	8	47	32	41.5	34	21.5
n	9	9	9	9	9	9
sum ranks	109	450	171.5	360	202.5	192
mean rank	12.11	50.00	19.06	40.00	22.50	21.33
Rank	1	6	2	5	4	3
Chi^2 calc (H)	37.59					
Chi crit	11.07					

Table C.4 Statistical analysis of *E. coli* O157 GNP biosensor specificity using non-parametric Student-Neumann Keuls tests (C: water, NT1: *E. coli* C-3000, NT2: *S.* Enteritidis, NT3: *Listeria* spp., NT4: *B. cereus*).

Initial Calculations					
Range	2	3	4	5	6
Pooled SE	16.02	23.81	31.61	39.40	47.20
Qcrit	2.77	3.31	3.63	3.86	4.03
Critical difference = Qcrit*pooled SE	44.40	78.91	114.83	152.01	190.20

Calculation of Individual Differences			
Comparison	**Difference**	**Range**	**Critical difference**
C vs T	341	6	190.20
C vs NT2	251	5	152.01
C vs NT4	83	4	114.83
C vs NT3	93.5	3	78.91
C vs NT1	62.5	2	44.40
NT1 vs T	278.5	5	152.01
NT1 vs NT2	188.5	4	114.83
NT1 vs NT3	31	3	78.91
NT1 vs NT4	20.5	2	44.40
NT4 vs T	258	4	114.83
NT4 vs NT2	168	3	78.91
NT4 vs NT3	10.5	2	44.40
NT3 vs T	247.5	3	78.91
NT3 vs NT2	157.5	2	44.40
NT2 vs T	90	2	44.40

Table C.5 Peak wavelength shift data for 6 replicates of *E. coli* O157 GNP biosensor with flour samples and 95% confidence interval testing (NC: water, T: *E. coli* O157 at 83.4 ng/µL, T60: *E. coli* O157 at 60 ng/µL, NT1: *E. coli* C-3000, NT2: *L. monocytogenes*, n: number of trials).

	NC	T	T60	NT1	NT2	NT3
Trial 1	663.5	597	596.5	618.5	618	628
Trial 2	662	606	597.5	618.5	617.5	628.5
Trial 3	670.5	597.5	596.5	618.5	610.5	621
Trial 4	680.5	597.5	596.5	619	619	624.5
Trial 5	681	597	596.5	617.5	629.5	625
Trial 6	679.5	597	594	625.5	618.5	625
Average	672.83	598.67	596.25	619.58	618.83	625.33
St. dev.	8.72	3.60	1.17	2.94	6.10	2.71
n	6	6	6	6	6	6
SE	3.56	1.47	0.48	1.20	2.49	1.11
tcrit	2.45	2.45	2.45	2.45	2.45	2.45
tcrit*SE	8.71	3.60	1.17	2.94	6.09	2.71
UL95%	681.54	602.26	597.42	622.52	624.92	628.04
LL95%	664.13	595.07	595.08	616.65	612.74	622.62

Table C.6 Statistical analysis of *E. coli* O157 GNP biosensor with flour samples using Kruskal-Wallis (NC: water, T: *E. coli* O157 at 83.4 ng/µL, T60: *E. coli* O157 at 60 ng/µL, NT1: *E. coli* C-3000, NT2: *L. monocytogenes*, n: number of trials).

	Ranked data - Kruskal-Wallis					
	C	**T**	**T60**	**NT1**	**NT2**	**NT3**
Trial 1	5	30	33.5	18.5	21	9
Trial 2	6	25	27	18.5	22.5	8
Trial 3	4	27	33.5	18.5	24	14
Trial 4	2	27	33.5	15.5	15.5	13
Trial 5	1	30	33.5	22.5	7	11.5
Trial 6	3	30	36	10	18.5	11.5
n	6	6	6	6	6	6
sum ranks	21	169	197	103.5	108.5	67
mean rank	3.50	28.17	32.83	17.25	18.08	11.17
Rank	1	5	6	3	4	2
Chi^2 calc (H)	31.32					
Chi crit	11.07					

Table C.7 Statistical analysis of *E. coli* O157 GNP biosensor with flour samples using Non-Parametric Student-Neumann-Keuls (NC: water, T: *E. coli* O157 at 83.4 ng/µL, T60: *E. coli* O157 at 60 ng/µL, NT1: *E. coli* C-3000, NT2: *L. monocytogenes*).

Initial Calculations					
Range	2	3	4	5	6
Pooled SE	8.83	13.08	17.32	21.56	25.81
Qcrit	2.77	3.31	3.63	3.86	4.03
Critical difference = Qcrit*pooled SE	24.48	43.34	62.93	83.19	104.00

Calculation of Individual Differences			
	Difference	**Range**	**Critical difference**
C vs T60	176	6	104.00
C vs T	148	5	83.19
C vs NT2	87.5	4	62.93
C vs NT1	82.5	3	43.34
C vs NT3	46	2	24.48
NT3 vs T60	130	5	83.19
NT3 vs T	102	4	62.93
NT3 vs NT2	41.5	3	43.34
NT3 vs NT1	36.5	2	24.48
NT1 vs T60	93.5	4	62.93
NT1 vs T	65.5	3	43.34
NT1 vs NT2	5	2	24.48
NT2 vs T60	88.5	3	43.34
NT2 vs T	60.5	2	24.48
T vs T60	28	2	24.48

BIBLIOGRAPHY

BIBLIOGRAPHY

[1] World Health Organization. *WHO estimates of the global burden of foodborne diseases: foodborne disease burden epidemiology reference group 2007-2015*. 2015. Available online: https://apps.who.int/iris/handle/10665/199350 (accessed on 12 November 2021).

[2] R. L. Scharff, "Economic burden from health losses due to foodborne illness in the United States," *J. Food Prot.*, vol. 75, no. 1, pp. 123–131, Jan. 2012, doi: 10.4315/0362-028X.JFP-11-058.

[3] T. Bintsis, "Foodborne pathogens," *AIMS Microbiol.*, vol. 3, no. 3, pp. 529–563, 2017, doi: 10.3934/MICROBIOL.2017.3.529.

[4] S. D. Bennett, S. V Sodha, T. L. Ayers, M. F. Lynch, L. H. Gould, and R. V Tauxe, "Produce-associated foodborne disease outbreaks, USA, 1998 – 2013," *Epidemiol. Infect.*, vol. 146, no. 11, pp. 1397–1406, 2018, doi: doi:10.1017/S0950268818001620.

[5] P. K. Mandal, A. K. Biswas, K. Choi, and U. K. Pal, "Methods for Rapid Detection of Foodborne Pathogens: An Overview," *Am. J. Food Technol.*, vol. 6, no. 2, pp. 87–102, Jan. 2011, doi: 10.3923/ajft.2011.87.102.

[6] J. W.-F. Law, N.-S. Ab Mutalib, K.-G. Chan, and L.-H. Lee, "Rapid methods for the detection of foodborne bacterial pathogens: principles, applications, advantages and limitations," *Front. Microbiol.*, vol. 5, Jan. 2015, doi: 10.3389/fmicb.2014.00770.

[7] M. A. Hussain and C. O. Dawson, "Economic impact of food safety outbreaks on food businesses," *Foods*, vol. 2, no. 4, pp. 585–589, 2013, doi: 10.3390/foods2040585.

[8] S. H. Park *et al.*, "Current and emerging technologies for rapid detection and characterization of Salmonella in poultry and poultry products," *Food Microbiol.*, vol. 38, pp. 250–262, Apr. 2014, doi: 10.1016/j.fm.2013.10.002.

[9] H. Yadav, D. Shah, S. Sayed, S. Horton, and L. F. Schroeder, "Availability of essential diagnostics in ten low-income and middle-income countries: results from national health facility surveys," *Lancet Glob. Heal.*, vol. 9, no. 11, pp. e1553–e1560, Nov. 2021, doi: 10.1016/ S2214-109X(21)00442-3.

[10] K. A. Fleming *et al.*, "The Lancet Commission on diagnostics: transforming access to diagnostics," *Lancet*, vol. 398, no. 10315, pp. 1997–2050, Nov. 2021, doi: 10.1016/ S0140-6736(21)00673-5.

[11] T. Di Febo *et al.*, "Development of a Capture ELISA for Rapid Detection of Salmonella enterica in Food Samples," *Food Anal. Methods*, vol. 12, no. 2, pp. 322–330, Feb. 2019, doi: 10.1007/S12161-018-1363-2/TABLES/5.

[12] Z. Zhang, J. Zhou, and X. Du, "Electrochemical Biosensors for Detection of Foodborne

Pathogens," *Micromachines 2019, Vol. 10, Page 222*, vol. 10, no. 4, p. 222, Mar. 2019, doi: 10.3390/MI10040222.

[13] M.-C. Lim, J. Y. Park, K. Park, G. Ok, H.-J. Jang, and S.-W. Choi, "An automated system for separation and concentration of food-borne pathogens using immunomagnetic separation," *Food Control*, vol. 73, no. Part B, pp. 1541–1547, 2016, doi: 10.1016/j.foodcont.2016.11.021.

[14] M. C. Thomas, M. J. Shields, K. R. Hahn, T. W. Janzen, N. Goji, and K. K. Amoako, "Evaluation of DNA extraction methods for Bacillus anthracis spores isolated from spiked food samples," *J. Appl. Microbiol.*, vol. 115, no. 1, pp. 156–162, Jul. 2013, doi: 10.1111/JAM.12206.

[15] U.S. Food and Drug Administration, "Bacteriological Analytical Manual (BAM)." 2021, Accessed: Oct. 04, 2021. [Online]. Available: https://www.fda.gov/food/laboratory-methods-food/bacteriological-analytical-manual-bam.

[16] Z. Wang, R. Cai, Z. Gao, Y. Yuan, and T. Yue, "Immunomagnetic separation: An effective pretreatment technology for isolation and enrichment in food microorganisms detection," *Compr. Rev. Food Sci. Food Saf.*, vol. 19, no. 6, pp. 3802–3824, Nov. 2020, doi: 10.1111/1541-4337.12656.

[17] A. C. Vinayaka *et al.*, "Rapid detection of Salmonella enterica in food samples by a novel approach with combination of sample concentration and direct PCR," *Biosens. Bioelectron.*, vol. 129, pp. 224–230, Mar. 2019, doi: 10.1016/j.bios.2018.09.078.

[18] L. Barre, E. Brasseur, C. Doux, B. Lombard, and N. G. Besse, "Sensitive enumeration of Listeria monocytogenes and other Listeria species in various naturally contaminated matrices using a membrane filtration method," *Food Microbiol.*, vol. 48, pp. 171–177, Jun. 2015, doi: 10.1016/j.fm.2014.10.012.

[19] C. Zhou, J. Wang, R. Li, and K. Ye, "High-throughput sequencing analysis of the bacterial community for assessing the differences in extraction methods of bacteria separation from chilled pork," *LWT*, vol. 134, no. 110213, Dec. 2020, doi: 10.1016/j.lwt.2020.110213.

[20] K. El-Boubbou, C. Gruden, and X. Huang, "Magnetic Glyco-nanoparticles: A Unique Tool for Rapid Pathogen Detection, Decontamination, and Strain Differentiation," *J. AM. CHEM. SOC*, vol. 129, p. 52, 2007, doi: 10.1021/ja076086e.

[21] L. L. Matta, "Biosensing total bacterial load in liquid matrices to improve food supply chain safety using carbohydrate-functionalized magnetic nanoparticles for cell capture and gold nanoparticles for signaling," Michigan State Univeristy, 2018.

[22] L. L. Matta and E. C. Alocilja, "Emerging nano-biosensing with suspended MNP microbial extraction and EANP labeling," *Biosens. Bioelectron.*, vol. 117, pp. 781–793, Oct. 2018, doi: 10.1016/j.bios.2018.07.007.

[23] F. Kveton, A. Blsakova, P. Kasak, and J. Tkac, "Glycan Nanobiosensors," *Nanomaterials*,

vol. 10, no. 7, p. 1406, Jul. 2020, doi: 10.3390/nano10071406.

[24] E. Uribe, T. J. Steele, R. C. Richards, and K. V. Ewart, “Ligand and pathogen specificity of the Atlantic salmon serum C-type lectin,” *Biochim. Biophys. Acta - Gen. Subj.*, vol. 1830, no. 1, pp. 2129–2138, 2013, doi: 10.1016/j.bbagen.2012.09.019.

[25] N. K. Broeker *et al.*, “Complex carbohydrate recognition by proteins: Fundamental insights from bacteriophage cell adhesion systems,” *Perspect. Sci.*, vol. 11, pp. 45–52, 2017, doi: 10.1016/j.pisc.2016.10.001.

[26] L. L. Matta and E. C. Alocilja, “Carbohydrate Ligands on Magnetic Nanoparticles for Centrifuge-Free Extraction of Pathogenic Contaminants in Pasteurized Milk,” *J. Food Prot.*, vol. 81, no. 12, pp. 1941–1949, Dec. 2018, doi: 10.4315/0362-028X.JFP-18-040.

[27] S.-M. You, K.-B. Jeong, K. Luo, J.-S. Park, J.-W. Park, and Y.-R. Kim, “Paper-based colorimetric detection of pathogenic bacteria in food through magnetic separation and enzyme-mediated signal amplification on paper disc,” *Anal. Chim. Acta*, vol. 1151, no. 338252, 2021, doi: 10.1016/j.aca.2021.338252.

[28] M. Cohen, “Notable aspects of glycan-protein interactions,” *Biomolecules*, vol. 5, no. 3, pp. 2056–2072, 2015, doi: 10.3390/biom5032056.

[29] R. K. Briceno, S. R. Sergent, S. M. Benites, and E. C. Alocilja, “Nanoparticle-Based Biosensing Assay for Universally Accessible Low-Cost TB Detection with Comparable Sensitivity as Culture,” *Diagnostics*, vol. 9, no. 4, p. 222, Dec. 2019, doi: 10.3390/diagnostics9040222.

[30] L. L. Matta, J. Harrison, G. S. Deol, and E. C. Alocilja, “Carbohydrate-Functionalized Nanobiosensor for Rapid Extraction of Pathogenic Bacteria Directly from Complex Liquids with Quick Detection Using Cyclic Voltammetry,” *IEEE Trans. Nanotechnol.*, vol. 17, no. 5, pp. 1006–1013, 2018, doi: 10.1109/TNANO.2018.2841320.

[31] I. A. Quintela, B. G. de los Reyes, C.-S. Lin, and V. C. H. Wu, “Simultaneous Colorimetric Detection of a Variety of Salmonella spp. in Food and Environmental Samples by Optical Biosensing Using Oligonucleotide-Gold Nanoparticles,” *Front. Microbiol.*, vol. 10, no. 1138, 2019, doi: 10.3389/FMICB.2019.01138.

[32] P. Bakthavathsalam, V. K. Rajendran, and J. A. Baquir Mohammed, “A direct detection of Escherichia coli genomic DNA using gold nanoprobes,” *J. Nanobiotechnology*, vol. 10, no. 8, Feb. 2012, doi: 10.1186/1477-3155-10-8.

[33] S. Ahmadi, H. Kamaladini, F. Haddadi, and M. R. Sharifmoghadam, “Thiol-Capped Gold Nanoparticle Biosensors for Rapid and Sensitive Visual Colorimetric Detection of Klebsiella pneumoniae,” *J. Fluoresc.*, vol. 28, pp. 987–998, Jul. 2018, doi: 10.1007/S10895-018-2262-z.

[34] E. Dester and E. Alocilja, “Current Methods for Extraction and Concentration of Foodborne Bacteria with Glycan-Coated Magnetic Nanoparticles: A Review,” *Biosens.*

2022, Vol. 12, Page 112, vol. 12, no. 2, p. 112, Feb. 2022, doi: 10.3390/BIOS12020112.

[35] J.-H. Kim and S.-W. Oh, "Pretreatment methods for nucleic acid-based rapid detection of pathogens in food: A review," *Food Control*, vol. 121, p. 107575, 2021, doi: 10.1016/j.foodcont.2020.107575.

[36] F. Huang, Y. Zhang, J. Lin, and Y. Liu, "Biosensors coupled with signal amplification technology for the detection of pathogenic bacteria: A review," *Biosensors*, vol. 11, no. 6, 2021, doi: 10.3390/bios11060190.

[37] H. V. Hsieh, J. L. Dantzler, and B. H. Weigl, "Analytical Tools to Improve Optimization Procedures for Lateral Flow Assays," *Diagnostics*, vol. 7, no. 2, p. 29, May 2017, doi: 10.3390/DIAGNOSTICS7020029.

[38] A. A. Ali, A. B. Altemimi, N. Alhelfi, and S. A. Ibrahim, "Application of Biosensors for Detection of Pathogenic Food Bacteria: A Review," *Biosensors*, vol. 10, no. 6, p. 58, May 2020, doi: 10.3390/bios10060058.

[39] D. Seinige, M. Von Köckritz-Blickwede, C. Krischek, G. Klein, and C. Kehrenberg, "Influencing factors and applicability of the viability Ema-qpcr for a detection and quantification of Campylobacter cells from water samples," *PLoS One*, vol. 9, no. 11, Nov. 2014, doi: 10.1371/journal.pone.0113812.

[40] Y. Choi *et al.*, "Comparison of Upgraded Methods for Detecting Pathogenic Escherichia coli in Foods Using Centrifugation or Filtration," *Korean J. Food Sci. An*, vol. 37, no. 6, pp. 799–803, 2017, doi: 10.5851/kosfa.2017.37.6.799.

[41] R. Wang, Y. Xu, H. Liu, J. Peng, J. Irudayaraj, and F. Cui, "An integrated microsystem with dielectrophoresis enrichment and impedance detection for detection of Escherichia coli," *Biomed. Microdevices*, vol. 19, no. 34, Apr. 2017, doi: 10.1007/S10544-017-0167-2.

[42] U. S. K. Rathnayaka and S. K. Rakshit, "Evaluation of metal hydroxide immobilization and DNA extraction methods on detection of Salmonella enterica from pork sausage by nested polymerase chain reaction," *J. Muscle Foods*, vol. 21, no. 4, pp. 801–812, Oct. 2010, doi: 10.1111/J.1745-4573.2010.00220.X.

[43] C.-T. Chen, P. M. Reddy, Y.-R. Ma, and Y.-P. Ho, "Mass spectrometric identification of pathogens in foods using a zirconium hydroxide immobilization approach," *Int. J. Mass Spectrom.*, vol. 312, pp. 45–52, Feb. 2012, doi: 10.1016/j.ijms.2011.05.014.

[44] O. A. Triplett, J. Xuan, S. Foley, R. Nayak, and W. H. Tolleson, "Immunomagnetic Capture of Big Six Shiga Toxin–Producing Escherichia coli Strains in Apple Juice with Detection by Multiplex Real-Time PCR Eliminates Interference from the Food Matrix," *J. Food Prot.*, vol. 82, no. 9, pp. 1512–1523, Sep. 2019, doi: 10.4315/0362-028X.JFP-19-134.

[45] M. F. Diouani *et al.*, "Magnetic separation and centri-chronoamperometric detection of

foodborne bacteria using antibiotic-coated metallic nanoparticles," *Biosensors*, vol. 11, no. 7, 2021, doi: 10.3390/bios11070205.

[46] K. A. Stevens and L. A. Jaykus, "Bacterial separation and concentration from complex sample matrices: A review," *Critical Reviews in Microbiology*, vol. 30, no. 1. pp. 7–24, 2004, doi: 10.1080/10408410490266410.

[47] N. Bhusal, S. Shrestha, N. Pote, and E. C. Alocilja, "Nanoparticle-based biosensing of tuberculosis, an affordable and practical alternative to current methods," *Biosensors*, vol. 9, no. 1, Mar. 2019, doi: 10.3390/BIOS9010001.

[48] J. Castelló, M. Gallardo, M. Antònia Busquets, and J. Estelrich, "Chitosan (or alginate)-coated iron oxide nanoparticles: A comparative study," *Physicochem. Eng. Asp.*, vol. 468, pp. 151–158, 2015, doi: 10.1016/j.colsurfa.2014.12.031.

[49] T. M. Ways, W. Lau, and V. Khutoryanskiy, "Chitosan and Its Derivatives for Application in Mucoadhesive Drug Delivery Systems," *Polymers (Basel).*, vol. 10, no. 3, p. 267, Mar. 2018, doi: 10.3390/polym10030267.

[50] P. W. Benoit and D. W. Donahue, "Methods for Rapid Separation and Concentration of Bacteria in Food that Bypass Time-Consuming Cultural Enrichment," *J. Food Prot.*, vol. 66, no. 10, pp. 1935–1948, 2003, Accessed: Jun. 15, 2021. [Online]. Available: http://meridian.allenpress.com/jfp/article-pdf/66/10/1935/1675695/0362-028x-66_10_1935.pdf.

[51] H. Fukushima, K. Katsube, Y. Hata, R. Kishi, and S. Fujiwara, "Rapid separation and concentration of food-borne pathogens in food samples prior to quantification by viable-cell counting and real-time PCR," *Appl. Environ. Microbiol.*, vol. 73, no. 1, pp. 92–100, Jan. 2007, doi: 10.1128/AEM.01772-06.

[52] R. Ágoston, "Rapid Concentration of Bacillus and Clostridium Spores from Large Volumes of Milk, Using Continuous Flow Centrifugation," *J. Food Prot.*, vol. 72, no. 3, pp. 666–668, 2009, Accessed: Jun. 15, 2021. [Online]. Available: https://www-proquest-com.proxy2.cl.msu.edu/docview/231345365.

[53] R. Lindqvist, "Preparation of PCR samples from food by a rapid and simple centrifugation technique evaluated by detection of Escherichia coli 0157:H7," *Int. J. Food Microbiol.*, vol. 37, pp. 73–82, 1997.

[54] C. M. Armstrong, A. G. Gehring, G. C. Paoli, C.-Y. Chen, Y. He, and J. A. Capobianco, "Impacts of Clarification Techniques on Sample Constituents and Pathogen Retention," *Foods*, vol. 8, no. 12, p. 636, Dec. 2019, doi: 10.3390/FOODS8120636.

[55] L. F. Stinson, J. Ma, A. Rea, M. Dymock, and D. T. Geddes, "Centrifugation does not remove bacteria from the fat fraction of human milk," *Sci. Rep.*, vol. 11, no. 1, Dec. 2021, doi: 10.1038/s41598-020-79793-y.

[56] P. F. G. Wolffs, K. Glencross, R. Thibaudeau, and M. W. Griffiths, "Direct quantitation

and detection of salmonellae in biological samples without enrichment, using two-step filtration and real-time PCR," *Appl. Environ. Microbiol.*, vol. 72, no. 6, pp. 3896–3900, Jun. 2006, doi: 10.1128/AEM.02112-05.

[57] J.-H. Kim and S.-W. Oh, "Pretreatment methods for nucleic acid-based rapid detection of pathogens in food: A review," *Food Control*, vol. 121, no. 107575, 2021, doi: 10.1016/j.foodcont.2020.107575.

[58] H. P. Dwivedi and L.-A. Jaykus, "Detection of pathogens in foods: the current state-of-the-art and future directions," *Crit. Rev. Microbiol.*, vol. 37, no. 1, pp. 40–63, Feb. 2011, doi: 10.3109/1040841X.2010.506430.

[59] B. Furrer, U. Candrian, C. Hoefelein, and J. Luethy, "Detection and identification of Listeria monocytogenes in cooked sausage products and in milk by in vitro amplification of haemolysin gene fragments," *J. Appl. Bacteriol.*, vol. 70, no. 5, pp. 372–379, 1991, doi: 10.1111/J.1365-2672.1991.TB02951.X.

[60] T. J. Silhavy, D. Kahne, and S. Walker, "The Bacterial Cell Envelope," *Cold Spring Harb. Perspect. Biol.*, vol. 2, no. a00414, May 2010, doi: 10.1101/CSHPERSPECT.A000414.

[61] J. F. Kennedy, S. A. Barker, and J. D. Humphreys, "Microbial cells living immobilised on metal hydroxides," *Nature*, vol. 261, no. 5557, pp. 242–244, 1976, doi: 10.1038/261242A0.

[62] L. Yang, "A Review of Multifunctions of Dielectrophoresis in Biosensors and Biochips for Bacteria Detection," *Anal. Lett.*, vol. 45, no. 2–3, pp. 187–201, Jan. 2012, doi: 10.1080/00032719.2011.633182.

[63] V. C. H. Wu and C.-C. Wu, "Filtration and removal of foodborne pathogens using dielectrophoretic phenomena," *J. Rapid Methods Autom. Microbiol.*, vol. 16, no. 1, pp. 62–72, Mar. 2008, doi: 10.1111/J.1745-4581.2008.00116.X.

[64] W. Choi, Y. W. Min, K. Y. Lee, S. Jun, and H. G. Lee, "Dielectrophoresis-based microwire biosensor for rapid detection of Escherichia coli K-12 in ground beef," *LWT*, vol. 132, p. 109230, Oct. 2020, doi: 10.1016/J.LWT.2020.109230.

[65] H. O. Yosief, A. A. Weiss, and S. S. Iyer, "Capture of Uropathogenic E. coli by Using Synthetic Glycan Ligands Specific for the Pap-Pilus," *ChemBioChem*, vol. 14, no. 2, pp. 251–259, Jan. 2013, doi: 10.1002/cbic.201200582.

[66] L. Wang *et al.*, "Combining impedance biosensor with immunomagnetic separation for rapid screening of Salmonella in poultry supply chains," *Poult. Sci.*, vol. 99, no. 3, pp. 1606–1614, Mar. 2020, doi: 10.1016/J.PSJ.2019.12.007.

[67] L. Yang, "Dielectrophoresis assisted immuno-capture and detection of foodborne pathogenic bacteria in biochips," *Talanta*, vol. 80, no. 2, pp. 551–558, Dec. 2009, doi: 10.1016/J.TALANTA.2009.07.024.

[68] A. B. Nowicka, M. Czaplicka, T. Szymborski, and A. Kamińska, “Combined negative dielectrophoresis with a flexible SERS platform as a novel strategy for rapid detection and identification of bacteria,” *Anal. Bioanal. Chem.*, vol. 413, no. 7, pp. 2007–2020, Jan. 2021, doi: 10.1007/s00216-021-03169-y.

[69] Q. Li *et al.*, “Rapid detection of Listeria monocytogenes using fluorescence immunochromatographic assay combined with immunomagnetic separation technique,” *Int. J. Food Sci. Technol.*, vol. 52, no. 7, pp. 1559–1566, Jul. 2017, doi: 10.1111/IJFS.13428.

[70] N. Lee, S.-W. Choi, H.-J. Chang, and H. S. Chun, “Rapid Detection of Escherichia coli O157:H7 in Fresh Lettuce Based on Localized Surface Plasmon Resonance Combined with Immunomagnetic Separation,” *J. Food Prot.*, vol. 81, no. 5, pp. 713–718, May 2018, doi: 10.4315/0362-028X.JFP-17-338.

[71] D. Bhandari, F. C. Chen, and R. C. Bridgman, “Detection of Salmonella Typhimurium in Romaine Lettuce Using a Surface Plasmon Resonance Biosensor,” *Biosensors*, vol. 9, no. 3, p. 94, Jul. 2019, doi: 10.3390/BIOS9030094.

[72] J. Y. Park *et al.*, “Detection of Escherichia coli O157:H7 Using Automated Immunomagnetic Separation and Enzyme-Based Colorimetric Assay,” *Sensors*, vol. 20, no. 5, p. 1395, Mar. 2020, doi: 10.3390/S20051395.

[73] S. Wei, B.-J. Park, S.-H. Kim, K.-H. Seo, Y.-G. Jin, and D.-H. Oh, “Detection of Listeria monocytogenes using Dynabeads ® anti-Listeria combined with real-time PCR in soybean sprouts,” *LWT*, vol. 99, pp. 533–539, 2019, doi: 10.1016/j.lwt.2018.10.023.

[74] R. Augustine, A. R. Abraham, N. Kalarikkal, and S. Thomas, “Monitoring and separation of foodborne pathogens using magnetic nanoparticles,” in *Novel Approaches of Nanotechnology in Food*, 1st ed., P. Osborn, Ed. London: Elsevier Inc., 2016, pp. 271–312.

[75] A. Akbarzadeh, M. Samiei, and S. Davaran, “Magnetic nanoparticles: preparation, physical properties, and applications in biomedicine,” *Nanoscale Res. Lett.*, vol. 7, no. 144, Feb. 2012, doi: 10.1186/1556-276X-7-144.

[76] M. E. Khosroshahi and L. Ghazanfari, “Synthesis and functionalization of SiO 2 coated Fe 3O 4 nanoparticles with amine groups based on self-assembly,” *Mater. Sci. Eng. C*, vol. 32, no. 5, pp. 1043–1049, Jul. 2012, doi: 10.1016/J.MSEC.2011.09.003.

[77] V. F. Cardoso, A. Francesko, C. Ribeiro, M. Bañobre-López, P. Martins, and S. Lanceros-Mendez, “Advances in Magnetic Nanoparticles for Biomedical Applications,” *Adv. Healthc. Mater.*, vol. 7, no. 5, p. 1700845, Mar. 2018, doi: 10.1002/ADHM.201700845.

[78] M. Bilal, Y. Zhao, T. Rasheed, and H. M. N. Iqbal, “Magnetic nanoparticles as versatile carriers for enzymes immobilization: A review,” *Int. J. Biol. Macromol.*, vol. 120, pp. 2530–2544, Dec. 2018, doi: 10.1016/J.IJBIOMAC.2018.09.025.

[79] A.-H. Lu, E. L. Salabas, and F. Schüth, “Magnetic Nanoparticles: Synthesis, Protection, Functionalization, and Application,” *Angew. Chemie Int. Ed.*, vol. 46, no. 8, pp. 1222–1244, Feb. 2007, doi: 10.1002/ANIE.200602866.

[80] J. He, M. Huang, D. Wang, Z. Zhang, and G. Li, “Magnetic separation techniques in sample preparation for biological analysis: A review,” *J. Pharm. Biomed. Anal.*, vol. 101, pp. 84–101, Dec. 2014, doi: 10.1016/J.JPBA.2014.04.017.

[81] D. V. Pryazhnikov and I. V. Kubrakova, “Surface-Modified Magnetic Nanoscale Materials: Preparation and Study of Their Structure, Composition, and Properties,” *J. Anal. Chem.*, vol. 76, no. 6, pp. 685–706, Jun. 2021, doi: 10.1134/S1061934821060095.

[82] R. M. Fratila, M. Moros, and J. M. de la Fuente, “Recent advances in biosensing using magnetic glyconanoparticles,” *Anal. Bioanal. Chem.*, vol. 408, no. 7, pp. 1783–1803, Mar. 2016, doi: 10.1007/s00216-015-8953-2.

[83] S. Park *et al.*, “Probing Cell-Surface Carbohydrate Binding Proteins with Dual-Modal Glycan-Conjugated Nanoparticles,” *J. Am. Chem. Soc.*, vol. 137, no. 18, pp. 5961–5968, May 2015, doi: 10.1021/JACS.5B00592.

[84] N. P. Pera and R. J. Pieters, “Towards bacterial adhesion-based therapeutics and detection methods,” *Medchemcomm*, vol. 5, no. 8, pp. 1027–1035, Jul. 2014, doi: 10.1039/C3MD00346A.

[85] M. M. Sauer *et al.*, “Catch-bond mechanism of the bacterial adhesin FimH,” *Nat. Commun. 2016 71*, vol. 7, no. 1, pp. 1–13, Mar. 2016, doi: 10.1038/NCOMMS10738.

[86] M. A. Campanero-Rhodes, A. S. Palma, M. Menéndez, and D. Solís, “Microarray Strategies for Exploring Bacterial Surface Glycans and Their Interactions With Glycan-Binding Proteins,” *Front. Microbiol.*, vol. 10, no. 2909, 2020, doi: 10.3389/fmicb.2019.02909.

[87] R. Sommer *et al.*, “Cinnamide Derivatives of d-Mannose as Inhibitors of the Bacterial Virulence Factor LecB from Pseudomonas aeruginosa,” *ChemistryOpen*, vol. 4, no. 6, pp. 756–767, Dec. 2015, doi: 10.1002/OPEN.201500162.

[88] V. P. Harden and J. O. Harris, “The isoelectric point of bacterial cells.,” *J. Bacteriol.*, vol. 65, no. 2, pp. 198–202, 1953, doi: 10.1128/JB.65.2.198-202.1953.

[89] M. E. Bayer and J. L. S. Jr, “The electrophoretic mobility of Gram-negative and Gram-positive bacteria: an electrokinetic analysis,” *Microbiology*, vol. 136, no. 5, pp. 867–874, May 1990, doi: 10.1099/00221287-136-5-867.

[90] C.-T. Chen, J.-W. Yu, and Y.-P. Ho, “Identification of bacteria in juice/lettuce using magnetic nanoparticles and selected reaction monitoring mass spectrometry,” *J. Food Drug Anal.*, vol. 27, pp. 575–584, 2019, doi: 10.1016/j.jfda.2018.09.006.

[91] X. Zhao, C. W. Lin, J. Wang, and D. H. Oh, “Advances in rapid detection methods for

foodborne pathogens," *J. Microbiol. Biotechnol.*, vol. 24, no. 3, pp. 297–312, 2014, doi: 10.4014/jmb.1310.10013.

[92] K. G. Maciorowski, P. Herrera, F. T. Jones, S. D. Pillai, and S. C. Ricke, "Cultural and Immunological Detection Methods for Salmonella spp. in Animal Feeds – A Review," *Vet. Res. Commun.*, vol. 30, no. 2, pp. 127–137, Feb. 2006, doi: 10.1007/S11259-006-3221-8.

[93] W. B. Valderrama, E. G. Dudley, S. Doores, and C. N. Cutter, "Commercially Available Rapid Methods for Detection of Selected Food-borne Pathogens," *Crit. Rev. Food Sci. Nutr.*, vol. 56, no. 9, pp. 1519–1531, Jul. 2016, doi: 10.1080/10408398.2013.775567.

[94] J. H. Shin *et al.*, "Multiplexed Detection of Foodborne Pathogens from Contaminated Lettuces Using a Handheld Multistep Lateral Flow Assay Device," *J. Agric. Food Chem.*, vol. 66, no. 1, pp. 290–297, Jan. 2018, doi: 10.1021/acs.jafc.7b03582.

[95] Y. Wang and J. K. Salazar, "Culture-Independent Rapid Detection Methods for Bacterial Pathogens and Toxins in Food Matrices," *Compr. Rev. Food Sci. Food Saf.*, vol. 15, no. 1, pp. 183–205, Jan. 2016, doi: 10.1111/1541-4337.12175.

[96] Z. Wu, "Simultaneous Detection of Listeria monocytogenes and Salmonella typhimurium by a SERS-Based Lateral Flow Immunochromatographic Assay," *Food Anal. Methods*, vol. 12, no. 5, pp. 1086–1091, May 2019, doi: 10.1007/S12161-019-01444-4/TABLES/1.

[97] Y. Liu, Y. Cao, T. Wang, Q. Dong, J. Li, and C. Niu, "Detection of 12 common food-borne bacterial pathogens by taq man real-time PCR using a single set of reaction conditions," *Front. Microbiol.*, vol. 10, no. 222, 2019, doi: 10.3389/FMICB.2019.00222/BIBTEX.

[98] S. He *et al.*, "Detection of four foodborne pathogens based on magnetic separation multiplex PCR and capillary electrophoresis," *Biotechnol. J.*, vol. 17, no. 2100335, Jan. 2022, doi: 10.1002/BIOT.202100335.

[99] Y. Shang, J. Sun, Y. Ye, J. Zhang, Y. Zhang, and X. Sun, "Loop-mediated isothermal amplification-based microfluidic chip for pathogen detection," *Crit. Rev. Food Sci. Nutr.*, vol. 60, no. 2, pp. 201–224, Jan. 2018, doi: 10.1080/10408398.2018.1518897.

[100] M. Zhang *et al.*, "A newly developed paper embedded microchip based on LAMP for rapid multiple detections of foodborne pathogens," *BMC Microbiol.*, vol. 21, no. 197, Dec. 2021, doi: 10.1186/S12866-021-02223-0/TABLES/1.

[101] F. Sun, J. Zhang, Q. Yang, and W. Wu, "Quantum dot biosensor combined with antibody and aptamer for tracing food-borne pathogens," *Food Qual. Saf.*, vol. 5, Jan. 2021, doi: 10.1093/FQSAFE/FYAB019.

[102] L. Xu, X. Bai, and A. K. Bhunia, "Current State of Development of Biosensors and Their Application in Foodborne Pathogen Detection," *J. Food Prot.*, vol. 84, no. 7, pp. 1213–1227, Jul. 2021, doi: 10.4315/JFP-20-464.

[103] P. Poltronieri, V. Mezzolla, E. Primiceri, and G. Maruccio, “Biosensors for the Detection of Food Pathogens,” *Foods*, vol. 3, pp. 511–526, Sep. 2014, doi: 10.3390/FOODS3030511.

[104] P. Poltronieri, M. D. De Blasi, and O. F. D’Urso, “Detection of Listeria monocytogenes through real-time PCR and biosensor methods,” *Plant, Soil Environ.*, vol. 55, no. 9, pp. 363–369, 2009, doi: 10.17221/139/2009-pse.

[105] B. Wang and B. Park, “Immunoassay Biosensing of Foodborne Pathogens with Surface Plasmon Resonance Imaging: A Review,” *J. Agric. Food Chem.*, vol. 68, no. 46, pp. 12927–12939, Nov. 2020, doi: 10.1021/ACS.JAFC.0C02295.

[106] H. Vaisocherová-Lísalová *et al.*, “Low-fouling surface plasmon resonance biosensor for multi-step detection of foodborne bacterial pathogens in complex food samples,” *Biosens. Bioelectron.*, vol. 80, pp. 84–90, Jun. 2016, doi: 10.1016/j.bios.2016.01.040.

[107] Z. Bagheryan, J. B. Raoof, M. Golabi, A. P. F. Turner, and V. Beni, “Diazonium-based impedimetric aptasensor for the rapid label-free detection of Salmonella typhimurium in food sample,” *Biosens. Bioelectron.*, vol. 80, pp. 566–573, Jun. 2016, doi: 10.1016/J.BIOS.2016.02.024.

[108] J. H. Lee, H. Y. Cho, H. K. Choi, J. Y. Lee, and J. W. Choi, “Application of Gold Nanoparticle to Plasmonic Biosensors,” *Int. J. Mol. Sci.*, vol. 19, no. 7, p. 2021, Jul. 2018, doi: 10.3390/IJMS19072021.

[109] J. Zhang, B. Liu, H. Liu, X. Zhang, and W. Tan, “Aptamer-conjugated gold nanoparticles for bioanalysis,” *Nanomedicine*, vol. 8, no. 6, pp. 983–993, Jun. 2013, doi: 10.2217/nnm.13.80.

[110] P. Zhao, N. Li, and D. Astruc, “State of the art in gold nanoparticle synthesis,” *Coord. Chem. Rev.*, vol. 257, no. 3–4, pp. 638–665, Feb. 2013, doi: 10.1016/j.ccr.2012.09.002.

[111] L. Yu and N. Li, “Noble Metal Nanoparticles-Based Colorimetric Biosensor for Visual Quantification: A Mini Review,” *Chemosensors*, vol. 7, no. 53, Oct. 2019, doi: 10.3390/CHEMOSENSORS7040053.

[112] J. Turkevich, P. C. Stevenson, and J. Hillier, “A study of the nucleation and growth processes in the synthesis of colloidal gold,” *Discuss. Faraday Soc.*, vol. 11, pp. 55–75, Jan. 1951, doi: 10.1039/DF9511100055.

[113] M. Brust, M. Walker, D. Bethell, D. J. Schiffrin, and R. Whyman, “Synthesis of thiol-derivatised gold nanoparticles in a two-phase Liquid–Liquid system,” *J. Chem. Soc. Chem. Commun.*, no. 7, pp. 801–802, Jan. 1994, doi: 10.1039/C39940000801.

[114] R. Ahirwar and P. Nahar, “Development of a label-free gold nanoparticle-based colorimetric aptasensor for detection of human estrogen receptor alpha,” *Anal. Bioanal. Chem.*, vol. 408, pp. 327–332, 2015.

[115] J. M. Pingarrón, P. Yáñez-Sedeño, and A. González-Cortés, “Gold nanoparticle-based electrochemical biosensors,” *Electrochim. Acta*, vol. 53, no. 19, pp. 5848–5866, Aug. 2008, doi: 10.1016/J.ELECTACTA.2008.03.005.

[116] S. Nooranian, A. Mohammadinejad, T. Mohajeri, G. Aleyaghoob, and R. Kazemi Oskuee, “Biosensors based on aptamer-conjugated gold nanoparticles: A review,” *Biotechnol. Appl. Biochem.*, pp. 1–18, 2021, doi: 10.1002/BAB.2224.

[117] F. Wei, R. Lam, S. Cheng, S. Lu, D. Ho, and N. Li, “Rapid detection of melamine in whole milk mediated by unmodified gold nanoparticles,” *Appl. Phys. Lett.*, vol. 96, no. 133702, Mar. 2010, doi: 10.1063/1.3373325.

[118] C. A. Mirkin, R. L. Letsinger, R. C. Mucic, and J. J. Storhoff, “A DNA-based method for rationally assembling nanoparticles into macroscopic materials,” *Nature*, vol. 382, no. 6592, pp. 607–609, Aug. 1996, doi: 10.1038/382607A0.

[119] Z. Heidari, S. E. Rezatofighi, and S. Rastegarzadeh, “Development and comparison of cross-linking and non-crosslinking probe-gold nanoparticle hybridization assays for direct detection of unamplified bovine viral diarrhea virus-RNA,” *BMC Biotechnol.*, vol. 21, no. 1, Dec. 2021, doi: 10.1186/S12896-021-00691-W.

[120] B. Kuswandi, A. A. Gani, N. Kristiningrum, and M. Ahmad, “Simple Colorimetric DNA Biosensor Based on Gold Nanoparticles for Pork Adulteration Detection in Processed Meats,” *Sensors & Transducers*, vol. 208, no. 1, pp. 7–13, 2017, Accessed: Jan. 31, 2022. [Online]. Available: http://www.sensorsportal.com.

[121] K. Mao, J. Ma, X. Li, and Z. Yang, “Rapid duplexed detection of illicit drugs in wastewater using gold nanoparticle conjugated aptamer sensors,” *Sci. Total Environ.*, vol. 688, pp. 771–779, Oct. 2019, doi: 10.1016/J.SCITOTENV.2019.06.325.

[122] Y. W. Hartati, A. A. Suryani, M. Agustina, S. Gaffar, and A. Anggraeni, “A Gold Nanoparticle–DNA Bioconjugate–Based Electrochemical Biosensor for Detection of Sus scrofa mtDNA in Raw and Processed Meat,” *Food Anal. Methods*, vol. 12, no. 11, pp. 2591–2600, Nov. 2019, doi: 10.1007/S12161-019-01593-6/TABLES/3.

[123] S. Brosel-Oliu *et al.*, “Novel impedimetric aptasensor for label-free detection of Escherichia coli O157:H7,” *Sensors Actuators B Chem.*, vol. 255, pp. 2988–2995, Feb. 2018, doi: 10.1016/J.SNB.2017.09.121.

[124] S. M. You *et al.*, “Gold Nanoparticle-Coated Starch Magnetic Beads for the Separation, Concentration, and SERS-Based Detection of E. coli O157:H7,” *ACS Appl. Mater. Interfaces*, vol. 12, no. 16, pp. 18292–18300, Apr. 2020, doi: 10.1021/ACSAMI.0C00418/SUPPL_FILE/AM0C00418_SI_001.PDF.

[125] C. Zhou, H. Zou, M. Li, C. Sun, D. Ren, and Y. Li, “Fiber optic surface plasmon resonance sensor for detection of E. coli O157:H7 based on antimicrobial peptides and AgNPs-rGO,” *Biosens. Bioelectron.*, vol. 117, pp. 347–353, Oct. 2018, doi: 10.1016/J.BIOS.2018.06.005.

[126] A. Gnanamani, P. Hariharan, Paul-, and M. Satyaseela, “Staphylococcus aureus: Overview of Bacteriology, Clinical Diseases, Epidemiology, Antibiotic Resistance and Therapeutic Approach,” in *Frontiers in Staphylococcus aureus*, S. Enany and L. C. Alexander, Eds. London: IntechOpen, 2017.

[127] B. Crago, C. Ferrato, S. J. Drews, L. W. Svenson, G. Tyrrell, and M. Louie, “Prevalence of Staphylococcus aureus and methicillin-resistant S. aureus (MRSA) in food samples associated with foodborne illness in Alberta, Canada from 2007 to 2010,” *Food Microbiol.*, vol. 32, no. 1, pp. 202–205, Oct. 2012, doi: 10.1016/J.FM.2012.04.012.

[128] A. E. Waters *et al.*, “Multidrug-Resistant Staphylococcus aureus in US Meat and Poultry,” *Clin. Infect. Dis.*, vol. 52, no. 10, pp. 1227–1230, May 2011, doi: 10.1093/CID/CIR181.

[129] M. Azimirad *et al.*, “Microbiological survey and occurrence of bacterial foodborne pathogens in raw and ready-to-eat green leafy vegetables marketed in Tehran, Iran,” *Int. J. Hyg. Environ. Health*, vol. 237, no. 113824, Aug. 2021, doi: 10.1016/j.ijheh.2021.113824.

[130] D. M. Tack *et al.*, “Preliminary Incidence and Trends of Infections with Pathogens Transmitted Commonly Through Food — Foodborne Diseases Active Surveillance Network, 10 U.S. Sites, 2016–2019,” *MMWR. Morb. Mortal. Wkly. Rep.*, vol. 69, no. 17, pp. 509–514, May 2020, doi: 10.15585/mmwr.mm6917a1.

[131] H. Pennington, “Escherichia coli O157,” *Lancet*, vol. 376, no. 9750, pp. 1428–1435, Oct. 2010, doi: 10.1016/S0140-6736(10)60963-4.

[132] X. Zhang, S. Wang, X. Chen, and C. Qu, “Review controlling Listeria monocytogenes in ready-to-eat meat and poultry products: An overview of outbreaks, current legislations, challenges, and future prospects,” *Trends Food Sci. Technol.*, vol. 116, pp. 24–35, Oct. 2021, doi: 10.1016/j.tifs.2021.07.014.

[133] C. D. K. Tchatchouang *et al.*, “Listeriosis Outbreak in South Africa: A Comparative Analysis with Previously Reported Cases Worldwide,” *Microorganisms*, vol. 8, no. 1, Jan. 2020, doi: 10.3390/MICROORGANISMS8010135.

[134] K. Xing, X. G. Chen, C. S. Liu, D. S. Cha, and H. J. Park, “Oleoyl-chitosan nanoparticles inhibits Escherichia coli and Staphylococcus aureus by damaging the cell membrane and putative binding to extracellular or intracellular targets,” *Int. J. Food Microbiol.*, vol. 132, no. 2–3, pp. 127–133, 2009, doi: 10.1016/j.ijfoodmicro.2009.04.013.

[135] N. Sharon, “Carbohydrates as future anti-adhesion drugs for infectious diseases,” *Biochim. Biophys. Acta - Gen. Subj.*, vol. 1760, no. 4, pp. 527–537, Apr. 2006, doi: 10.1016/J.BBAGEN.2005.12.008.

[136] M. S. Riaz Rajoka *et al.*, “Chitin/chitosan derivatives and their interactions with microorganisms: a comprehensive review and future perspectives,” *Crit. Rev. Biotechnol.*, vol. 40, no. 3, pp. 365–379, Apr. 2020, doi: 10.1080/07388551.2020.1713719.

[137] E. T. Sumrall, A. P. Keller, Y. Shen, and M. J. Loessner, “Structure and function of

Listeria teichoic acids and their implications," *Mol. Microbiol.*, vol. 113, no. 3, pp. 627–637, Mar. 2020, doi: 10.1111/MMI.14472.

[138] N. T. Reichmann and A. Gründling, "Location, synthesis and function of glycolipids and polyglycerolphosphate lipoteichoic acid in Gram-positive bacteria of the phylum Firmicutes," *FEMS Microbiol. Lett.*, vol. 319, no. 2, pp. 97–105, Jun. 2011, doi: 10.1111/J.1574-6968.2011.02260.X.

[139] I. M. Helander, E. L. Nurmiaho-Lassila, R. Ahvenainen, J. Rhoades, and S. Roller, "Chitosan disrupts the barrier properties of the outer membrane of Gram-negative bacteria," *Int. J. Food Microbiol.*, vol. 71, no. 2–3, pp. 235–244, Dec. 2001, doi: 10.1016/S0168-1605(01)00609-2.

[140] Y. Liu, H. Tang, Z. Lin, and P. Xu, "Mechanisms of acid tolerance in bacteria and prospects in biotechnology and bioremediation," *Biotechnol. Adv.*, vol. 33, no. 7, pp. 1484–1492, Nov. 2015, doi: 10.1016/J.BIOTECHADV.2015.06.001.

[141] C. Zhou and P. D. Fey, "The Acid Response Network of Staphylococcus aureus," *Curr. Opin. Microbiol.*, vol. 55, p. 67, Jun. 2020, doi: 10.1016/J.MIB.2020.03.006.

[142] B. A. Diep *et al.*, "The arginine catabolic mobile element and staphylococcal chromosomal cassette mec linkage: convergence of virulence and resistance in the USA300 clone of methicillin-resistant Staphylococcus aureus," *J. Infect. Dis.*, vol. 197, no. 11, pp. 1523–1530, Jun. 2008, doi: 10.1086/587907.

[143] S. Ryan, M. Begley, C. G. M. Gahan, and C. Hill, "Molecular characterization of the arginine deiminase system in Listeria monocytogenes: regulation and role in acid tolerance," *Environ. Microbiol.*, vol. 11, no. 2, pp. 432–445, Feb. 2009, doi: 10.1111/J.1462-2920.2008.01782.X.

[144] D. Verheyen, X. M. Xu, M. Govaert, M. Baka, T. Skåra, and J. F. Van Impe, "Food microstructure and fat content affect growth morphology, growth kinetics, and preferred phase for cell growth of Listeria monocytogenes in fish-based model systems," *Appl. Environ. Microbiol.*, vol. 85, no. 16, Aug. 2019, doi: 10.1128/AEM.00707-19/ASSET/53712AA3-28DA-43FE-9712-0AE802F5566A/ASSETS/GRAPHIC/AEM.00707-19-F0006.JPEG.

[145] W. M. Leong, R. Geier, S. Engstrom, S. Ingham, B. Ingham, and M. Smukowski, "Growth of Listeria monocytogenes, Salmonella spp., Escherichia coli O157:H7, and Staphylococcus aureus on Cheese during Extended Storage at 25uC," *J. Food Prot.*, vol. 77, no. 8, 2014, doi: 10.4315/0362-028X.JFP-14-047.

[146] K. A. Floyd, A. R. Eberly, and M. Hadjifrangiskou, "Adhesion of bacteria to surfaces and biofilm formation on medical devices," in *Biofilms and Implantable Medical Devices: Infection and Control*, L. Overend, Ed. Duxford, United Kingdom: Elsevier Ltd, 2017, pp. 47–95.

[147] F. Sarti and A. Bernkop-Schnürch, "Chitosan and thiolated chitosan," *Adv. Polym. Sci.*,

vol. 243, no. 1, pp. 93–110, 2011, doi: 10.1007/12_2011_109.

[148] Centers for Disease Control and Prevention, "Listeria Outbreaks," *Centers for Disease Control and Prevention*, 2021. https://www.cdc.gov/listeria/outbreaks/index.html (accessed May 07, 2021).

[149] Centers for Disease Control and Prevention, "Reports of Selected E. coli Outbreak Investigations," *Centers for Disease Control and Prevention*, 2021. https://www.cdc.gov/ecoli/outbreaks.html (accessed Jan. 24, 2022).

[150] J. Kadariya, T. C. Smith, and D. Thapaliya, "Staphylococcus aureus and Staphylococcal Food-Borne Disease: An Ongoing Challenge in Public Health," *Biomed Res. Int.*, vol. 2014, no. 827965, 2014, doi: 10.1155/2014/827965.

[151] "pH Values of Foods and Food Products," *Arrow Scientific*, 2021. http://www.arrowscientific.com.au/index.php?option=com_content&view=article&id=61:ph-values-of-foods-and-food-products&catid=17&Itemid=31 (accessed Jan. 24, 2022).

[152] J.-Y. Hyeon and X. Deng, "Rapid detection of Salmonella in raw chicken breast using real-time PCR combined with immunomagnetic separation and whole genome amplification," *Food Microbiol.*, vol. 63, pp. 111–116, 2016, doi: 10.1016/j.fm.2016.11.007.

[153] E. Dester, K. Kao, and E. C. Alocilja, "Detection of Unamplified E. coli O157 DNA Extracted from Large Food Samples Using a Gold Nanoparticle Colorimetric Biosensor," *Biosensors*, vol. 12, no. 5, p. 274, Apr. 2022, doi: 10.3390/BIOS12050274.

[154] N. Al-Awwal, M. Masjedi, M. El-Dweik, S. H. Anderson, and J. Ansari, "Nanoparticle immuno-fluorescent probes as a method for detection of viable E. coli O157:H7," *J. Microbiol. Methods*, vol. 193, p. 106403, Feb. 2022, doi: 10.1016/j.mimet.2021.106403.

[155] M. H. Tu, T. Sun, and K. T. V. Grattan, "Optimization of gold-nanoparticle-based optical fibre surface plasmon resonance (SPR)-based sensors," *Sensors Actuators B Chem.*, vol. 164, no. 1, pp. 43–53, Mar. 2012, doi: 10.1016/J.SNB.2012.01.060.

[156] T. Bu *et al.*, "Diversely positive-charged gold nanoparticles based biosensor: A label-free and sensitive tool for foodborne pathogen detection," *Food Chem. X*, vol. 3, p. 100052, Sep. 2019, doi: 10.1016/J.FOCHX.2019.100052.

[157] F. Zhan, T. Wang, L. Iradukunda, and J. Zhan, "A gold nanoparticle-based lateral flow biosensor for sensitive visual detection of the potato late blight pathogen, Phytophthora infestans," *Anal. Chim. Acta*, vol. 1036, pp. 153–161, Dec. 2018, doi: 10.1016/J.ACA.2018.06.083.

[158] E. Gorodkiewicz and Z. Lukaszewski, "Recent Progress in Surface Plasmon Resonance Biosensors (2016 to Mid-2018)," *Biosensors*, vol. 8, no. 4, p. 132, Dec. 2018, doi: 10.3390/BIOS8040132.

[159] S. Balbinot, A. M. Srivastav, J. Vidic, I. Abdulhalim, and M. Manzano, "Plasmonic biosensors for food control," *Trends Food Sci. Technol.*, vol. 111, pp. 128–140, May 2021, doi: 10.1016/J.TIFS.2021.02.057.

[160] National Center for Biotechnology Information, "Escherichia coli (ID 167)." https://www-ncbi-nlm-nih-gov.proxy1.cl.msu.edu/genome/?term=e. coli O157 (accessed Mar. 30, 2022).

[161] P. Feng, S. Weagant, and K. Jinneman, "BAM Chapter 4A: Diarrheagenic Escherichia coli | FDA," in *Bacteriological Analytical Manual*, 2020.

[162] A. Surendraraj, N. Thampuran, and T. C. Joseph, "Molecular Screening, Isolation, and Characterization of Enterohemorrhagic Escherichia coli O157:H7 from Retail Shrimp," *J. Food Prot.*, vol. 73, no. 1, pp. 97–103, 2010, doi: 10.4315/0362-028x-73.1.97.

[163] F. M. Yrad, J. M. Castañares, and E. C. Alocilja, "Visual Detection of Dengue-1 RNA Using Gold Nanoparticle-Based Lateral Flow Biosensor," *Diagnostics*, vol. 9, no. 3, Sep. 2019, doi: 10.3390/DIAGNOSTICS9030074.

[164] R. Hunter, *Foundations of Colloid Science*, 2nd ed. Oxford University Press, 2001.

[165] C. L. Gyles, "Shiga toxin-producing Escherichia coli: An overview," *J. Anim. Sci.*, vol. 85, no. supp_13, pp. E45–E62, Mar. 2007, doi: 10.2527/JAS.2006-508.

[166] G. M. S. Ross, D. Filippini, M. W. F. Nielen, and G. I. J. Salentijn, "Unraveling the Hook Effect: A Comprehensive Study of High Antigen Concentration Effects in Sandwich Lateral Flow Immunoassays," *Anal. Chem.*, vol. 92, no. 23, pp. 15587–15595, Dec. 2020, doi: 10.1021/ACS.ANALCHEM.0C03740/SUPPL_FILE/AC0C03740_SI_001.PDF.

[167] S. A. Vetrone, M. C. Huarng, and E. C. Alocilja, "Detection of Non-PCR Amplified S. enteritidis Genomic DNA from Food Matrices Using a Gold-Nanoparticle DNA Biosensor: A Proof-of-Concept Study," *Sensors*, vol. 12, pp. 10487–10499, Aug. 2012, doi: 10.3390/S120810487.

[168] M. E. Arnold, J. J. Carrique-Mas, I. McLaren, and R. H. Davies, "A comparison of pooled and individual bird sampling for detection of Salmonella in commercial egg laying flocks," *Prev. Vet. Med.*, vol. 99, no. 2–4, pp. 176–184, May 2011, doi: 10.1016/J.PREVETMED.2010.12.007.

[169] M. Sidstedt *et al.*, "Humic substances cause fluorescence inhibition in real-time polymerase chain reaction," *Anal. Biochem.*, vol. 487, pp. 30–37, Oct. 2015, doi: 10.1016/J.AB.2015.07.002.

[170] Qiagen, "DNeasy PowerLyzer PowerSoil Kit," 2022. https://www.qiagen.com/us/products/discovery-and-translational-research/dna-rna-purification/dna-purification/microbial-dna/dneasy-powerlyzer-powersoil-kit/ (accessed May 09, 2022).

[171] Y. Qu *et al.*, “SSEL, a selective enrichment broth for simultaneous growth of Salmonella enterica, Staphylococcus aureus, Escherichia coli O157: H7, and Listeria monocytogenes,” *J. Food Saf.*, vol. 40, no. 5, p. e12837, Oct. 2020, doi: 10.1111/JFS.12837.

[172] Y. Suo *et al.*, “A multipathogen selective enrichment broth for simultaneous growth of Salmonella enteria, Escherichia coli O157:H7, and Shigella flexneri,” *J. Food Saf.*, vol. 38, no. 1, p. e12388, Feb. 2018, doi: 10.1111/JFS.12388.

[173] L. Zheng, G. Cai, S. Wang, M. Liao, Y. Li, and J. Lin, “A microfluidic colorimetric biosensor for rapid detection of Escherichia coli O157:H7 using gold nanoparticle aggregation and smart phone imaging,” *Biosens. Bioelectron.*, vol. 124–125, pp. 143–149, Jan. 2019, doi: 10.1016/J.BIOS.2018.10.006.